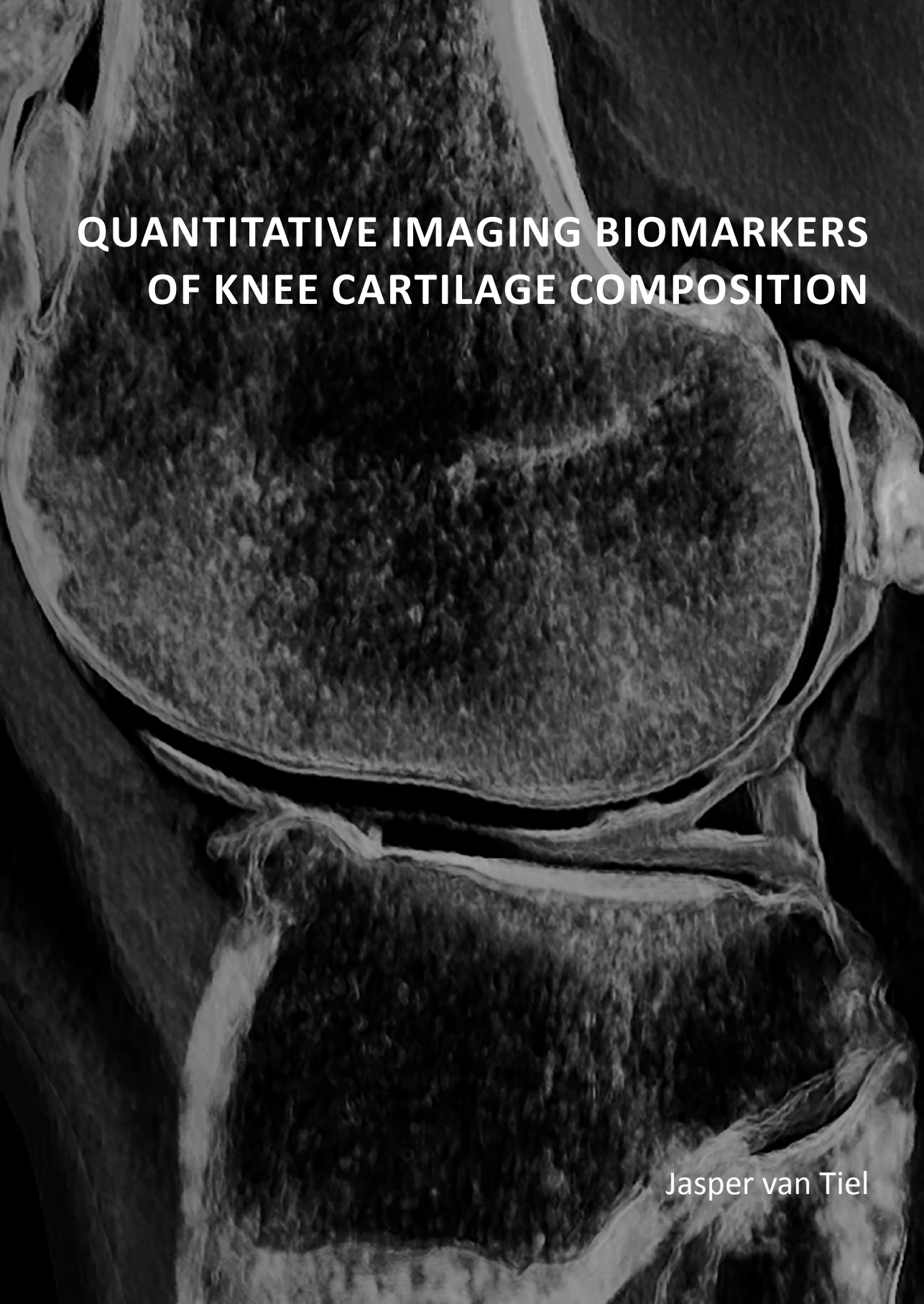

QUANTITATIVE IMAGING BIOMARKERS OF KNEE CARTILAGE COMPOSITION

Jasper van Tiel

Quantitative Imaging Biomarkers of Knee Cartilage Composition

Jasper van Tiel
j.vantiel@erasmusmc.nl

The printing of this thesis was financially supported by:
- Department of Orthopedic Surgery, Erasmus Medical Center, Rotterdam
- Department of Radiology, Erasmus Medical Center, Rotterdam
- The Dutch Orthopedic Society, 's Hertogenbosch
- The Anna | NOREF foundation, Leiden
- Centrum Orthopedie Rotterdam b.v., Rotterdam
- Chipsoft b.v., Amsterdam
- ABN AMRO Bank, Amsterdam
- Guerbet Nederland b.v., Gorichem
- Livit orthopedie, Amsterdam
- Push Braces, Maastricht
- Össur, Son en Breugel
- Bayer Healthcare b.v., Mijdrecht
- Spomed, Capelle aan den IJssel

ISBN: 978-94-91487-25-5
Layout: Ridderprint BV - www.ridderprint.nl
Printed by: Ridderprint BV - www.ridderprint.nl
Publisher: YourThesis published by Medix Publishers BV, Keizersgracht 317A, 1016 EE Amsterdam, the Netherlands

Quantitative Imaging Biomarkers of Knee Cartilage Composition

Beeldvormende technieken om de samenstelling van
kniekraakbeen in maat en getal te bepalen

Proefschrift

ter verkrijging van de graad van doctor aan de
Erasmus Universiteit Rotterdam
op gezag van de
rector magnificus

Prof.dr. H.A.P. Pols

en volgens besluit van het College voor Promoties.
De openbare verdediging zal plaatsvinden op

17 november 2015 om 13:30 uur

Jasper van Tiel
geboren te Utrecht

Erasmus University Rotterdam

Promotiecommissie

Promotores:
Prof.dr.ir. H.H. Weinans
Prof.dr. G.P. Krestin

Co-promotor:
Dr. E.H.G. Oei

Overige leden:
Prof.dr. S.M.A. Bierma - Zeinstra
Prof.dr. M. Maas
Prof.dr. W.J. Niessen

TABLE OF CONTENTS

Chapter 1

General introduction

Part of this chapter is based on the following publications:

Quantitative MRI Techniques of Cartilage Composition.
S. Matzat, J. van Tiel, G.E. Gold, E.H. Oei.
Quant Imaging Med Surg. 2013 Jun;3(3):162-74.

Quantitative Radiological Imaging Techniques for Articular Cartilage Composition: Towards Early Diagnosis and Development of Disease-Modifying Therapeutics for Osteoarthritis.
E.H. Oei, J. van Tiel, W.H. Robinson, G.E. Gold
Arthritis Care Res (Hoboken). 2014 Aug;66(8):1129-41.

OSTEOARTHRITIS

Osteoarthritis (OA) is the most common joint disease among middle-aged and elderly in Western countries [1-4]. Hip and knee joints are more frequently affected by OA than other joints. For example, 40% of the population aged 70 years and above suffers from knee OA [5]. OA is a chronic disease that, because of its high prevalence, contributes most to impaired physical well-being and quality of life on a population level. In the year 2011, over 1.000.000 persons in The Netherlands visited their general practitioner because of symptomatic hip or knee OA [2, 3]. Due to the ageing of the population in Western countries, the prevalence of OA is expected to increase further with another 40% in the coming decades [3, 6]. When increased rates of obesity in Western societies are additionally taken into consideration as an important risk factor for the development of OA, the prevalence is expected to increase by almost 50% in 2040 [3, 6].

Besides impairment in physical well-being and quality of life, OA also results in more costs to society than other musculoskeletal diseases such as rheumatoid arthritis and osteoporosis [7-9]. Due to the ageing population, this financial burden to society is also expected to increase over the coming decades. The economic burden of arthritis is estimated at 1 to 2.5% of the gross national product of Western countries [8, 10]. Symptomatic OA accounts for the majority of this burden because it is by far the most prevalent form of arthritis. The total medical costs for symptomatic OA in The Netherlands were estimated at €1.1 billion in 2011 [3, 11]. Most of the medical costs for OA are made in secondary care, mainly due to expensive joint replacement surgeries and associated costs for end-stage OA [12].

Given the absence of definitive treatment options other than joint replacement and the high burden of OA both in terms of health and costs, research in the OA field focuses on therapies that may modify the course of OA, e.g. disease-modifying osteoarthritis drugs (DMOADs) [13, 14], stem cell therapy [14, 15], joint distraction [16, 17] or more established intervention methods such as high tibial osteotomy [18]. Especially the first two strategies aim at targeting OA at an early stage when they are expected to be most effective, thereby aiming at avoiding or delaying progression of the disease to its end-stage and reducing the large socio-economic impact of OA. In addition to these therapeutic interventions, high-risk populations for development of OA are being studied which might be a candidate for targeted OA prevention studies in the future [19-21]. Successful application of the aforementioned therapeutic or preventive strategies could reduce the need for invasive and irreversible joint replacement, which is associated with complications, high costs and limited lifetime of the prosthesis.

It is known from previous research that OA is not a disease of only bone and cartilage. OA is rather a disease of the whole joint in which bone, cartilage, menisci and synovium play a role in the development and progression of the disease [22]. As cartilage

is an important tissue in the joint that is known to be affected by OA at early stages, research concerning DMOADs or preventive interventions focuses on articular cartilage as a target tissue in knee OA. These interventions can only be developed, assessed, improved and implemented successfully if their clinical and structural effect can be monitored and measured accurately, sensitively, and objectively in cross-sectional and longitudinal studies. Clinical efficacy of these interventions can be assessed by validated questionnaires that include patient's clinical history and physical examination. However, these measurements, which represent clinical disease severity, are prone to subjectivity and poorly correlate with radiological disease severity [23, 24]. Therefore, it is of utmost importance to also assess the structural efficacy of an intervention. The structural effects of a certain treatment on articular cartilage structure can be assessed non-invasively using radiological imaging [25, 26]. Thus, radiological imaging can be used as an imaging biomarker to assess the structural efficacy of a certain treatment in the development of novel therapeutic strategies for OA, but also for assessment of disease status or progression.

TRADITIONAL IMAGING TECHNIQUES IN OSTEOARTHRITIS

Radiography

Radiography is the most commonly applied radiological technique to image OA and an accepted imaging biomarker to evaluate progression both in clinical practice and in research settings [27]. A frequently used grading system for diagnosing and following OA was developed by Kellgren and Lawrence which allows the differentiation of radiographic OA in 4 categories of severity: no OA (*Figure 1A*), mild or early OA (*Figure 1B*) and more advanced, e.g. moderate and severe OA (*Figure 1C*) [28]. Radiography is a frequently used modality both in clinical and in OA research settings since it is relatively inexpensive and is easily accessible for general physicians, medical specialists and researchers.

There are, however, major limitations of radiography applied as an imaging biomarker for OA. The most important limitation is its inability of directly visualizing cartilage and its weak correlation with cartilage damage on arthroscopy [29, 30]. Instead, radiography can only detect joint space narrowing used as a representation of gross cartilage loss or meniscal damage in moderate to advanced stage OA [31, 32]. Furthermore, radiographic assessment of early stage OA is associated with substantial inaccuracy and subjectivity [33] and there is major disagreement concerning the definition and grading of OA using the Kellgren and Lawrence classification system [34]. In addition, radiography is incapable of detecting disease progression with sufficient sensitivity within a reasonable time window, i.e. progression of OA on radiography is only detectable after years instead of months [35, 36]. This makes large-scale studies, which use radiography as an outcome

measure less feasible since it would be necessary to have a follow-up period of several years, while a shorter follow-up period is desirable in clinical research. Another limitation of radiography is its incapacity to depict any soft tissues in and around the joint

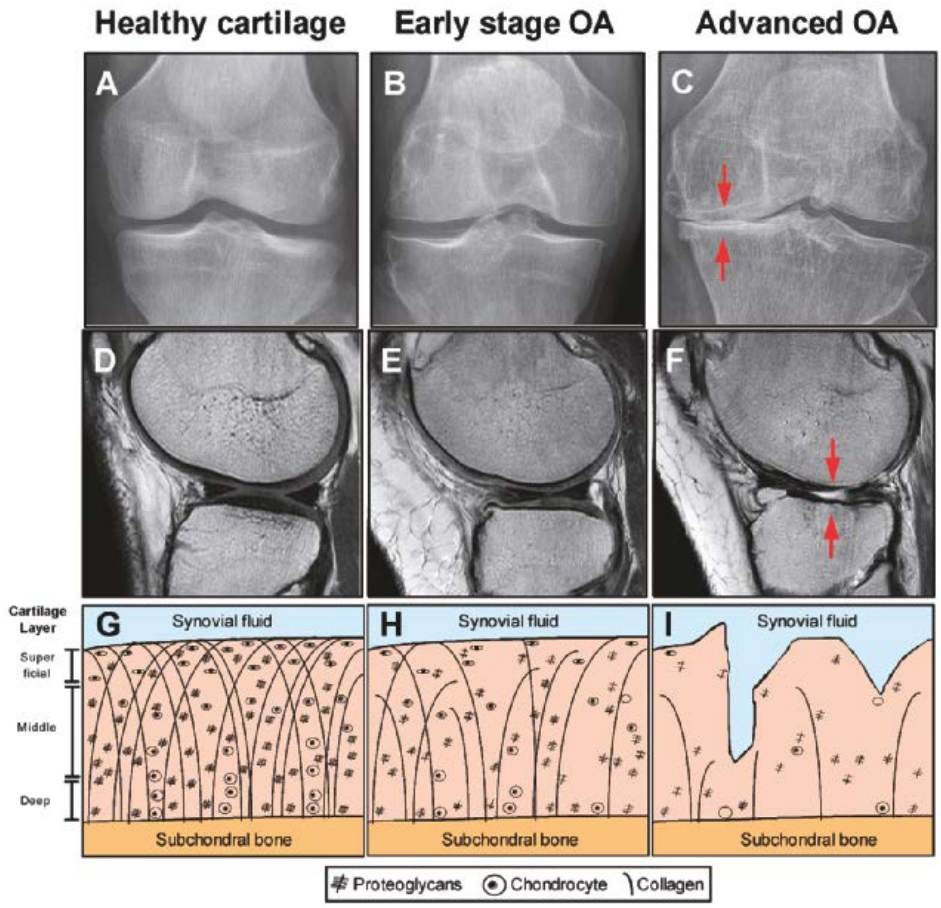

Figure 1: *Radiographic, conventional morphological MRI and schematic representation of articular cartilage in healthy (A, D, G), early stage osteoarthritic (B, E, H) and moderate (right side of the tibiofemoral compartment in C) or end stage osteoarthritic cartilage (left side of the tibiofemoral compartment in C, F, I). In healthy cartilage on radiography and conventional MRI, no morphological abnormalities are present (A, D). In healthy cartilage the orientation and density of the collagen fibers varies by location within the cartilage layer and regionally within the joint. Relative to the articular surface, their prevailing orientation is parallel in the superficial layer, oblique in the transitional (middle) layer, and perpendicular in the deep radial zone (G). Similarly, the concentration of proteoglycans varies according to location and is highest in the middle layer (G). In the early phase of OA no morphological changes of the cartilage are visible on radiography and conventional MRI (B, E), but sulphated glycosaminoglycans leak from the cartilage and the collagen fibers change in size and orientation (H). In advanced stage OA, morphological changes (thinning and defects) of the cartilage appear on radiography or conventional MRI (C, F), while the whole original microscopic structure is destroyed (I).*

that are believed to play an important role in OA, e.g. synovium, menisci, ligaments, joint capsule and muscle [22]. Finally, OA related findings derived from radiographs correlate poorly with clinical OA symptoms, e.g. pain, stiffness and disability [37, 38].

Magnetic resonance imaging

Because of the aforementioned limitations of radiography, magnetic resonance imaging (MRI) is increasingly applied as an imaging biomarker to assess and follow-up OA, both in clinical trials and epidemiological studies. Unlike radiography, MRI is a three-dimensional technique that can directly visualize cartilage and other soft tissues of the joint (*Figure 1D*), and is substantially more accurate than radiography in detecting cartilage damage [33]. Therefore, several semi-quantitative MRI scoring systems for OA features in different tissues of the knee have been developed over the last decade [39]. The Knee Osteoarthritis Scoring System (KOSS) [40], the Whole-Organ MRI Score (WORMS) [41], the Boston Leeds Osteoarthritis Knee Score (BLOKS) [42], and MRI Osteoarthritis Knee Score (MOAKS) [43, 44] are commonly used scoring systems [25]. In addition to these semi-quantitative scoring systems for OA features on MRI, quantitative morphometric methods that involve cartilage segmentation followed by thickness and volume measurements were developed to further increase sensitivity of MRI as an OA biomarker to determine and follow articular cartilage quality in OA [45, 46].

Despite these advantages of MRI over radiography, there are also limitations of MRI, especially if it is used as an outcome measure in early stage OA. Current "conventional MRI techniques" are usually aimed at assessing morphology alterations (thinning or defects) of cartilage in moderate or end stage OA (*Figure 1F*) [47, 48]. These morphological cartilage changes are, however, not present in early stage OA (*Figure 1E*) and may not be manifest with subtle OA progression [49, 50]. Moreover, morphological MRI assessment of cartilage is a subjective outcome measure for cartilage quality.

QUANTITATIVE IMAGING BIOMARKERS OF CARTILAGE COMPOSITION AND ITS BASIC PRINCIPLES

To overcome the limitations of radiography and conventional MRI methods, there is increasing interest in novel imaging techniques that enable measurement of the biochemical composition of cartilage rather than its morphology [51-53]. These quantitative techniques offer a numeric outcome measure that can be used as an imaging biomarker for cartilage composition in cross-sectional studies, as well as in longitudinal research of OA in an early stage of the disease. In addition, they may enhance understanding of the pathogenesis of OA, much of which is still unknown.

The basic principles of these novel quantitative imaging biomarkers are based on the microscopic changes in composition of cartilage during early stage OA. Articular cartilage which is also known as hyaline cartilage, is largely acellular as chondrocytes constitute only 4% of its wet weight [54]. Instead, the main components of cartilage are water (65%-85% depending on depth from the articular surface) and the extracellular matrix (ECM). The ECM is synthesized and maintained by the chondrocytes and mainly consists of type II collagen (15-20%) and proteoglycans (PG) (3-10%) (*Figure 1G*) [55-57]. PGs mainly consist of sulphated glycosaminoglycans (sGAG), which are negatively charged due to ionized sulfate and carboxyl groups. These strong negative electrostatic charges, collectively responsible for the so-called fixed-charge density (FCD), are important contributors to the structure and biomechanical properties of articular cartilage [55, 56]. They allow sGAG molecules to be fixed to the collagen network of the extracellular matrix and attract positive counter-ions, mainly sodium, which lead to a firm increase of the cartilage osmotic pressure. As a consequence cartilage attracts water molecules resulting in a swelling of cartilage, which is counteracted by the surrounding collagen meshwork. This balance between swelling pressure and collagen tension contributes to a large extent to the tremendous tensile and compressive strength of cartilage under normal physiological conditions [55, 56, 58, 59]. Articular cartilage can be subdivided in three layers: the superficial, middle and deep layer. In healthy cartilage, PG density and the orientation of the collagen fibers varies by location within the cartilage layer and regionally within the joint [55, 60-62] (*Figure 1G*).

In early stages of OA, the microstructure of the ECM breaks down and the tissue begins to lose its functional capacity. These early changes are indicated by a decreasing FCD due to loss of PGs, a decreased organization of the collagen matrix, and increased water content (*Figure 1H*) [56]. These changes compromise the ability of cartilage to resist stress, resulting in further strain on the ECM and leaving cartilage prone to more advanced morphological degenerative changes [57, 63] that radiography and conventional MRI techniques are sensitive to (*Figure 1I*). Quantitative imaging biomarkers for cartilage composition are advocated to visualize and measure the microscopic biochemical changes during the early stage of OA, which are described above. In this thesis, the focus will be on the techniques that can measure the sGAG content present in the ECM of articular cartilage.

QUANTITATIVE IMAGING BIOMARKERS MEASURE SULPHATED GLYCOSAMINOGLYCAN CONTENT OF ARTICULAR CARTILAGE

Delayed gadolinium-enhanced MRI of cartilage

Most quantitative imaging biomarkers for articular cartilage composition are MRI based. The most established method of these is delayed gadolinium-enhanced MRI of cartilage (dGEMRIC) [64, 65]. The technique was introduced in 1996 and makes use of the repulsive force between a negatively charged contrast agent (gadopentetate dimeglumine) and the negative charge of the sGAG present in the extracellular matrix of cartilage. This results in contrast agent accumulation in cartilage inversely proportional to its sGAG content [64]. The outcome parameter is the T1 relaxation time, usually averaged for the pixels in a region of interest and presented as the dGEMRIC index. T1 relaxation time is reduced by the contrast agent and consequently is lower in areas with decreased sGAG content compared to healthy cartilage with relative high and homogeneous sGAG distribution (*Figure 2A*). Because dGEMRIC is one of the first quantitative biomarkers for cartilage composition, it has become the standard biomarker in clinical research during the last decade [25, 26].

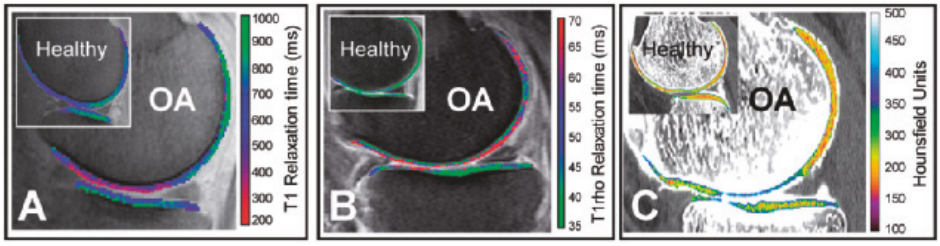

Figure 2: *dGEMRIC, T1rho-mapping and CT arthrography applied in healthy subjects and early and moderate stage knee OA patients. Sagittal slices through the center of the medial or lateral tibiofemoral compartment of knee OA patients and healthy volunteers (insets) acquired using different quantitative radiological techniques (all images acquired in different subjects). None of the early OA patients showed clear abnormalities on the conventional MRI sequences (not shown). The dGEMRIC color map A shows a clear decrease in T1 relaxation times (purple/red) in early OA representing loss of sGAG. T1rho mapping (B) shows increased T1rho relaxation times (red) in a patient with moderate knee OA. CT arthrography color map C shows a clear increase in Hounsfield units (blue/white) in early OA representing loss of sGAG.*

T1rho-mapping

Another quantitative MRI biomarker to measure cartilage composition is T1rho-mapping [66, 67]. T1rho-mapping, also described as relaxation in the rotating frame, uses a constant radiofrequency field referred to as a "spin lock" pulse to change relaxation rates of water associated with large macromolecules in cartilage. As T1rho relaxation time is proposed to be sensitive to protons associated with sGAG, several authors have suggested a direct relationship between T1rho relaxation time and sGAG concentration [66, 68, 69]. Decreased sGAG content may lead to increased mobile proton density in bulk water and therefore

increased T1rho relaxation times (*Figure 2B*). Since T1rho-mapping does not involve the use of a contrast agent, the technique has been advocated as a non-contrast-enhanced alternative to dGEMRIC and is therefore increasingly applied in clinical OA research [25, 26, 70].

Other potential MRI based biomarkers for cartilage sulphated glycosaminoglycan content

Chemical exchange saturation transfer (CEST) is an MRI method to measure the difference in free water and water which has been bound by certain macromolecules [71]. Applied to cartilage, CEST can be used to assess the amount of water, which has been bound by the sGAG molecules in the cartilage ECM to provide a direct measurement of cartilage sGAG content (referred to as gagCEST) [72]. When less sGAG is present in the ECM, the free water signal increases as a result of the loss of sGAG from the cartilage.

Unlike previously discussed MRI biomarkers that rely on proton imaging, sodium MRI measures sodium signal [73]. As positive sodium ions are associated with negatively charged sGAG of the cartilage ECM extracellular matrix [74], sodium MRI outcomes correlate with sGAG content. GAG loss from cartilage in early cartilage degeneration is accompanied by reduced sodium concentration resulting in decreased sodium MRI signal [75].

GagCEST and sodium MRI are promising imaging biomarkers which are mainly applied *in vitro* [72, 74], but are also already applied *in vivo* in human research [76, 77]. However, they mostly needs specific MRI equipment, coils and imaging post processing software which makes these techniques less feasible compared to dGEMRIC and T1rho-mapping.

Contrast-enhanced computed tomography

In addition to MRI based biomarkers for cartilage composition, there are also contrast-enhanced computed tomography (CT) based quantitative imaging techniques, such as equilibrium partitioning of an ionic contrast agent using microCT (EPIC-µCT) [78, 79] and µCT arthrography (µCTa) [80, 81]. Like dGEMRIC, EPIC-µCT and µCTa use the inverse relation between a negatively charged contrast agent (ioxaglate) and the sGAG content of cartilage [80, 81]. The quantitative outcome of contrast-enhanced CT is the X-ray attenuation measured in Hounsfield units and is higher in sGAG depleted compared to healthy, non-sGAG-depleted, cartilage (*Figure 2C*). In µCTa, the contrast agent is injected intra-articularly and is also used for cartilage delineation and segmentation [80, 81]. After contrast injection, the injected joint is passively or actively moved to promote contrast distribution throughout the joint cavity. Although CT arthrography has been used extensively in the past to assess cartilage morphology [82, 83], quantitative CT arthrography is not yet applied as biomarker of cartilage biochemical composition in a clinical human research setting and is only used in *in vitro* research or in *in vivo* animal research.

CURRENT USE OF QUANTITATIVE IMAGING BIOMARKERS OF CARTILAGE SULPHATED GLYCOSAMINOGLYCAN CONTENT IN HUMAN OSTEOARTHRITIS RESEARCH

As previously mentioned, dGEMRIC and T1rho-mapping are already applied as imaging biomarkers for cartilage sGAG content in human OA research. To generate correct and reliable outcomes from quantitative MRI biomarkers, robust image processing tools are of great importance. Until now, only little research has been performed to develop such image processing tools [84-86]. Therefore, future research is warranted to optimize image processing of quantitative MRI data. In addition to robust imaging processing tools, the reproducibility is also of importance when using a quantitative technique, i.e. dGEMRIC, as an outcome measure in cross-sectional or longitudinal research. dGEMRIC has been shown to be a reproducible measure for cartilage sGAG content in healthy human knees [87, 88], but the reproducibility in OA knee cartilage, which constitute an important target population for quantitative imaging techniques for cartilage composition, has not yet been determined.

T1rho-mapping has been shown to yield reproducible results in an OA population [89] and could therefore possibly be a non-contrast-enhanced alternative for dGEMRIC to quantify sGAG content in OA cartilage, as advocated. Even though both dGEMRIC and T1rho-mapping are used as outcome measure for cartilage sGAG content in clinical OA research, no thorough validation studies have been performed that compare both techniques within the same OA patients using a reference standard for cartilage sGAG content. Both techniques were only validated *in vivo* in humans in one (dGEMRIC) or two (T1rho-mapping) studies with relatively small sample size [69, 90, 91].

Assuming that the aforementioned research shows that both dGEMRIC and T1rho-mapping yield reproducible and valid outcomes in terms sGAG content of OA cartilage, the techniques could indeed be used as a quantitative imaging biomarker for cartilage composition, for example to assess the efficacy of a potential DMOAD. In addition, since MRI images multiple tissues in the knee joint, quantitative assessment of non-cartilaginous tissues might be studied.

Unlike MRI based quantitative imaging biomarkers for cartilage sGAG content that are already applied in human OA research, contrast-enhanced CT or CT arthrography (CTa) have not yet been used for this purpose in human OA research. If properly translated and implemented in clinical setting, CT based techniques may be a potential valuable alternate to MRI based techniques for cartilage sGAG imaging in clinical OA research, for example in indications to undergo MRI.

AIMS AND OUTLINE OF THIS THESIS

The main aims of this thesis are divided between MRI and CT based quantitative imaging biomarkers of cartilage sGAG content, which relates to their different stage of application in research. MRI is already applied in human OA research, whereas CT is still to be translated and implemented in clinical research.

The first part of this thesis focuses on MRI based biomarkers for cartilage sGAG content and aims at optimization of image post processing, assessing reproducibility, comparison of different MRI sequences and application in clinical OA research. In chapter 2, the development of a sophisticated image processing algorithm to analyze quantitative MRI datasets is described. This algorithm is used in all following chapters in which MRI biomarkers are applied. In chapter 3, the reproducibility of dGEMRIC in early stage OA patients is assessed. In chapter 4 an *in vivo* validation and comparison study is performed for dGEMRIC and T1rho-mapping, which is advocated to be a non-contrast alternative to dGEMRIC in human knee OA patients. In chapter 5, dGEMRIC is used to investigate if improvement of cartilage sGAG content could be measured after treating early stage OA patients with hyaluronic acid and in chapter 6, the possibility to analyze both cartilage, as well as meniscus composition using dGEMRIC is assessed.

The second part of this thesis focuses on CT based imaging biomarkers and aims at translating CTa from a microscopic to a macroscopic setup and making it suitable to be used in clinical OA research. In chapter 7 μCT arthrography is translated to a clinically applicable protocol for CTa of human knee joints. The ability of this protocol to measure cartilage sGAG content using low radiation dose is assessed in chapter 8. In chapter 9, the CTa technique is validated *in vivo* in human patients with knee OA.

In chapter 10, the results of the research on which this thesis is based are discussed followed by the overall conclusions of this thesis and future perspectives towards quantitative imaging biomarkers in the human OA research. Chapter 11 summarizes all results and the conclusions in English and chapter 12 in Dutch.

Part 1

MRI based quantitative imaging biomarkers of cartilage sulphated glycosaminoglycan content

Optimization of post processing and reproducibility of dGEMRIC

1.1

Chapter 2

Image registration improves human knee cartilage T1 mapping with delayed gadolinium-enhanced MRI of cartilage (dGEMRIC)

E.E. Bron, J. van Tiel, H. Smit, D.H.J. Poot, W.J. Niessen, G.P. Krestin, H. Weinans, E.H. Oei, G. Kotek, S. Klein.

Eur Radiol. 2013 Jan;23(1):246-52.

ABSTRACT

Introduction

To evaluate the effect of automated registration in delayed gadolinium-enhanced MRI of cartilage (dGEMRIC) of the knee on the occurrence of movement artifacts on the T1 map and the reproducibility of region of interest (ROI)-based measurements.

Materials and Methods

Eleven patients with early stage knee osteoarthritis and ten healthy controls underwent dGEMRIC twice at 3-T. Controls underwent unenhanced imaging. ROIs were manually drawn on the femoral and tibial cartilage. T1 calculation was performed with and without registration of the T1-weighted images. Automated 3D rigid registration was performed on the femur and tibia cartilage separately. Registration quality was evaluated using the square root Cramér–Rao lower bound ($CRLB_\sigma$). Additionally, the reproducibility of dGEMRIC was assessed by comparing automated registration with manual slice matching.

Results

Automated registration of the T1-weighted images improved the T1 maps as the 90% percentile of the $CRLB_\sigma$ was significantly ($P<0.05$) reduced with a median reduction of 55.8 ms (patients) and 112.9 ms (controls). Manual matching and automated registration of the reimaged T1 map gave comparable intraclass correlation coefficients of respectively 0.89/0.90 (patients) and 0.85/0.85 (controls).

Conclusion

Registration in dGEMRIC reduces movement artifacts on T1 maps and provides a good alternative to manual slice matching in longitudinal studies.

INTRODUCTION

Osteoarthritis, the most common form of arthritis, is characterized by the degradation and loss of cartilage [92]. Delayed gadolinium-enhanced MRI of cartilage (dGEMRIC) has been introduced as a non-invasive quantitative technique to measure cartilage quality by evaluating its glycosaminoglycan content [64, 65, 93]. Imaging is performed after administration of a negatively charged contrast agent that diffuses into cartilage in reverse relationship to the charge of glycosaminoglycan molecules. A quantitative T1 map is reconstructed from images acquired consecutively with different inversion times.

Automated image registration may improve dGEMRIC studies in two ways. First, T1 map quality may be improved by registration of the T1-weighted images to correct for patient movement during the acquisition process. Only a few papers on dGEMRIC used image registration to correct for motion artifacts [84, 85]. Moreover, registration of the T1-weighted images has not been evaluated before in patients with knee osteoarthritis. Second, automated image registration can be applied in longitudinal studies to compare T1 maps acquired at different time points. Previous studies did not use registration for this purpose, but instead relied on manual matching of slices [87, 88], which is operator-dependent and time-consuming. Automated image registration eliminates the subjective manual slice matching and manually outlined ROIs are required only once. This can be of value in follow-up studies evaluating for example the effect of a treatment.

The present study evaluates the effects of both image registration steps on the outcome of dGEMRIC in patients with knee osteoarthritis as well as in healthy controls.

MATERIALS AND METHODS

Subjects

This study was approved by the institutional review board of Erasmus MC, Rotterdam, The Netherlands. Informed consent was obtained from all subjects.

Two subject groups were included in this study. Group I consisted of 11 patients (age 52.2±11.0 years, 7 male) with early stage knee osteoarthritis (knee complaints > 3 months, visual analogue pain scale > 20 mm and Kellgren–Lawrence grade I or II on radiography [28]). Group II consisted of 10 healthy controls (age 26.7±8.6 years, 4 male).

Imaging protocol

Images were acquired on a 3-T MRI (Discovery MR750, General Electric Healthcare, Milwaukee, WI, USA). The 3D protocol for T1-weighted imaging consisted of an inversion recovery fast spoiled gradient-recalled echo (FSPGR) sequence with five inversion times (TI = 100, 200, 400, 800, 2100 ms) [94]. The repetition time (TR) was the inversion

time plus the time after read-out (TS = 3.9ms). Other parameters were: flip angle = 15º, echo time = 1.5 ms, field of view = 15x15 cm, slice thickness = 3 mm, slice spacing = 3 mm, in-plane voxel size = 0.6x0.6 mm, number of slices in the sagittal plane = 36. The dGEMRIC MR protocol lasted approximately 15 min.

In patients, the dGEMRIC protocol [94] was performed twice with an interval of 7 days (range 5–14 days). A double dose (0.2 mmol/kg) of Magnevist® (Bayer, Berlin, Germany) was injected intravenously. Next, the patients were asked to cycle for 10 min on a home trainer to promote contrast agent distribution into and throughout the knee and the cartilage [95]. After cycling, there was a delay of 80 min before the participants underwent MRI. An open design three-channel knee coil (Flick Engineering Solutions B.V., Winterswijk, The Netherlands) was used which enabled imaging of patients with a large knee diameter. Controls underwent MRI with the standard eight-channel knee coil (General Electric Healthcare) requiring a knee diameter less than 14 cm. For the controls no contrast agent was used and the second MR examination was acquired after a short break and repositioning of the knee.

Definition of regions of interest

For each subject two regions of interest (ROIs) on the femoral and tibial cartilage were outlined by a trained researcher with a medical degree (JvT). The femoral cartilage ROI consisted of the adjacent trochlear, weight-bearing and posterior cartilage of the femur and the tibial cartilage ROI consisted of the weight-bearing tibial plateau cartilage. The ROI outlining was performed on the central slice through the medial and lateral tibio-femoral joint, for both the first and second MR examination, resulting in eight cartilage ROIs per subject.

T1 calculation and uncertainty estimate

The T1 map was reconstructed by voxel wise fitting of the relation $SI(TI)=S_0 \cdot (1-A \cdot \exp(-TI/T1)+\exp(-TR/T1))$ [94] to the T1-weighted images acquired at a range of inversion times. The fitting was performed with a maximum likelihood estimator of T1, S_0 (fully relaxed signal) and A (inversion efficiency) which takes into account the Rician distribution of the data because, for magnitude MR images, this is more accurate than the commonly used normal distribution [96].

The uncertainty of the estimated parameters at each voxel can be expressed by the Cramér–Rao lower bound (CRLB), which gives a lower bound for the variance [96-98]. The square root of the T1 CRLB ($CRLB_\sigma$) can therefore be interpreted as a lower bound for the standard deviation of the T1 value, which quantifies how noise on the MR signal propagates to uncertainty of the estimated T1 value. In quantitative MRI, $CRLB_\sigma$ has previously been used for optimization of MR sequences [99-101], but it can also be used as an indicator of misalignment. Misalignment of the T1-weighted images, especially

at tissue boundaries, results in biologically implausible values of S_0, A and T1, often associated with a high uncertainty, which is expressed by $CRLB_\sigma$. The T1 calculations were performed using in-house developed Matlab software (R2008a, The MathWorks, Natick, MA, USA), which produces both the T1 map and the $CRLB_\sigma$ map. As a summary statistic for the $CRLB_\sigma$ values, we computed the 90% percentile (90%-$CRLB_\sigma$) over all voxels in each annotated ROI; the lower this value, the better. We also computed the 90%-$CRLB_\sigma$ over all voxels in all ROIs together, to obtain a single measure per subject.

Registration of T1-weighted images

All T1-weighted images were registered in 3D with respect to that T1-weighted image showing the highest contrast between cartilage and surrounding synovial fluid, and between cartilage and bone cortex ($FSPGR_{TI=2100}$). Registrations were performed using Elastix software [102] using a rigid transformation model (translations and rotations). Femoral and tibial regions were registered separately based on sub volumes containing only the specific bone and surrounding tissue to allow correction for motion of the knee joint (*Figure 1*). The registration was optimized over 1000 iterations with localized mutual information (LMI) as a similarity measure [103]. Per iteration, LMI was calculated using 2048 random samples obtained from a sample region of size 50x50x50 mm. Cubic B-spline interpolation was used when applying the deformation to the moving image. The exact registration settings can be found on the parameter file database on the Elastix website: http://elastix.isi.uu.nl/wiki.php.

T1 maps were calculated with and without registration. A Wilcoxon signed rank test was used to test for a significant effect of registration on the 90%-$CRLB_\sigma$ values.

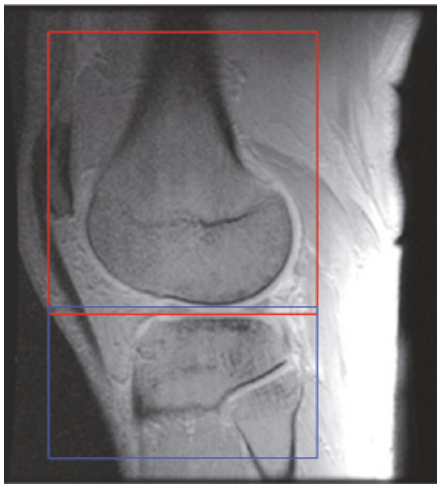

Figure 1: *Registration is performed separately on the femoral (red) and tibial (blue) sub volumes to correct for motion of the knee joint. The background grayscale image is a T1-weighted image ($FSPGR_{TI=2100}$)*

Registration between the first and second MR examinations

To align the $FSPGR_{TI=2100}$ images from the first and second MR examinations, registration was performed with the same method as in the previous section. Based on this registration, the T1 maps from the second MR examination were transformed to the T1 maps obtained at the initial study. The result of this alignment was compared with the reference standard of manually selecting matching slices, which was performed by a trained researcher (JvT.) visually inspecting $FSPGR_{TI=2100}$ images from the first and second MR examinations for matching slices.

Analysis of the reproducibility between the first and second MR examinations was based on correlations of a weighted mean T1 value per ROI. A weighted mean was computed to reduce the effect of outliers which are for example caused by bone voxels accidently included in the cartilage ROIs. As outliers are expected to have a high $CRLB_\sigma$, the reciprocal of the $CRLB_\sigma$ was used as the weight of each voxel to reduce their effect.

The reproducibility of the weighted mean T1 values was assessed using the intraclass correlation coefficient (ICC), Pearson's correlation coefficient, and total least squares regression. In these analyses we treated the four ROIs on each image as independent measurements. The ICC describes the resemblance of two sets of data with identical unit and an equal variance [104, 105] and can therefore be used to measure the agreement between the first and the registered second MR examination. A total least squares fit [106, 107] was performed to estimate a linear relation between measurements obtained at the two examinations. A fit with a slope significantly different from 1 would imply a systematic difference.

RESULTS

Registration of T1-weighted images

Registration of the T1-weighted images improved the T1 mapping, as $CRLB_\sigma$ was reduced and the homogeneity of the T1 maps was increased (*Figure 2*). Visual inspection of all ROIs showed an improvement in the alignment of the T1-weighted images due to registration. This effect was similar in the femoral and tibial cartilage ROIs. In only 3 out of 84 tibial cartilage ROIs, the severity of movement artifacts was increased by registration, which was caused by misalignment of the $FSGPR_{TI=100}$ image in 2 of the cases.

Table 1 reports per subject the 90%-$CRLB_\sigma$ over all voxels in the eight ROIs, with and without registration. *Table 2* shows the statistics for these measurements (first row) and for each ROI separately (rows 2–9). The 90%-$CRLB_\sigma$ decreased significantly in patients ($P=0.003$) and controls ($P=0.005$) owing to automated registration. The effect of registration was more pronounced in the femoral cartilage than in the tibial cartilage. With a Bonferroni correction for multiple testing, the registration effect in the femoral ROIs was still significant ($P<0.05$).

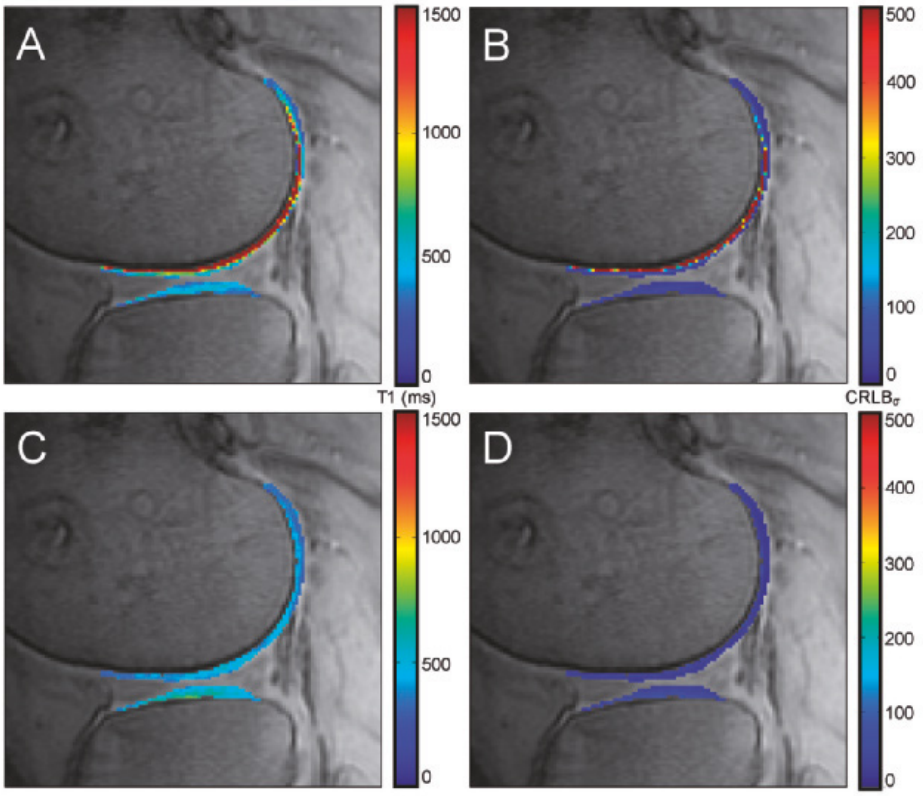

Figure 2: *Comparison of T1 map and square root of Cramér–Rao lower bound ($CRLB_\sigma$) map of a patient with and without automated registration to correct for patient movement (color overlay). The $CRLB_\sigma$ (ms) provides a lower bound for standard deviation of T1 (ms) and is a measure for registration quality. The background grayscale image is a T1-weighted image ($FSPGR_{TI=2100}$). (a) T1 map without registration, (b) $CRLB_\sigma$ map without registration showing high uncertainty in the T1 estimates, (c) improved T1 map with registration, (d) $CRLB_\sigma$ map with registration showing reduced uncertainty in the T1 estimates*

Registration between the first and second MR examinations

Figure 3 shows scatter plots of the weighted mean T1 measurements on the first versus the second MR examination. *Table 3* summarizes the statistics. In patients, the ICC for the manual slice matching was 0.89 and with registration similar results were obtained (ICC=0.90). In controls, an ICC of 0.85 was found with both manual matching and registration. These ICC values indicate a similar reproducibility for both methods as the ICC values lie in each other's 95% confidence interval. The Pearson correlation coefficients show the same pattern. Linear total least squares regression resulted in a slope of approximately 1 in patients and controls, with both manual matching and automated registration, which confirms that there are no systematic differences.

Subject	Patients		Controls	
	No registration (ms)	Automated registration (ms)	No registration (ms)	Automated registration (ms)
1	1753	177	260	244
2	43	34	>10000	605
3	142	84	443	298
4	96	74	410	360
5	765	152	176	164
6	178	120	>10000	712
7	111	74	456	385
8	>10000	762	441	267
9	128	105	>10000	2609
10	152	86	165	141
11	91	69	-	-

Table 1: *The 90%-CRLB$_\sigma$ calculated over all voxels in the eight cartilage ROIs. In 1 patient and 3 control subjects the 90%-CRLB$_\sigma$ value without registration is over 10000 (ms). This resulted from voxels where the maximum likelihood fit indicated an 'infinitely' long T1 time*

ROI	Patients		Controls	
	median difference (ms) [1]	P value [2]	median difference (ms)	P-value
All voxels in the eight ROIs	55.8	0.003	112.9	0.005
Femoral cartilage in the selected slice in the lateral compartment: Initial MRI	71.6	0.004	1561.6	0.005
Femoral cartilage in the selected slice in the medial compartment: Initial MRI	223.2	0.003	210.9	0.005
Lateral femoral cartilage on second MRI	73.8	0.003	677.6	0.005
Medial femoral cartilage on second MRI	104.8	0.003	72.8	0.009
Tibial cartilage in the selected slice in the lateral compartment: Initial MRI	-5.7	0.374	-63.1	0.647
Tibial cartilage in the selected slice in the medial compartment: Initial MRI	-7.4	0.350	-5.1	0.508
Lateral tibial cartilage on second MRI	3.0	0.424	-45.0	0.959
Medial tibial cartilage on second MRI	-15.4	0.286	148.6	0.037

Table 2: *The effect of registration on the 90%-CRLB$_\sigma$ of all voxels in the eight ROIs combined and of each ROI separately. [1] Differences in the median of the 90%-CRLB$_\sigma$ for all subjects between no registration and automated registration. [2] P values of the Wilcoxon signed rank test*

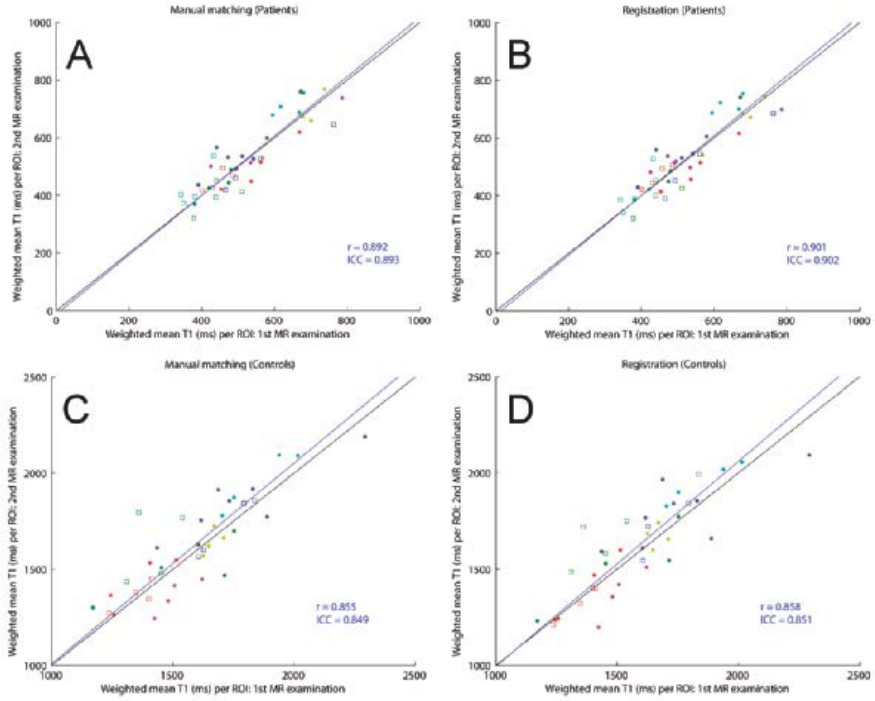

Figure 3: *Weighted mean T1 value per ROI for all patients (a, b) and controls (c, d). Subjects are represented by different colored markers. The weighted means of the T1 maps from the first and second MR examinations are plotted against each other with manual slice-matching (a, c) and automated registration (b, d). The black line represents y=x which is the expected result at perfect registration and reproducibility. The blue line is a linear total least squares fit through the points. r represents the Pearson's correlation coefficient of the points and ICC the intraclass correlation coefficient*

	Patients		Controls	
	Manual matching	**Registration**	**Manual matching**	**Registration**
ICC(2,1)	0.893	0.902	0.849	0.851
(CI)	(0.813–0.940)	(0.827–0.945)	(0.732–0.917)	(0.736–0.919)
r	0.892	0.901	0.855	0.858
(CI)	(0.809–0.940)	(0.824–0.945)	(0.742–0.921)	(0.745–0.923)
slope	1.030	1.036	1.044	1.065
(CI)	(0.412–1.649)	(0.383–1.688)	(0.589–1.499)	(0.506–1.624)

Table 3: *Comparison between first and second MR examinations: weighted mean T1 values of each ROI with manual slice-matching and automated registration. ICC(2,1) = Two-way random intraclass correlation coefficient based on single measures, r = Pearson's correlation coefficient, slope = the slope obtained with a total least squares fit, CI = 95% confidence interval*

DISCUSSION

Our study demonstrates that automated registration can improve two aspects of dGEMRIC studies in the setting of knee osteoarthritis: the T1 map calculation and the reproducibility of T1 maps obtained at different MR examinations.

First, applying automated image registration in the calculation of T1 maps from T1-weighted images improves the T1 maps and reduces the uncertainty in the estimated T1 value. In finger and hand arthritis, analysis by the coefficient of variation (CV) and visual grading analysis (VGA) showed that registration improves image quality and reduces variability [84]. In knee dGEMRIC, this has only been investigated in five healthy volunteers [85] where the goodness of the T1 fit was evaluated using χ^2 analysis. In our paper the $CRLB_\sigma$ was used to measure the effect of registration on the T1 map. Like χ^2 analysis, $CRLB_\sigma$ provides a quantitative measure to express the quality of the T1 fit, which is not provided by CV or VGA. However, χ^2 and $CRLB_\sigma$ express different properties of the quality of fit: χ^2 quantifies the difference between the fit and the measurements, and $CRLB_\sigma$ quantifies how noise on the MR signal propagates to the fit. $CRLB_\sigma$ has the advantage over χ^2 of being an absolute measure expressed in the same unit (ms) as T1. The results of our study show a reduction of $CRLB_\sigma$ due to registration, with a more pronounced effect in the femoral cartilage than in tibial cartilage. The 90%-$CRLB_\sigma$ did not show a significant effect of registration on the tibial ROIs (*Table 2*). This may be explained by the smaller signal intensity difference between cartilage and bone observed in the tibia compared with the femur. Misalignments in the tibial area will therefore have less effect on the $CRLB_\sigma$ than misalignments in the femoral region.

Second, automated image registration in evaluation of dGEMRIC reproducibility has been addressed. Using manual slice matching, Multanen et al [87] reported an ICC of 0.95 in femoral cartilage and 0.87 in tibial cartilage of control subjects and Siversson et al [88] found a femur ICC of approximately 0.68 in patients. We found an ICC of 0.89 with the manual slice-matching method in patients. For the control group, the manual approach resulted in an ICC of 0.85, which is comparable to the aforementioned studies. The automated registration method presented in our study requires only one manually drawn cartilage mask for evaluating the same ROI in two or more MR examinations. Therefore, analysis of dGEMRIC is less time consuming using the automated registration method. The actual amount of time that can be saved depends on the number of ROIs, slices and MR examinations to be analyzed. This is particularly of interest if two or more MR examinations need to be analyzed for large cohorts of patients. Automated registration yielded similar results to the manual method (ICC = 0.90 in patients and 0.85 in controls). The reproducibility in patients was slightly higher than in controls, which could be explained by differences in signal-to-noise ratio (SNR) owing to different coils, or by the difference in T1 values as controls underwent unenhanced MR

imaging. The SNR was actually higher in controls than in patients (132±38 vs. 67±37), so the better reproducibility in patients is most likely explained by the presence of contrast agent leading to shorter T1 values. The range of inversion times in the FSPGR sequence is optimized for these typical T1 values in the presence of contrast agent. The lower 90%-$CRLB_\sigma$ values for patients reflect this (*Table 1*).

Although this paper focuses on dGEMRIC, the registration method used is not specifically developed for dGEMRIC. The method should therefore be applicable to other MR mapping methods as well, such as T1ρ and T2.

In conclusion, automated registration of dGEMRIC in knee cartilage improves the quality of T1 maps and provides a good alternative to manual slice-matching in longitudinal studies as it leads to equal reproducibility and is operator-independent.

chapter

Reproducibility of 3D delayed gadolinium-enhanced MRI of cartilage (dGEMRIC) of the knee at 3.0 T in patients with early stage osteoarthritis

J. van Tiel, E.E. Bron, C.J. Tiderius, P.K. Bos, M. Reijman, S. Klein, J.A. Verhaar, G.P. Krestin, H. Weinans, G. Kotek, E.H. Oei.

Eur Radiol. 2013 Feb;23(2):496-504.

ABSTRACT

Introduction

To assess the reproducibility of 3D delayed Gadolinium Enhanced MRI of cartilage (dGEMRIC) at 3 T in early stage knee osteoarthritis (OA) patients.

Materials and Methods

In 20 patients, 3D dGEMRIC at 3 T was acquired twice within 7 days. To correct for patient motion during acquisition, all images were rigidly registered in 3D. Eight anatomical cartilage ROIs were analyzed on both images of each patient. Capability of dGEMRIC to yield T1 maps that reproducibly distinguish spatial differences in cartilage quality was assessed in two ROIs within a single slice in each patient. Reproducibility was assessed using ICCs and Bland–Altman plots.

Results

ICCs ranged from 0.87 to 0.95, indicating good reproducibility. T1 maps revealed reproducible spatial differences in cartilage quality (ICC 0.79). Based on the Bland–Altman plots, we defined a threshold of 95 ms to determine if a change in dGEMRIC outcome in longitudinal research was statistically significant.

Conclusion

3D knee dGEMRIC at 3 T combined with 3D image registration is a highly reproducible measure of cartilage quality in early stage OA. Therefore, dGEMRIC may be a valuable tool in the non-invasive evaluation of cartilage quality changes in longitudinal research in patients with early stage OA and focal cartilage defects.

INTRODUCTION

Knee osteoarthritis (OA) is the most common joint disease in the middle-aged and elderly, causing serious morbidity and having a large socio-economic impact [7, 108, 109]. As the current radiological reference standard for grading the severity of OA on radiographs [28], is not sensitive enough to detect or follow structural changes in the cartilage present in early stage OA, sophisticated imaging techniques have been developed that can quantitatively measure cartilage quality [13, 33]. An example of such a quantitative technique is delayed gadolinium enhanced magnetic resonance imaging of cartilage (dGEMRIC) which has been validated both *in vitro* and *in vivo* [65, 95]. This technique has become a standard for the non-invasive assessment of articular cartilage quality in OA research and after articular cartilage repair techniques in the knee [110-114].

Potentially, dGEMRIC could also be an excellent technique for the follow-up of cartilage quality over time. However, both for quality assessment of the technique and especially before the dGEMRIC technique can be used in longitudinal research, its reproducibility must be evaluated. Since the introduction of dGEMRIC by Bashir *et al*. in 1996 [65], only three small studies on the reproducibility of dGEMRIC have been published, reporting good reproducibility in healthy volunteers and patients with an anterior cruciate ligament tear (ACLT) with only limited changes related to OA on radiography [87, 88, 115]. To our knowledge, for early stage OA patients, who might have a higher and possibly more variable penetration of contrast agent into the cartilage [116], the reproducibility of dGEMRIC has not been reported. As the results of the previous reproducibility studies are not directly generalizable to the early stage OA patient population, the reproducibility of dGEMRIC needs to be reassessed accordingly.

The aim of this study was to assess the reproducibility of three-dimensional (3D) dGEMRIC at 3.0 Tesla (T) in patients with clinical and radiological signs of early stage OA of the knee. We also assessed whether the dGEMRIC protocol is capable of yielding T1 maps that reproducibly distinguish spatial differences in cartilage quality within a single slice. This information is important for using dGEMRIC to follow both OA development and the repair of cartilage defects over time.

MATERIALS AND METHODS

Participants

Between March and September 2011, 20 patients with early stage OA of the knee were recruited and included from the outpatient clinic of the Department of Orthopedic Surgery of Erasmus Medical Centre, Rotterdam, The Netherlands.

The inclusion criteria were: age > 18 years, duration of knee pain > 3 months, severity of knee pain > 2 out of 10 on a numeric rating scale [117, 118], and radiographic knee OA with a Kellgren and Lawrence grade of 1 or 2 [28]. Exclusion criteria were: absolute contra-indications to undergo magnetic resonance imaging (MRI), renal insufficiency (glomerular filtration rate < 60 ml/min), a history of previous reactions to contrast agent, significant co-morbidities in the lower extremity of the index knee joint, inflammatory arthritis in the index knee or knee surgery in the index knee < 1 year ago.

Written informed consent was obtained from all participants and the study was approved by the Institutional Review Board (protocol number MEC-2010-088).

MRI system and knee coil

Magnetic resonance imaging was performed on 3.0-T MRI (Discovery MR750, General Electric Healthcare, Milwaukee, WI, USA) using a custom made three-channel knee coil (Flick Engineering Solutions B.V., Winterswijk, the Netherlands) with a SNR comparable to the dedicated knee coil, which was delivered with the MRI. The design of the custom-made knee coil allowed the imaging of participants with a knee diameter > 14 cm which would not fit into the dedicated knee coil supplied by the manufacturer of the MRI system (*Figure 1*). From a previous study using identical selection criteria to ours [7], we estimated that approximately 30% of our patient population has a knee diameter > 14 cm and exclusion of these patients from our study could potentially cause a selection bias.

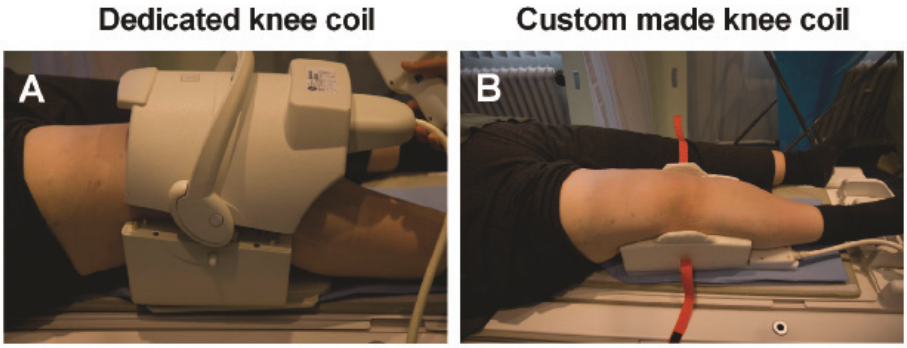

Figure 1: *Example of a patient with a knee diameter of > 14 cm who does not fit in the dedicated knee coil (A) requiring the custom-made knee coil (B)*

Study protocol

With an interval of 7 days two dGEMRIC MR images were acquired of the index knee of all participants. On both occasions, we tried to image patients at the same time of the day and asked them to not overload the index knee with sports or other activities the

day before and during the day of the examination. By doing so, we tried to minimize any possible impact of daily or sports activities on the sulphated glycosaminoglycan (sGAG) distribution in the cartilage, and hence the dGEMRIC results [119] which could negatively influence the reproducibility results. Before imaging, a double dose (0.2 mmol/kg) of gadopentetate dimeglumine (Magnevist®, Bayer Schering Ag, Berlin, Germany) was injected intravenously. After the injection, the participants were asked to cycle at a constant speed for 10 min on a home trainer to promote contrast distribution into the articular cartilage [95]. After cycling and a delay of 80 min, dGEMRIC was acquired, i.e. approximately 90 min after contrast agent injection. The participants were imaged in the supine position with the index knee fixed into the knee coil.

We used a 3D dGEMRIC protocol which was published by McKenzie et al [94] and consisted of an inversion recovery fast spoiled gradient-echo sequence with five different inversion times (TI=2100, 800, 400, 200 and 100 ms). The other MR parameters were kept constant during imaging: matrix 256 x 230 pixels; field of view 150 mm; slice thickness 3 mm; flip angle 15º; echo time 1.5 ms and repetition time 3.9 ms. The total acquisition time was approximately 14 min, resulting in 36 sagittal slices with complete coverage of the knee joint.

Region of interest selection

Using Matlab (R2007b, The MathWorks, Natick, MA, USA), four cartilage regions of interest (ROIs) were drawn manually on three consecutive slices through the lateral and medial tibiofemoral joint (central slice and one adjacent slice on each side), resulting in

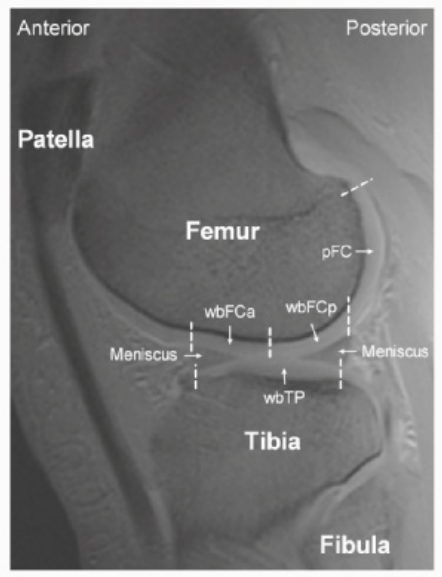

Figure 2: *Representation of the four anatomical cartilage ROIs in which the weighted mean T1 was calculated in three consecutive slices in each compartment of the tibiofemoral joint (lateral side shown in this example). wbFCa and wbFCp: anterior and posterior weight-bearing cartilage of the femoral condyle. pFC: posterior non-weight-bearing cartilage of the femoral condyle. wbTP: weight-bearing cartilage of the tibial plateau.*

three ROIs in each anatomical location for each patient. This ROI selection was based on the scheme suggested by Eckstein et al [120]. Tiderius et al [121] showed low inter- and intraobserver variability in anatomical landmark based ROI drawing independent from experience in reading MR images. Therefore, all ROIs in our study were drawn by a trained researcher with a medical degree. The anatomical landmark-based ROIs were drawn on the TI=2100 ms images of the first dGEMRIC and consisted of the anterior and posterior weight-bearing cartilage of the femoral condyles (wbFCa and wbFCp), the posterior non-weight-bearing cartilage of the femoral condyles (pFC) and the weight-bearing cartilage of the tibial plateaus (wbTP) (*Figure 2*). The mean number of voxels in each anatomical cartilage ROI was: wbFCa 112 (± 28) voxels, wbFCp 200 (± 31) voxels, pFC 135 (± 31) voxels and wbTP 192 (± 60) voxels.

To assess if the 3D dGEMRIC protocol yields T1 maps that reproducibly distinguish spatial differences in cartilage quality within a single slice, we defined two additional ROIs on 28 slices of the first dGEMRIC examination of 20 patients. These ROIs (we will refer to them as quality-based ROIs) were visually selected on the T1 maps of the cartilage in all first dGEMRIC examinations of every patient. On those maps, we identified slices with cartilage regions with a long T1 relaxation time, indicating a relatively high sGAG content and hence a relatively high cartilage quality compared with a cartilage region on the same slice with shorter T1 relaxation time which indicates a relatively low sGAG content and hence quality [65, 95, 122].

dGEMRIC analysis

During acquisition of dGEMRIC, patient motion, which may cause errors in the T1 calculation, might occur. However, such motion artifacts can be reduced by image registration and subsequent post-imaging compensations [84, 85]. Therefore, we developed an automated registration algorithm that first aligns all images with different TI values to the TI=2100 ms images within the first and second dGEMRIC separately [123]. The registration method consisted of two 3D rigid registrations (the femoral condyle and tibial plateau were registered separately) and was implemented using open source registration software (Elastix, http://elastix.isi.uu.nl/) [102]. After the first step, the algorithm automatically registers the acquisition and the reacquisition. This eliminates subjective visual slice matching between acquisition and reacquisition and also eliminates the need to manually outline the cartilage ROIs in the reacquisition

After registration, T1 maps were created and further analyzed using a T1 fitting tool developed in-house using Matlab. In all ROIs, the weighted mean T1 relaxation time per ROI was calculated, where the estimated T1 relaxation time of each voxel was weighted by the reciprocal of its uncertainty. The uncertainty was measured by the square root of the Cramér-Rao Lower Bound, which gives a lower bound for the standard deviation of the estimated T1 [96-98]. Misalignment of the T1-weighted images, especially at tissue

boundaries, results in biologically implausible values of T1, often associated with great uncertainty. Using the weighted mean, these implausible T1 values will not heavily influence the calculated mean T1 values in the determined cartilage ROIs [123].

After calculating the T1 values in the anatomical ROIs, we calculated the average T1 of the three similar anatomical cartilage ROIs. By doing so, we use the 3D information we have available instead of only using a separate slice (2D analysis) in both the medial and lateral compartment of the knee which has been done in most previous studies using dGEMRIC. After calculating the average T1 values, there were eight weighted mean T1 values of eight anatomical cartilage ROIs for each participant.

Statistical analysis

We calculated the mean of all weighted mean T1 relaxation times in each anatomical cartilage ROI in the first and second acquisitions. We also calculated the standard error of mean of all anatomical ROIs.

To assess the reproducibility of dGEMRIC in each separate anatomical cartilage ROI, we used the intraclass correlation coefficient (ICC) measuring the absolute agreement in a two-way random effect model [124]. We calculated eight ICC values for eight anatomical cartilage ROIs in the medial and lateral tibiofemoral joint. In addition to the ICC values, according to the method suggested by Bland and Altman [125], we plotted the difference between the weighted mean T1 of the first and second dGEMRIC against the mean outcome in weighted mean T1 of both images of the anatomical ROIs separately. In these plots, the 95% limits of agreement were expected to be comparable to two standard deviations [125].

Finally, to analyze whether the 3D dGEMRIC protocol is capable of yielding T1 maps that reproducibly distinguish spatial differences in cartilage quality, we subtracted the T1 relaxation time of the low cartilage quality ROI from the T1 relaxation time of the high cartilage quality ROI resulting in the difference in T1 relaxation times of the two ROIs. We did this in both the first and the second acquisitions, resulting in 28 difference measurements of which we calculated the ICC value.

We interpreted ICC values > 0.75 as good, whereas ICC values between 0.74 and 0.40 were interpreted as moderate and values < 0.40 were interpreted as poor reproducibility [87, 88, 124]. All analyses were performed using SPSS 17.0 (SPSS Inc., Chicago, IL, USA) and all P values < 0.05 were considered to be statistically significant.

RESULTS

Participants

All included participants completed both dGEMRIC examinations. The median interval between the first and second acquisitions was 7 days (range 5–14 days).

Three participants were excluded from our statistical analysis because of technical errors during the acquisition of dGEMRIC (e.g. differences in pre-imaging settings between the first and second acquisitions). Therefore, we included 17 participants (7 women and 5 left knee joints) in our data analysis. The mean age of the participants was 50 (± 10) years and their mean body mass index was 30 (± 5) kg/m^2.

dGEMRIC reproducibility

The mean T1 relaxation times in the different anatomical cartilage ROIs ranged from 458 to 574 ms with higher mean T1 values in the lateral compartment of the tibiofemoral joint (*Figure 3*). All mean T1 relaxation times of the anatomical cartilage ROIs and the associated standard error of the mean are displayed in *Table 1*. We pooled the mean and

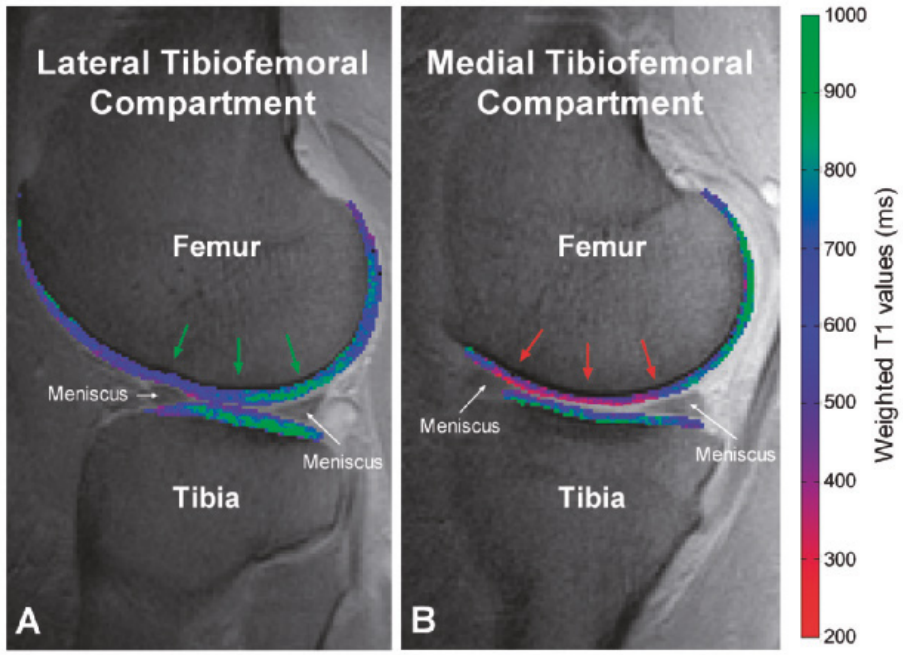

Figure 3: *Sagittal central slices through the lateral (A) and medial (B) tibiofemoral compartment of an early stage medial OA knee. The T1 color map of the cartilage clearly shows lower T1 values (red arrows in B), indicating relatively lower sGAG content in the weight-bearing femoral cartilage in the medial compartment compared to the relatively higher T1 values (green arrows in A) in the same cartilage region in the lateral knee compartment.*

Cartilage ROI	Mean T1 (S.E. mean)	ICC (95% CI)
Medial tibiofemoral compartment		
Anterior weight-bearing femoral	458 (17) ms	0.87 (0.69–0.95)
Posterior weight-bearing femoral	475 (17) ms	0.91 (0.78–0.97)
Posterior femoral	492 (22) ms	0.88 (0.69–0.96)
Weight-bearing tibia	489 (18) ms	0.90 (0.74–0.96)
Lateral tibiofemoral compartment		
Anterior weight-bearing femoral	490 (14) ms	0.87 (0.68–0.95)
Posterior weight-bearing femoral	542 (14) ms	0.88 (0.70–0.96)
Posterior femoral	477 (16) ms	0.95 (0.85–0.98)
Weight-bearing tibia	574 (19) ms	0.91 (0.76–0.97)

Table 1: *Mean T1 relaxation times in milliseconds, standard error of the mean in milliseconds and ICC value for reproducibility between the first and second dGEMRIC in each anatomical cartilage ROI (n=17 for each ROI). S.E. mean: standard error of the mean. ICC: intraclass correlation coefficient. 95% CI: 95% confidence interval*

the standard error of the means of the first and the second MR examination, since those values were equal in all anatomical ROIs.

The reproducibility of dGEMRIC in the different anatomical cartilage ROIs, in terms of the ICC values together with the 95% confidence intervals (95% CI), are shown in *Table 1*. The reproducibility was good in all anatomical cartilage ROIs (n=17 for each ROI), as all ICC values were > 0.75 [124]. No large differences in ICC values were observed among the different anatomical ROIs. Scatter plots of weighted mean T1 values in acquisitions and reacquisitions are shown in *Figure 4*. In these plots, the range of observed T1 values was 300 to 750 ms in the cartilage.

In agreement with the ICC values, the Bland–Altman plots of the different anatomical cartilage ROIs suggest the good reproducibility of dGEMRIC (*Figure 5*). In addition, based on the 95% limits of agreement of the Bland–Altman plots, we defined a threshold of 95 ms to determine whether a change in dGEMRIC outcome is statistically significant or not.

The capability of the 3D dGEMRIC protocol to yield T1 maps that reproducibly distinguish spatial differences in cartilage quality within a single slice (n=25 because 3 patients with three difference measurements were excluded from the analysis) was also considered good (ICC 0.79, 95% CI 0.57–0.90). A scatter plot of the difference measurements is shown in *Figure 6*.

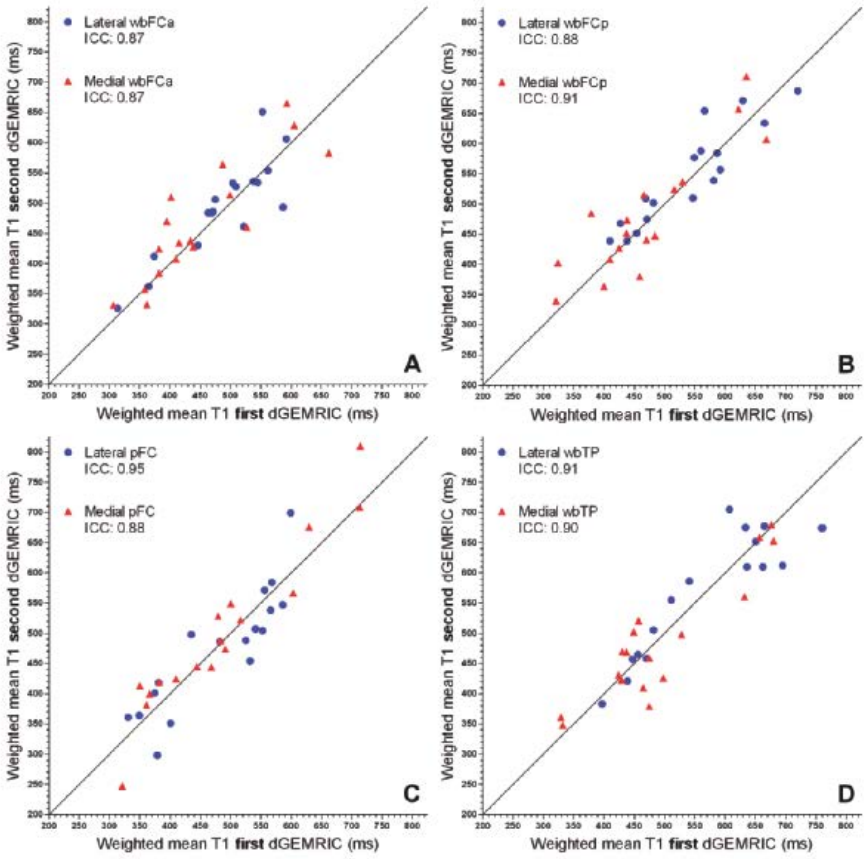

Figure 4: *Scatter plots of the first and second dGEMRIC of all patients. Every anatomical cartilage region (n=17) is represented by a blue dot (lateral) or red triangle (medial), depending on the location in the tibiofemoral joint. A: anterior weight-bearing cartilage of the femoral condyle. B: posterior weight-bearing cartilage of the femoral condyle. C: posterior non-weight-bearing cartilage of the femoral condyle. D: weight-bearing cartilage of the tibial plateau. The black line represents the relation x=y (perfect reproducibility). ICC: intraclass correlation coefficient.*

DISCUSSION

Reproducible outcome measures to follow cartilage quality non-invasively over time in longitudinal studies are important in OA research, as they might enhance understanding of the pathogenesis of (early stage) OA. Furthermore, accurate, objective and reproducible imaging techniques are essential to develop and monitor disease-modifying OA drugs and other novel OA therapies.

The first aim of the present study was to assess the reproducibility of dGEMRIC using a 3D sequence on 3.0-T MRI equipment in patients with early stage knee OA. The results of our study demonstrate that the reproducibility of individual anatomical cartilage

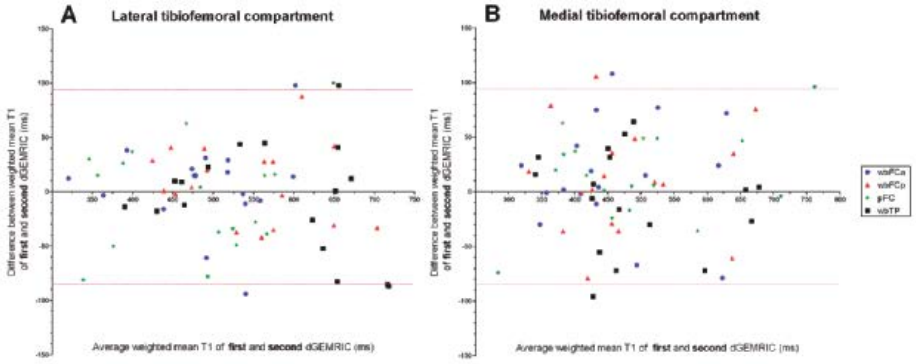

Figure 5: *Bland–Altman plots of the difference in the weighted mean T1 values between the first and second dGEMRIC plotted against the weighted mean T1 values of both acquisitions in each separate anatomical ROI in the lateral (A) and medial (B) tibiofemoral compartment (n=17 participants x 8 ROIs for each participant = 136). The red lines indicate the 95% limits of agreement of the anatomical cartilage ROIs. wbFCa (blue dots) and wbFCp (red triangles): anterior and posterior weight-bearing cartilage of the femoral condyle. pFC (green stars): posterior non-weight-bearing cartilage of the femoral condyle. wbTP (black squares): weight-bearing cartilage of the tibial plateau*

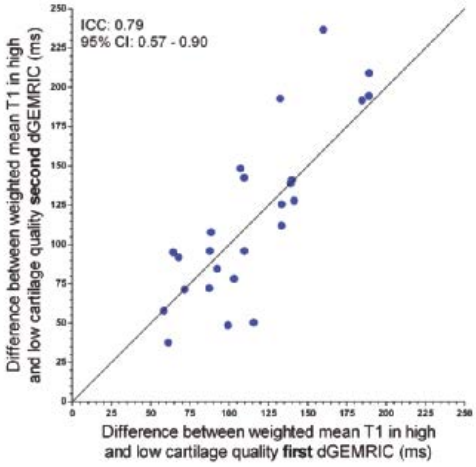

Figure 6: *Scatter plot of the difference measurements between weighted mean T1 in adherent cartilage with relatively high and low quality cartilage within one slice in the first and second dGEMRIC (n=25). Every difference measurement is represented by a blue dot. The black line represents the relation x=y (perfect reproducibility). ICC: intraclass correlation coefficient, 95% CI: 95% confidence interval*

ROIs is good, regardless of the anatomical location within the knee joint (*Table 1*). The Bland–Altman plot of the anatomical cartilage ROIs (*Figure 5*) agrees with the calculated ICC values in the anatomical ROIs. However, the 95% limits of agreement indicate a relatively large variation between the first MR acquisition and reacquisition in the anatomical cartilage ROIs. This is also revealed by the relatively large standard error of the mean in all ROIs (*Table 1*) indicating a relatively large variation in the calculated weighted mean T1 values within a single MR examination, but also between the first and second dGEMRIC.

Our reproducibility results in terms of ICC values are similar to those of previous studies assessing the reproducibility of 2D and 3D dGEMRIC in healthy volunteers and patients with an ACLT [87, 88, 115]. As this is the first study assessing the reproducibility of dGEMRIC in OA, we aimed to investigate whether the impaired cartilage quality, including loss of sGAG, in early OA [56, 116] causes less reproducible results in comparison to studies conducted in healthy volunteers or patients with an ACLT without radiographical signs of OA [87, 88, 115]. The use of an automated image registration method, which allowed us to analyze exactly the same voxels on the same slice in the first and the second acquisitions, might have been beneficial to the ICC values we observed in our study. It solves the issue of visual slice and ROI selection, which could have a negative influence on the reproducibility [88].

The second aim of our study was to analyze the capability of the 3D dGEMRIC protocol to yield T1 maps that distinguish spatial differences in cartilage quality within a single slice. This ability is important for longitudinal non-invasive follow-up measurement for (surgical) techniques to treat (focal) cartilage defects (e.g. microfracturing and autologous chondrocyte implantation [14, 126]). The T1 maps generated revealed reproducible spatial differences in cartilage quality (ICC value of 0.79 with a 95% CI ranging from 0.57 to 0.90). This ICC is lower than the anatomical ROIs (*Table 1*) and might be caused by using relatively small ROIs (mean number of voxels 115) compared with the anatomical cartilage ROIs (mean number of voxels 180). An outlier in the weighted mean T1 of one pixel in such an ROI might have a relatively large negative impact on the ICC value.

The clinical significance of this work is that, to our knowledge, this is the first study, which assesses the reproducibility of 3D dGEMRIC in early stage OA knees. Compared with previous research [87, 88], we used a higher field strength MR system and an automated registration method to analyze the dGEMRIC [123]. In addition, our study population (n=17) is two to three times larger than the populations of previous studies on dGEMRIC reproducibility. Based on the Bland–Altman plots, we determined a change of 95 ms in the weighted mean T1 relaxation time as a threshold to define a significant change in dGEMRIC outcome if a single person is followed over time in future studies, e.g. treatment efficacy studies, using our study protocol. Because of the differences in the dGEMRIC protocols, MRI equipment and post processing algorithms compared with other groups using dGEMRIC, we think that our threshold might not be generalizable to other centers. Therefore, we recommend that every group should calculate a threshold value as presented in this study for their own setup (dGEMRIC protocol, MRI system, etc.). We believe that establishing such a threshold value is absolutely essential in every longitudinal quantitative study, regardless of it being specific to the actual setup.

Despite the promising results, this study also has some limitations. We used a custom-built knee coil to enable imaging of knees with a diameter > 14 cm. However, because of the open design, the SNR in the patellar cartilage region was insufficient. This may

have influenced the outcomes of the dGEMRIC analysis in the patellar cartilage and therefore, we decided not to analyze the patellar cartilage in our study. Another limitation may be that we only analyzed the reproducibility of dGEMRIC in full thickness cartilage ROIs. This is contrary to Multanen et al [87], who described the reproducibility of dGEMRIC for each different zone (superficial, middle and deep) of the articular cartilage. However, because of the relatively low in-plane spatial resolution of the MR images in this study, we decided to analyze full thickness ROIs only.

Future research should focus on developing a pulse sequence for dGEMRIC with a higher in-plane resolution. Using such a sequence could enable an accurate visualization and ROI selection of different zones within the cartilage as suggested recently [127]. Other future research should focus on developing an automated segmentation algorithm for articular cartilage. Combining such an auto-segmentation algorithm with an automated post processing pipeline, will enable analysis of all slices of the dGEMRIC procedure within a limited time instead of the laborious and time-consuming process of slice and ROI selection by hand.

In conclusion, the results of the present study show that in patients with early stage OA, 3D dGEMRIC of the knee at 3.0 T combined with 3D image registration is a highly reproducible measure of articular cartilage quality in anatomical ROIs. The technique also yields T1 maps that reproducibly distinguish spatial differences in cartilage quality over time. Finally, we defined a threshold of 95 ms to determine a significant change in dGEMRIC outcome if a single person is followed over time in future studies using our study protocol. Therefore, dGEMRIC may be a valuable tool to non-invasively evaluate cartilage quality changes in longitudinal research in patients with early stage OA and focal cartilage defects.

Validation and comparison of dGEMRIC and T1rho-mapping as imaging biomarker in human osteoarthritis research

1.2

Chapter 4

Is T1rho-mapping an alternative to delayed gadolinium-enhanced MRI of cartilage (dGEMRIC) in assessing sulphated glycosaminoglycan content in human osteoarthritic knees? An in vivo validation study

J. van Tiel, G. Kotek, M. Reijman, P.K. Bos, E.E. Bron,
S. Klein, K. Nasserinejad, G.J. van Osch,
J.A. Verhaar, G.P. Krestin, H. Weinans, E.H. Oei.

Radiology. 2015. Accepted for publication

ABSTRACT

Introduction

T1rho-mapping has been proposed as a non-contrast-enhanced alternative to delayed gadolinium-enhanced MRI of cartilage (dGEMRIC) to quantify cartilage sulphated glycosaminoglycan (sGAG) content. However, no thorough validation studies have been performed that compare both imaging biomarkers within the same osteoarthritis (OA) patients using reference standards for cartilage composition. We assessed if T1rho-mapping can be used as an alternative to dGEMRIC for quantifying cartilage biochemical composition *in vivo* in human OA knees

Materials and Methods

Institutional review board study approval and written informed consent from participants was obtained. Twelve knee OA patients underwent dGEMRIC and T1rho-mapping at 3T before total knee replacement (TKR). Outcomes of dGEMRIC and T1rho-mapping were calculated in 6 cartilage regions of interest (ROI). Femoral and tibial cartilage were harvested during TKR. Cartilage sGAG and collagen content were assessed with dimethylmethylene blue and hydroxyproline assays, respectively. DGEMRIC and T1rho-mapping were correlated with cartilage sGAG and collagen content.

Results

dGEMRIC T1 relaxation times correlated strongly with cartilage sGAG (r=0.73, 95% confidence interval (95%CI) 0.60-0.83) and weakly with cartilage collagen content (r=0.40, 95%CI 0.18-0.58). T1rho relaxation times did not correlate with cartilage sGAG (r=0.04, 95%CI -0.21-0.28), nor with cartilage collagen content (r=-0.05, 95%CI -0.31-0.20).

Conclusion

dGEMRIC can accurately measure cartilage sGAG content *in vivo* in human knee OA subjects whereas T1rho-mapping appears not suitable for this purpose. Although the technique is not completely sGAG specific and requires a contrast agent, dGEMRIC is a validated and robust method for quantifying cartilage sGAG content in human OA subjects in clinical research.

INTRODUCTION

Knee osteoarthritis (OA) is the most common joint disease in middle-aged and elderly, causing serious morbidity and large socio-economic impact [8]. Since no definitive treatment options other than joint replacement surgery in end stage OA are available, research mainly focuses on novel interventions such as disease-modifying OA drugs. These should be effective in the early stages of OA by modifying the course of the disease, for example by improving cartilage biochemical composition [13, 128]. To monitor the structural effectiveness of such novel interventions in early OA, accurate *in vivo* imaging biomarkers are essential. Therefore, quantitative biomarkers that measure cartilage biochemical composites, e.g. sulphated glycosaminoglycan (sGAG) content, have become of interest during the last decade [129].

An example of such a quantitative imaging biomarker to measure articular cartilage sGAG content is delayed gadolinium-enhanced MRI of cartilage (dGEMRIC) [65]. This technique utilizes the inverse relation between the amount of sGAG in cartilage and an intravenously administered negatively charged contrast agent. Although dGEMRIC is an established imaging biomarker for quantitative imaging of articular cartilage, the technique has disadvantages. These are mainly related to the contrast administration that increases costs and is potentially harmful for patients with impaired renal function, and the long delay between contrast administration and MR acquisition. Because of these drawbacks, T1rho-mapping was suggested as a non-contrast-enhanced alternative to dGEMRIC to measure cartilage sGAG content [128-130]. T1rho-mapping quantifies the spin relaxation in the rotating frame by using a constant radiofrequency field referred to as a "spin lock" pulse to change relaxation rates of water associated with large macromolecules in cartilage such as sGAG [131, 132].

Although both dGEMRIC and T1rho-mapping are increasingly used as outcome measures for cartilage biochemical composition in clinical OA research, they have been validated mainly *in vitro* [67, 68] or *ex vivo* [133, 134] using bovine and cadaveric human cartilage. *In vivo* validation was performed in only one study for dGEMRIC [91] and only two studies for T1rho-mapping [69, 90]. Besides, no study applied both imaging biomarkers in humans *in vivo* and compared the outcomes with a reference standard for cartilage sGAG content to validate and compare their performance. Finally, the influence of the cartilage extracellular matrix integrity, mainly provided by the collagen network, has not yet been studied in detail for dGEMRIC and T1rho-mapping.

The aim of this study was to assess if T1rho-mapping can be used as an alternative to dGEMRIC for quantifying cartilage biochemical composition *in vivo* in human OA knees.

MATERIALS AND METHODS

Study design and participants

For this prospective observational study, conducted between October 2012 and December 2013, all consecutive patients scheduled for total knee replacement (TKR) at our institution were approached.

The inclusion criteria were: age ≥ 18 years and radiographic knee OA with asymmetric distribution and a maximum of grade 1-2 (doubtful or definite osteophyte formation without definite joint space narrowing) according to Kellgren & Lawrence (KL) grading [28] in the least affected tibiofemoral compartment. Exclusion criteria were: renal insufficiency (glomerular filtration rate < 60 ml/min), history of previous reactions to contrast agent, or significant co-morbidities in the ipsilateral lower extremity (e.g. severe hip OA, neurologic or muscular diseases causing hip or knee disability), which prohibit exercising after contrast administration for dGEMRIC.

The study was approved by the Medical Ethical Committee of Erasmus MC (MEC-2012-218) and written informed consent was obtained from all participants

MRI acquisition

One day before TKR, MRI was performed using a 3.0 Tesla MRI scanner (Discovery MR750, General Electric Healthcare, Milwaukee, USA) using a dedicated 8-channel knee coil (Invivo Inc., Gainesville, USA).

The MRI protocol included the following three pulse sequences, all acquired in the sagittal plane (specific imaging parameters shown in *Table 1*): (I) a 3D high resolution fat-saturated spoiled gradient-echo (SPGR) sequence, (II) a 3D fast spin-echo (FSE) T1rho-mapping sequence with five different spin lock times (TSL) [135] and (III) a 3D inversion recovery (IR) non-fat-saturated SPGR sequence with five different inversion times (TI) for dGEMRIC [94].

Before dGEMRIC acquisition, a double dose (0.2 mmol per kg body weight) of gadopentetate dimeglumine (Magnevist®, Bayer Schering AG, Berlin, Germany) was injected intravenously as advocated previously [122]. Subsequently, participants cycled for 10 minutes on a home trainer at constant speed to promote contrast distribution into and throughout the knee. After a delay of 90 minutes, the IR SPGR sequence was acquired [95].

MRI analysis

Using Matlab (R2011a, The MathWorks, Natick, MA, USA), three cartilage regions of interest (ROIs) in both tibiofemoral compartments were drawn: weight-bearing cartilage of the femoral condyles (wbFC), posterior non weight-bearing cartilage of the femoral condyles (pFC) and weight-bearing cartilage of the tibial plateaus (wbTP) (*Figure 1*). All ROIs consisted of 15 consecutive slices: the most central slice through the medial or

Sequence	High resolution SPGR	T1rho-mapping	dGEMRIC
Plane	Sagittal	Sagittal	Sagittal
Imaging mode	3D	3D	3D
Sequence	SPGR	FSE	IR SPGR
Matrix (frequency)	512	288	288
Matrix (phase)	512	192	192
Number of slices	108	36	36
FOV (mm)	150	150	150
Slice thickness (mm)	1.0	3.0	3.0
TSL (ms)	NA	1 / 16 / 32 / 64 / 125	NA
FSL (Hz)	NA	500	NA
TI (ms)	NA	NA	2100 / 800 / 400 / 200 / 100
Flip angle (°)	12	90	15
Bandwidth (Hz/pixel)	122	244	244
Number excitations averaged	0.75	0.5	1
Fat saturated	Yes	Yes	No
Acquisition time (min)	05:37	05:43	14:18

Table 1: *MRI protocol parameters. FOV: field of view; FSE: fast spin-echo; FSL: spin lock frequency; IR SPGR: inversion recovery spoiled gradient-echo; NA: not applicable; SPGR: spoiled gradient-echo; TI: inversion time; TSL: spin lock time*

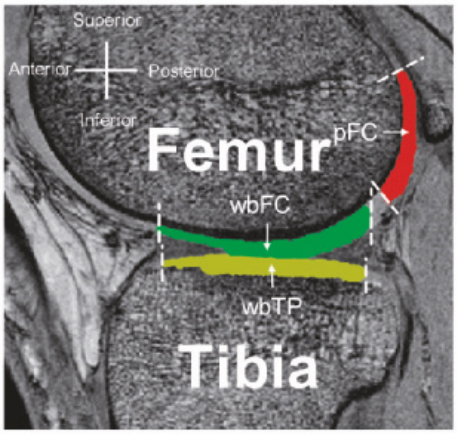

Figure 1: *Representation of the three anatomical cartilage ROIs in which outcomes of dGEMRIC and T1rho-mapping were calculated in 15 consecutive slices in each compartment of the tibiofemoral joint (lateral side shown in this example). The posterior non-weight-bearing cartilage of the femoral condyle (pFC) is shown in red, the weight-bearing cartilage of the femoral condyle (wbFC) is shown in green and the weight-bearing cartilage of the tibial plateaus (wbTP) is shown in yellow.*

lateral tibiofemoral compartment (defined as the sagittal section depicting the most caudal point of the femoral condyle identified on multiplanar reconstructions of the 3D high resolution fat-saturated SPGR sequence) along with the neighboring seven slices medially and laterally. All ROIs were drawn on the high resolution SPGR images by a researcher with a medical degree and 4 years' experience in musculoskeletal research (JvT).

Image analysis was performed with Software for Post processing And Registration of Cartilage of the Knee [123, 136]. The image analysis pipeline included registration to correct for patient motion and performed fitting of dGEMRIC post-contrast T1 ($T1_{GD}$) and T1rho relaxation times. First, all images of the T1rho-mapping and dGEMRIC sequence with different TSL and TI values were registered to the TSL=1 ms and TI=2100 ms images. The femoral condyle and tibial plateau were registered separately. The images were registered using a 3D rigid transformation model by maximization of localized mutual information [103]. To minimize the blurring of the registered images, cubic interpolation was used. All registrations were performed using open source registration software (Elastix, http://elastix.isi.uu.nl/) [144102]. Second, both registered T1rho-mapping and dGEMRIC datasets were registered to the high resolution SPGR images. This registration was based on the TSL=1 ms and TI=2100 ms images; the other TSL and TI images were transformed accordingly. This second registration step allows analyzing matching cartilage ROIs on matching slices in both sequences.

After registration, T1rho- and dGEMRIC $T1_{GD}$ maps were estimated using a maximum likelihood fit. Before fitting, partial volume voxels for cortical bone within the cartilage ROIs were excluded by using a threshold. Next, weighted T1rho and $T1_{GD}$ relaxation times were calculated using the reciprocal of the uncertainty of the estimated T1rho and $T1_{GD}$ relaxation time in each voxel [123]. This uncertainty was measured by the square root of the Cramér-Rao Lower Bound, which gives a lower bound for the standard deviation of the estimated T1rho or $T1_{GD}$ [96-98]. If after registration T1rho- and $T1_{GD}$-weighted images are not yet perfectly aligned, this might result in implausible T1rho and $T1_{GD}$ relaxation times especially at tissue boundaries. Using the weighted mean, these implausible T1rho and $T1_{GD}$ relaxation times will not heavily influence the results of the analyses [123]. Finally, as proposed by Tiderius *et al.*, $T1_{GD}$ relaxation times were corrected for the participants' body mass index (BMI) [137].

The weighted T1rho and $T1_{GD}$ relaxation times for each anatomical cartilage ROI were averaged over the 15 consecutive MR images. Thus, for each patient six mean T1rho and $T1_{GD}$ relaxation times from six cartilage ROIs were obtained.

Harvesting of cartilage and biochemical cartilage analyses

During TKR, weight-bearing and non-weight-bearing femoral cartilage and weight-bearing tibial cartilage were harvested and stored in saline for 30 minutes to one hour before further processing in the laboratory. Depending on size of the specimen, four (posterior femoral cartilage), six or eight (weight-bearing femoral and plateau cartilage, number of explants depending on specimen size) full thickness cartilage explants of 6 mm diameter were taken using a biopsy punch, corresponding with cartilage of the ROIs analyzed with dGEMRIC and T1rho-mapping. All explants were cut in halves and stored separately in airtight tubes at -20 °C.

Before biochemical analysis, explants were thawed at room temperature. One half was digested in a papain solution overnight and used to quantify sGAG content with the dimethylmethylene blue (DMMB) assay as described by Farndale *et al.* [138]. The other half of each explant was not digested and used to quantify collagen content based on the hydroxyproline content as described by Bank *et al.* [139]. This assay quantifies the degraded as well as the intact collagen content. The outcomes of both measures were summed together resulting in the total collagen content per explant. For each cartilage ROI, the mean sGAG or collagen content was calculated by adding up the sGAG or collagen content of each explant analyzed and dividing this by the numbers of explants taken from that specific ROI.

Statistical analysis

To assess the correlation between $T1_{GD}$ and T1rho relaxation times and the reference tests (sGAG and collagen content) simultaneously, a multivariate mixed-effects model was applied. To take into account the potential intrinsic correlation between outcomes of different anatomical ROIs within one participant, a random intercept was included in the model. The Pearson's correlation coefficient of dGEMRIC or T1rho-mapping and each reference test were extracted from the results of this model. The analysis was performed using a Bayesian approach with Markov chain Monte Carlo (McMC) sampling using WinBugs [140]. For all Pearson's correlation coefficients the 95% confidence interval (95%CI) were calculated via McMC samples. All p-values < 0.05 were considered to be statistically significant.

RESULTS

Participants

Fourteen patients participated in the study. Two participants were excluded because their TKR was postponed after inclusion. Therefore, 12 participants (6 women and 6 left knee joints) were analyzed. In one participant T1rho-mapping data were unavailable since its acquisition failed. Three cartilage specimens (one posterior non weight-bearing cartilage specimen of the lateral femoral condyle and two weight-bearing cartilage specimens of the medial tibial plateau) were severely damaged during surgery and were excluded from the analysis. Mean age of the participants was 64 (standard deviation ± 6) years and their mean body mass index was 33 (± 6) kg/m^2. The KL grades in the medial tibiofemoral compartments were 3 or 4 in 7 participants and 1 or 2 in 4 participants. The KL grades in the lateral tibiofemoral compartments were 1 or 2 in 9 participants and 3 in 2 participants.

Correlation of dGEMRIC and T1rho-mapping with biochemical cartilage analyses

$T1_{GD}$ relaxation times for all femoral and tibial cartilage ROIs correlated strongly with cartilage sGAG content measured using the DMMB assay (n=69, r=0.73, 95% confidence interval (95%CI) 0.60 to 0.83; *Figure 2A*) and weakly with cartilage collagen content measured using the hydroxyproline assay (n=69, r=0.40, 95%CI 0.18 to 0.58; *Figure 2B*). When each ROI was analyzed separately, the correlation coefficients between outcomes of dGEMRIC and sGAG content ranged from 0.70 to 0.80. For the correlation between dGEMRIC and collagen content, the range of correlation coefficients was 0.30 to 0.49.

T1rho relaxation times for all femoral and tibial cartilage ROIs did neither correlate with cartilage sGAG content (n=63, r=0.04, 95%CI -0.21 to 0.28; *Figure 3A*), nor with cartilage collagen content (n=63, r=-0.05, 95%CI -0.31 to 0.20; *Figure 3B*). A range of -0.07 to 0.06 was observed for the correlation coefficients between T1rho relaxation

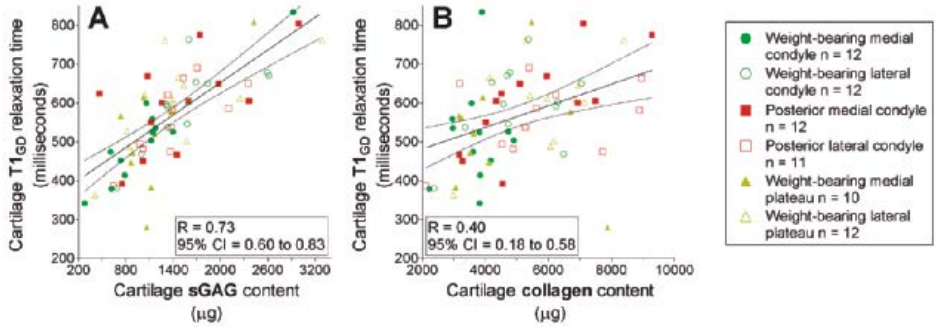

Figure 2: *Correlation plots of mean $T1_{GD}$ relaxation times in all anatomical ROIs with sGAG content of the cartilage measured and DMMB assay (A) and outcomes of dGEMRIC and collagen content of the cartilage measured with hydroxyproline assay (B). The dashed lines indicate the 95% confidence interval of the Pearson's correlation coefficient.*

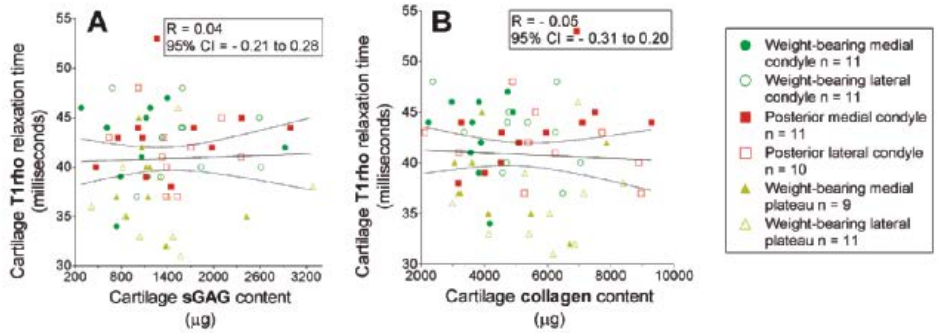

Figure 3: *Correlation plots of mean T1rho relaxation times in all anatomical ROIs with sGAG content of the cartilage measured and DMMB assay (A) and outcomes of T1rho-mapping and collagen content of the cartilage measured with hydroxyproline assay (B). The dashed lines indicate the 95% confidence interval of the Pearson's correlation coefficient.*

times and sGAG content for all separate cartilage ROIs in both knee compartments. This range was -0.18 to 0.10 for the correlation between T1rho-mapping and collagen content.

Figure 4 shows images representative for cartilage with relatively high and low sGAG content measured using dGEMRIC, T1rho-mapping, equilibrium partitioning of an ionic contrast agent using micro-CT (EPIC-µCT: visual representation of sGAG content) and histology (visual representation of sGAG content using Safranin-O staining). These images confirm the strong correlation between dGEMRIC and cartilage sGAG.

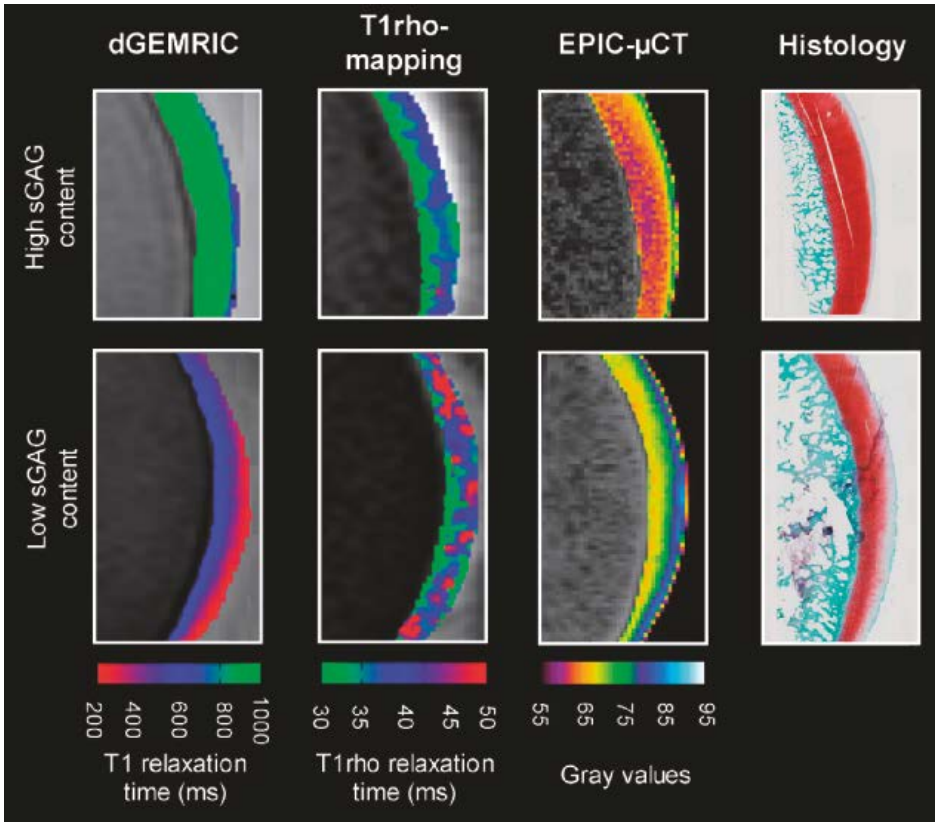

Figure 4: *Spatial agreement between MRI, EPIC-µCT and histology. Representative images of matching sagittal slides of dGEMRIC and T1rho-mapping, EPIC-µCT and histology. The relaxation time and/or attenuation of cartilage are visualized in color and representative for sGAG content. In dGEMRIC high $T1_{GD}$ represent high sGAG content and low $T1_{GD}$ represent low sGAG content. In T1rho mapping the opposite is true for T1rho relaxation times. In EPIC-µCT high attenuation represents a low sGAG content of cartilage and a low attenuation represents high sGAG content. The intensity of the sGAG staining in histology is representative for sGAG content. A high intensity represents high sGAG content and a low intensity or discoloration represents a low or absent sGAG content. The top row shows visual agreement for dGEMRIC and disagreement for T1rho-mapping in relative high cartilage sGAG content and the bottom row shows the same for a relative low cartilage sGAG content in the superficial and partially mid zone of the cartilage. Visual slice matching was performed for the histological slices.*

DISCUSSION

Quantitative imaging biomarkers that measure cartilage biochemical composition non-invasively are needed for development and monitoring of new treatments for osteoarthritis. For this purpose, dGEMRIC is increasingly used to measure cartilage sGAG content, but the technique has drawbacks related to the use of a contrast agent. Therefore, T1rho-mapping was proposed as a non-contrast-enhanced alternative. Since, to our knowledge, a thorough *in vivo* comparison and validation study was lacking, our aim was to assess if T1rho-mapping can be used as an alternative to dGEMRIC for quantifying cartilage biochemical composition *in vivo* in human OA knees.

Our results showed that outcomes of *in vivo* dGEMRIC in OA patients correlated strongly with cartilage sGAG content measured using the DMMB assay. This indicates that dGEMRIC acquired *in vivo* accurately measures sGAG content in OA patients. These results are consistent with previous research showing a strong correlation between $T1_{GD}$ relaxation times acquired *in vitro* and ex *vivo* in cadaveric animal cartilage post microfracture treatment and human OA cartilage [65, 141]. The results are also in agreement with the only *in vivo* validation study of dGEMRIC performed by Watanabe *et al*. in 2006 reporting a strong correlation (r=0.82) between outcomes of dGEMRIC after treatment of focal cartilage defects and cartilage sGAG content measured using high-performance liquid chromatography in nine cartilage explants [91].

We found a weak correlation between outcomes of dGEMRIC and the amount of collagen in the articular cartilage (correlation with intact collagen content measured using the hydroxyproline assay was comparable, no correlation between dGEMRIC and degraded collagen content: data not shown). Despite the weak correlation, this finding suggests that in addition to sGAG content, the integrity of cartilage extracellular matrix also influences contrast influx into cartilage. Therefore, dGEMRIC outcomes appear not only dependent on sGAG content, which was recently also suggested by others [142, 143]. The difference between the strength in correlation between the outcomes of dGEMRIC and cartilage sGAG and collagen content, however, suggests that sGAG is the composite that influences contrast distribution throughout articular cartilage most.

We did not observe any correlation between T1rho relaxation times and cartilage sGAG content. These results are surprising when compared to previous *in vitro* and *ex vivo* research in which T1rho relaxation times correlated moderately to strongly with sGAG amount in bovine and human cartilage [68, 69]. Our results, however, are more consistent with one of the two previous *in vivo* validation studies of T1rho-mapping which showed only a weak correlation (r=0.44) between T1rho relaxation times and sGAG content in the lateral tibial plateau cartilage of 20 OA patients [90]. A possible explanation for the difference in strength of reported correlation values between *in vivo* and *in vitro* or *ex vivo* acquired T1rho-mapping and cartilage sGAG content may be

the differences in specific acquisition parameters. For example, number and duration of TSLs, field of view and in-plane image matrix are usually different for *in vitro* or *ex vivo* [67, 68, 133] compared to *in vivo* experiments [69, 90, 131]. Optimizing these parameters might improve the ability of T1rho-mapping to assess cartilage sGAG content, but will likely increase acquisition time. Moreover, the spin lock frequency (FSL) was usually higher *in vitro* or *ex vivo* [67, 132] compared to *in vivo* [69, 90]. Higher FSL causes less B0 inhomogeneity, possibly improving accuracy of T1rho-mapping, but increased FSL is a limiting factor *in vivo* since it induces higher specific absorption rate [129]. T1rho-mapping acquired with an FSL higher than 500 Hz has been described to be safe [132], but we applied a 500 Hz FSL since this is most commonly used *in vivo*, enabling us to compare our results with previous literature. Another option to improve T1rho-mapping would be to acquire a B0 map to correct for B0 inhomogeneity. Thus, different results may be obtained if the acquisition is optimized in future research.

T1rho relaxation times also did not correlate with cartilage collagen content (also no correlation with intact and degraded collagen content measured using the hydroxyproline assay: data not shown). While this finding is consistent with previous research in human cartilage after TKR [134], it suggests that T1rho-mapping measures other elements of cartilage, e.g. water content or a combination of composites of the cartilage extracellular matrix.

The results of our study suggest that, despite the need of contrast agent and relatively long delay between contrast administration and MR acquisition, dGEMRIC can still be regarded a good method to quantify cartilage sGAG content in human knee OA. T1rho-mapping appears less suitable for this purpose. However, because of its ability to discriminate between healthy subjects, mild and moderate OA patients [89], relatively short acquisition time and the fact that T1rho-mapping does not require a contrast agent, it may still be a valuable imaging biomarker in large clinical or population based OA research studies.

A potential drawback of our study is the use of OA patients undergoing TKR, whereas dGEMRIC and T1rho-mapping are advocated as imaging biomarkers in early stage OA [13, 128]. However, in our opinion this is the only human study population that allows comparison of *in vivo* acquired imaging biomarkers against *ex vivo* references standards performed on cartilage specimens. To minimize the potential of bias we included patients with asymmetrical radiographic OA distribution who nevertheless were indicated for TKR. This way we ended up analyzing cartilage with a relatively wide range in quality and sGAG content.

Furthermore, it is important to note that the dGEMRIC sequence we used consisted of an IR SPGR protocol, while dGEMRIC can also be acquired using IR FSE or gradient echo sequences with variable flip angles or a Look-Locker method [129]. Likewise, our T1rho-mapping protocol consisted of a 3D FSE pulse sequence while others may have

used different approaches. Therefore, our results may not be directly generalizable to other research institutes applying other acquisition protocols for dGEMRIC and T1rho-mapping. However, the $T1_{GD}$ and T1rho relaxation times obtained in our study are within the same range as those reported by others using different dGEMRIC and T1rho-mapping protocols at 3.0 T [129]. Future research may compare the outcomes of different protocols for dGEMRIC and T1rho-mapping in patients with knee OA. Such studies may also compare dGEMRIC and T1rho-mapping with other recently introduced biomarkers to measure cartilage sGAG content, e.g. gagCEST or sodium MRI [129].

In conclusion, our results show that dGEMRIC can accurately measure cartilage sGAG content *in vivo* in human knee OA subjects whereas T1rho-mapping appears not suitable for this purpose. Although the technique is not completely sGAG specific and requires a contrast agent, dGEMRIC is a validated and robust method for quantifying cartilage sGAG content in human OA subjects in clinical research.

Application of dGEMRIC in clinical osteoarthritis research

1.3

Chapter 4

Delayed gadolinium-enhanced MRI of cartilage (dGEMRIC) shows no change in cartilage structural composition after viscosupplementation in patients with early stage knee osteoarthritis

J. van Tiel, M. Reijman, P.K. Bos, J. Hermans, G.M. van Buul, E.E. Bron, S. Klein, J.A. Verhaar, G.P. Krestin, S.M. Bierma - Zeinstra, H. Weinans, G. Kotek, E.H. Oei.

PLoS One. 2013 Nov;8(11):e79785.

ABSTRACT

Introduction

Viscosupplementation with hyaluronic acid (HA) of osteoarthritic (OA) knee joints has a well-established positive effect on clinical symptoms. This effect, however, is only temporary and the working mechanism of HA injections is not clear. It was suggested that HA might have disease-modifying properties because of its beneficial effect on cartilage sulphated glycosaminoglycan (sGAG) content. Delayed gadolinium-enhanced MRI of cartilage (dGEMRIC) is a highly reproducible, non-invasive surrogate measure for sGAG content and hence composition of cartilage. The aim of this study was to assess whether improvement in cartilage structural composition is detected using dGEMRIC 14 weeks after 3 weekly injections with HA in patients with early stage knee OA.

Materials and Methods

In 20 early stage knee OA patients (KLG I-II), 3D dGEMRIC at 3T was acquired before and 14 weeks after 3 weekly injections with HA. To evaluate patient symptoms, the knee injury and osteoarthritis outcome score (KOOS) and a numeric rating scale (NRS) for pain were recorded. To evaluate cartilage composition, six cartilage regions in the knee were analyzed on dGEMRIC. Outcomes of dGEMRIC, KOOS and NRS before and after HA were compared using paired *t*-testing. Since we performed multiple *t*-tests, we applied a Bonferroni-Holm correction to determine statistical significance for these analyses.

Results

All KOOS subscales ('pain', 'symptoms', 'daily activities', 'sports' and 'quality of life') and the NRS pain improved significantly 14 weeks after viscosupplementation with HA. Outcomes of dGEMRIC did not change significantly after HA compared to baseline in any of the cartilage regions analyzed in the knee.

Conclusion

Our results confirm previous findings reported in the literature, showing persisting improvement in symptomatic outcome measures in early stage knee OA patients 14 weeks after viscosupplementation. Outcomes of dGEMRIC, however, did not change after viscosupplementation, indicating no change in cartilage structural composition as an explanation for the improvement of clinical symptoms.

INTRODUCTION

Knee osteoarthritis (OA) is the most common joint disease in middle-aged and elderly, causing serious morbidity and large socio-economic impact [7, 108, 109]. The current treatment strategies for OA, however, are limited and end-stage OA is treated with invasive joint replacement surgery. An important drawback of this surgery is the limited durability of joint prostheses and hence the need for revision if implanted in relatively young patients. Therefore, OA research focuses on the development of disease-modifying osteoarthritic drugs (DMOADs) which may allow treatment before OA reaches its end-stage [13]. Hyaluronic acid (HA) improves the viscoelastic properties of synovial fluid [144] and intra-articular injections with HA are nowadays frequently used as a viscosupplement in the treatment of knee OA [145]. Recently, a Cochrane review on the efficacy of viscosupplementation with HA in knee OA reported significantly good, but temporary clinical effects on pain, function and patient global assessment with the highest effect sizes between 5 and 14 weeks after viscosupplementation if high-molecular-weight HA derivatives are used [146].

The working mechanism of HA injections, however, is not yet clear. It has been suggested that viscosupplementation, in addition to symptomatic benefits, may also have disease-modifying properties in OA [147, 148]. As a possible pathway for disease modification, previous *in vitro* research showed that HA has a beneficial effect on chondrocytes that are stimulated to produce proteoglycans (PG) [149-152]. PGs, which mainly consist of sulphated glycosaminoglycan (sGAG), are one of the main components of the extracellular matrix of articular cartilage [56, 153]. It is known that PGs are depleted in the early stages of OA, long before cartilage degeneration is visible as joint space narrowing on radiography [116]. Therefore, radiography is considered an inappropriate imaging tool for detection and follow-up of early stage OA in clinical research [33]. Moreover, common magnetic resonance imaging (MRI) techniques that assess cartilage morphology alterations have also shown to be insensitive to detect subtle changes in biochemical cartilage composition [49, 50]. In order to diagnose OA in early stage disease and detect intervention-caused biochemical changes sensitively during follow up, sophisticated MRI techniques have been developed during the last decade. These techniques provide a quantitative measure of the amount of sGAG, collagen or sodium of articular cartilage and therefore are a measure for cartilage structural composition [154, 155].

An example of such a MRI technique to measure cartilage structural composition is delayed gadolinium-enhanced MRI of cartilage (dGEMRIC). The technique uses the inverse relation between a negatively charged contrast agent and the sGAG content of cartilage and therefore provides an indirect quantitative outcome measure for cartilage sGAG content [65, 93]. Because of its ability to serve as a non-invasive indirect measure for cartilage structural composition, dGEMRIC has become a standard for assessment of

articular cartilage sGAG content in OA research. Recently, dGEMRIC was also shown to be a highly reproducible surrogate outcome measure of cartilage sGAG content over time in early stage OA knees [136]. Since other direct outcome measures such as cartilage biopsies are usually not ethically accepted, dGEMRIC is considered a suitable tool to non-invasively evaluate potential structure modification in terms of sGAG content improvement in articular cartilage.

Based on the aforementioned literature, we hypothesize that the improvement in clinical symptoms after HA injections will be corroborated by an improvement in sGAG content in the articular cartilage. Therefore, the aim of this study was to assess whether improvement in structural composition of cartilage is detected using dGEMRIC 14 weeks after 3 weekly injections with HA in patients with early stage knee OA.

MATERIALS AND METHODS

Study design and participants

For this prospective follow-up study conducted between March and September 2011, we recruited and included 20 participants with early stage OA of the knee from the outpatient clinic of the Department of Orthopedic Surgery of our institution. This sample size was based on an expected difference in T1 relaxation time of at least 95 ms which has been shown to represent a clinically relevant improvement in cartilage sGAG content as measured by 3D dGEMRIC of early stage OA knees acquired at 3.0 Tesla [136], a standard deviation of 100 ms of T1 relaxation times with 3D dGEMRIC of early stage OA knees acquired at 3.0 Tesla, an α of 0.008 (corrected for multiple testing using Bonferroni-Holm method: see statistical analysis), a power of 0.8 and a maximum lost to follow-up of 10% of the included participants.

We were not able to include a control group in this study, because this was considered unethical by the Institutional Review Board (IRB). However, this was not a problem because it was not our aim to assess the potential clinical improvement of HA injections compared to a placebo or non-treated participant group. Such studies have already been performed and have shown a clinical improvement of HA injections compared to placebo [145, 146]. Moreover, OA is generally a slow progressing disease in which no significant change in dGEMRIC outcomes was found at 14, 24 and 48 weeks follow-up compared to baseline in the control groups (n=15 and n=10 respectively) of two randomized controlled trials consisting of mild to moderate knee OA patients [156, 157]. Thus, the absence of a control group was not considered a limitation to address our study aim, i.e. the assessment of potential sGAG *increase* in an index group treated with viscosupplementation. Based on the aforementioned results we expect that dGEMRIC would have detected minor and non-significant changes in sGAG content of the car-

tilage in a control group of non-treated early stage OA patients between the baseline and follow-up measurement 14 weeks later.

The inclusion criteria for our study were: participants age > 18 years, knee pain duration > 3 months, severity of knee pain > 2 out of 10 on a numeric rating scale (NRS) for pain (score from 0 - 10: the higher the score, the more knee pain) [117], and radiographic knee OA with a Kellgren and Lawrence grade of 1 or 2 [28]. Exclusion criteria were: viscosupplementation in the index knee within the last year, glucocorticoid injection(s) in the index knee within the last three months, absolute contra-indications to undergo MRI, renal insufficiency (glomerular filtration rate < 60 ml/min), a history of contrast medium allergy, significant co-morbidities in the lower extremity containing the index knee joint, knee surgery in the index knee within the last year or knee surgery scheduled in the index knee within the next half year.

Written informed consent was obtained from all participants and the study was approved by the IRB (Medical Ethical committee of the Erasmus MC, protocol number MEC-2010-088).

Study protocol

Within two weeks before viscosupplementation of the index knee, a baseline dGEMRIC examination and routine MRI sequences of the index knee were acquired in all participants. Participants were also asked to rate their knee complaints on the Knee injury and Osteoarthritis Outcome Score (KOOS) [158]. The KOOS consists of 5 subscales (score from 0-100, the lower the score, the more knee symptoms in that subscale): 'pain', 'symptoms', 'activities of daily living' (ADL), 'sport and function' (sport), and 'knee-related quality of life' (QoL) and was validated in Dutch for early stage OA patients by De Groot *et al.* in 2008 [159]. In addition to the KOOS, all participants were asked to rate their knee pain on a NRS for pain. The NRS is a numeric rating scale for pain (score from 0 – 10: the higher the score, the more knee pain) comparable with the visual analogue scale for pain, but is easier to use for patients because pain can be expressed as a number [117].

After obtaining the baseline measurements, viscosupplementation was performed using an intra-articular injection with Hylan G-F 20 (Synvisc®, Genzyme Corp, Cambridge, USA). With a time interval of one week between the injections, three injections with Hylan G-F 20 were provided by an experienced orthopedic surgeon according to a standardized protocol using a superolateral approach [160].

Follow-up measurements (dGEMRIC examination and routine MRI sequences, KOOS questionnaire, and NRS for pain) were obtained 14 weeks after viscosupplementation with HA. We chose a 14 weeks interval between viscosupplementation and follow-up measurements because the highest clinical effect sizes of intra-articular injections with HA have been reported between 5 and 14 weeks after treatment [146].

Acquisition of dGEMRIC and routine MRI sequences

Before MR imaging, a double dose (0.2 mmol/kg) of gadopentetate dimeglumine (Magnevist®, Bayer Schering AG, Berlin, Germany) was injected intravenously based on the participants' weight [122]. For the follow-up dGEMRIC examination, we used the same amount of contrast agent as we used for the baseline dGEMRIC examination. This way, the outcomes of the follow-up dGEMRIC are not biased by the participants' body mass index (BMI) [137]. After contrast administration, the participants were asked to cycle for 10 minutes on a home trainer at constant speed to promote contrast distribution into and throughout the knee and the articular cartilage [95]. After cycling and a delay of 80 minutes, the dGEMRIC images were acquired.

MR imaging was performed on a 3.0 Tesla MRI scanner (Discovery MR750, General Electric Healthcare, Milwaukee, WI, USA) using a custom made 3 channel knee coil (Flick Engineering Solutions B.V., Winterswijk, The Netherlands) [123, 136]. We used a three-dimensional (3D) dGEMRIC protocol, which was acquired in the sagittal plane and was previously published by McKenzie *et al.* [94]. The dGEMRIC protocol consisted of an inversion recovery fast spoiled gradient-echo sequence, which was acquired for five times with different inversion times (TI=2100; 800; 400; 200 and 100 ms). The other scanning parameters were constant during scanning: matrix 256 x 232 pixels; field of view 150 mm; slice thickness 3 mm; flip angle 15º; echo time 1.5 ms and repetition time (TR) 3.9 ms, pixel bandwidth 488 Hz/voxel and number of averages 1. The total acquisition time was approximately 14 minutes, resulting in 36 sagittal MR images with complete coverage of the knee joint.

In addition to dGEMRIC scans, three routine sequences consisting of a fast spin echo (FSE) proton density weighted sequence (sagittal and axial plane) and a coronal FSE T2-weighted sequence with fat suppression were acquired to allow morphological evaluation of the cartilage and incidental findings (e.g., chondroid tumors, bone tumors, etc.) in the knee. The scanning time of the additional sequences was approximately 11 minutes, resulting in a total scanning time of approximately 25 minutes for the entire MRI protocol.

dGEMRIC analysis

Using Matlab (R2011a, The MathWorks, Natick, MA, USA), three cartilage regions of interest (ROIs) were drawn manually on three consecutive images through the lateral and medial tibiofemoral joint (central image and one adjacent image on each side) by a researcher with a medical degree and 4 years of experience in this research field (JvT). These qualifications were considered sufficient, especially since Tiderius and colleagues showed that the experience of the investigator does not affect the variability of manual ROI selection in dGEMRIC [121].

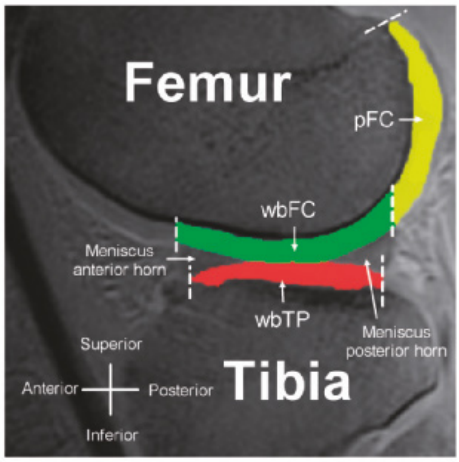

Figure 1: *Central sagittal MR image through the lateral tibiofemoral joint. The three anatomical cartilage ROIs which were drawn and analyzed on three consecutive images in each compartment of the tibiofemoral joint are shown. wbFC (green): weight-bearing cartilage of the femoral condyle. pFC (yellow): posterior non weight-bearing cartilage of the femoral condyle. wbTP (red): weight-bearing cartilage of the tibial plateau.*

ROI selection was standardized and based on the scheme suggested by Eckstein *et al.* [120]. These anatomical landmark based ROIs were drawn on the TI=2100 ms images of the first dGEMRIC examination and consisted of the weight-bearing cartilage of the femoral condyles (wbFC), the posterior non weight-bearing cartilage of the femoral condyles (pFC) and the weight-bearing cartilage of the tibial plateaus (wbTP) (*Figure 1*).

During acquisition of dGEMRIC, patient motion might occur. This patient motion may cause errors and imprecision in the outcomes of dGEMRIC, but image registration can correct for patient motion within dGEMRIC [85]. To correct for patient motion, we used an in-house developed registration and T1-fitting algorithm (Software for Post processing And Registration of Cartilage of the Knee: SPARCK) that was previously published [123]. In the registration part of the algorithm, first all images with different TI values were aligned to the TI=2100 ms images. The femoral condyle and tibial plateau were registered separately. The images were registered using a 3D rigid transformation model by maximization of localized mutual information. To minimize the blurring of the registered images, cubic interpolation was used [103]. The registration was performed separately for the baseline and follow-up dGEMRIC acquisitions. All registrations were performed using open source registration software (Elastix, http://elastix.isi.uu.nl/) [102]. After the first step, the follow-up examination is registered to the baseline examination based on the images with TI=2100 ms, the other TI images of the follow-up acquisition are transformed accordingly. Automated registration of baseline and follow-up scans eliminates subjective visual slice matching and also eliminates the need to manually outline the cartilage ROIs in the follow-up scan.

For the registered dGEMRIC baseline and follow-up datasets, T1 maps were estimated using a maximum likelihood fit [123]. After injection with Magnevist®, cartilage regions with long T1 relaxation time have relatively high sGAG content compared to cartilage regions

with short T1 relaxation time which indicates reduced sGAG content [65, 95]. All possible partial volume pixels for the cortical bone in the cartilage ROIs were automatically excluded for the ROIs using a patient specific bone-cartilage threshold which removed bone pixels for the manually drawn ROI before calculating the T1 relaxation time in all ROIs. Finally, in all cartilage ROIs, the weighted T1 relaxation time per ROI was calculated, where the estimated T1 relaxation time of each voxel was weighted by the reciprocal of its uncertainty. The uncertainty was measured by the square root of the Cramér-Rao Lower Bound, which gives a lower bound for the standard deviation of the estimated T1 [96-98]. Residual misalignment of the T1-weighted images, especially at tissue boundaries, results in biologically implausible values of T1, often associated with great uncertainty. Using the weighted mean, these implausible T1 relaxation times will not heavily influence the calculated mean T1 relaxation times in the determined cartilage ROIs [123].

The weighted T1 relaxation times for each anatomical cartilage ROI were averaged over the three consecutive MR images. This way we used the available 3D information instead of only using a single MR slice (2D analysis) in both the medial and lateral compartment of the knee as in most previous studies using dGEMRIC. Thus, for each patient in each dGEMRIC examination, six weighted average T1 relaxation times from six anatomical cartilage ROIs were obtained.

Morphological cartilage analysis

On the routine MRI sequences, the articular cartilage was scored for cartilage defects according to the MRI Osteoarthritis Knee Score (MOAKS) as described by Hunter *et al*. [43]. Both the baseline and the follow-up MRI were read by an experienced musculoskeletal radiologist (EO).

Statistical analysis

We tested our data for normality and equal variance using the Kolmogorov-Smirnov and Levene's test. The outcomes of these tests showed normality and equal variance of our data. We used paired *t*-tests to compare the outcomes of dGEMRIC in each anatomically defined cartilage ROI between follow-up and baseline. The same tests were used to compare the outcomes of each KOOS subscale and the NRS for pain 14 weeks after HA injections with the baseline outcomes. Since six cartilage ROIs and six subscales of questionnaires (KOOS and NRS were analyzed together) were compared between baseline and follow-up using six paired *t*-tests, we applied a Bonferroni-Holm correction [161] to define statistically significant *p*-values for these analyses. We present both the crude, as well as the adjusted *p*-values to determine whether a particular test result is statistically significant after Holm's adjustment of the *p*-values [162]. *P*-values of < 0.05 were considered statistically significant. All analyses were performed using SPSS 20.0 (SPSS Inc., Chicago, IL, USA).

RESULTS

Participants

We included 20 participants (eight female) with early stage OA of the knee (seven left knee joints). Their mean age at the time of inclusion was 48 ± 11 years and their mean BMI was 29 ± 5 kg/m^2.

On radiography, 11 participants had early stage OA in the medial tibiofemoral compartment. Two participants only had OA in the lateral tibiofemoral and 7 participants had OA in both knee compartments. No incidental findings were observed on routine MRI.

All baseline measurements were obtained two weeks (range 8 – 16 days) before viscosupplementation of the index knee with HA. The mean time between the first and second and second and third HA injection was 7 ± 0 days for all participants. All follow-up measurements were obtained 14 weeks (range 14 - 16 weeks) after viscosupplementation. All included patients completed both the baseline and the follow-up measurements.

dGEMRIC outcomes

At baseline, mean T1 relaxation times ranged from 461 to 491 ms in the three different cartilage regions in the medial tibiofemoral compartment. The mean T1 relaxation times in the lateral compartment were higher than those in the medial compartment and ranged from 475 to 581 ms in the different regions (*p*-value = 0.0006) (*Table 1*). At 14 weeks follow-up, the mean T1 relaxation times in the medial compartment of the knee ranged from 456 to 520 ms and in the lateral compartment from 498 to 579 (*p*-value = 0.04) (*Table 1*).

We did not observe a statistically significant change in T1 relaxation times in any of the analyzed cartilage regions between the baseline measurements and the follow-up measurements (all adjusted *p*-values > 0.05) (*Table 1*). In *Figure 2*, an example of a participant without change in cartilage T1 relaxation times and hence cartilage composition after HA injections is shown.

In two ROIs (wbFC and wbTP) in the lateral knee compartment and one ROI in the medial compartment (wbFC), a trend towards a decrease in indirectly measured cartilage sGAG content in terms of lower mean T1 relaxation times was observed (*Figure 3*). In one ROI in the lateral compartment (pFC) and in two ROIs in the medial compartment (pFC and wbTP), mean T1 relaxation times after viscosupplementation showed a trend towards improvement compared to baseline (*Figure 3*). These trends were, however, neither statistically significant, nor exceeded a previously determined threshold of 95 ms for clinically relevant improvement in cartilage sGAG content measured using dGEMRIC [136].

Cartilage ROI	Mean T1 at baseline (95% CI)	Mean T1 at follow-up (95% CI)	Crude *p*-value from paired *t*-tests	Adjusted p-value using Holm's method
Lateral tibiofemoral compartment				
Weight-bearing femoral	512 (478 – 546) ms	510 (482 – 538) ms	0.89	0.89
Posterior femoral	475 (434 – 516) ms	487 (450 – 524) ms	0.42	> 0.99
Weight-bearing tibia	581 (529 – 633) ms	579 (526 – 630) ms	0.85	> 0.99
Medial tibiofemoral compartment				
Weight-bearing femoral	461 (417 – 505) ms	456 (411 – 500) ms	0.64	> 0.99
Posterior femoral	488 (432 – 544) ms	520 (470 – 569) ms	0.04	0.24
Weight-bearing tibia	491 (441 – 541) ms	512 (466 – 558) ms	0.09	0.45

Table 1: *Mean T1 relaxation times with 95% confidence interval for the mean in milliseconds at baseline and at 14 weeks follow-up after HA injections (n=20 for each anatomical cartilage ROI). 95% CI: 95% confidence interval.*

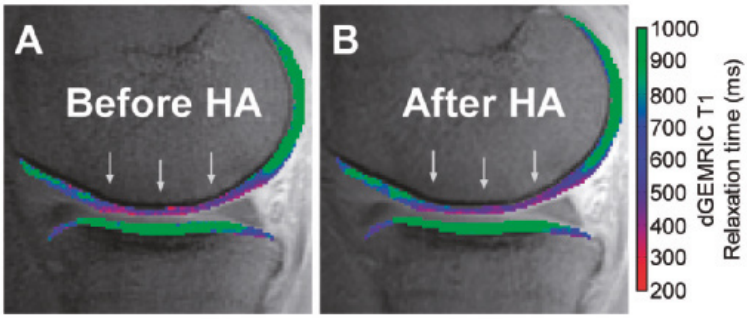

Figure 2: *Representative sagittal central MR image through the medial tibiofemoral compartment of an early stage OA knee before (A) and after (B) viscosupplementation with HA. The T1 color map of the cartilage clearly shows a region with relatively lower T1 relaxation times (grey arrows in A), indicating relatively lower sGAG content in the weight-bearing femoral cartilage before viscosupplementation (A). After HA injections (B), however, the region with relatively low T1 relaxation times is still present (grey arrows in B).*

Differences in T1 relaxation times at follow-up reached this threshold only in seven participants in a single cartilage ROI (3 times lateral pFC, 3 times medial pFC and 1 time lateral wbTP: data for each individual participant not shown). In the other ROIs in these participants, this 95 ms threshold was not reached. In the remaining 13 participants, the threshold for T1 improvement was not reached in any of the analyzed cartilage ROIs.

Morphological cartilage analysis

On the routine MRI sequences, a total of 240 cartilage regions were assessed for cartilage lesions using the MOAKS criteria. A total of 21 regions were diagnosed with a

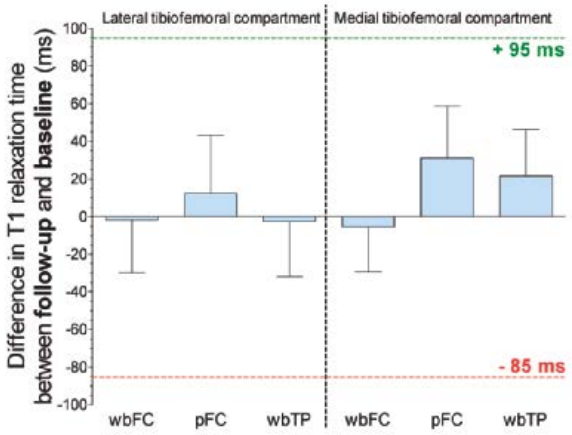

Figure 3: *Bar graphs showing the differences in dGEMRIC T1 relaxation times in each anatomical cartilage ROI at follow-up, 14 weeks after HA injections compared to baseline. The bar represents the mean and the whiskers represent the 95% confidence interval for the mean. +95 ms: clinically relevant threshold for improvement in cartilage sGAG content if a single patient is followed over time using dGEMRIC. -85 ms: clinically relevant threshold for impairment of cartilage sGAG content if a single patient is followed over time using dGEMRIC. wbFC: weight-bearing cartilage of the femoral condyle. pFC: posterior non weight-bearing cartilage of the femoral condyle. wbTP: weight-bearing cartilage of the tibial plateau.*

cartilage lesion (6 in the lateral and 15 in the medial compartment) and 219 regions showed normal cartilage morphology. Eight full thickness cartilage defects were observed at baseline in 3 participants. Thirteen partial cartilage lesions were observed in 11 participants. All cartilage lesions had a size of either <10% or 10-75% of the region of cartilage surface area. No progression in any partial and full thickness size or progression from partial to full thickness cartilage lesions was observed at 14 weeks follow-up.

KOOS and NRS outcomes

All KOOS subscales, 'pain' (mean at baseline: 48, mean at follow-up: 66, crude *p*-value = 0.0003, adjusted *p*-value = 0.002), 'symptoms' (mean at baseline: 49, mean at follow-up: 56, crude *p*-value = 0.03, adjusted *p*-value = 0.03), 'ADL' (mean at baseline: 55, mean at follow-up: 72, crude *p*-value = 0.0007, adjusted *p*-value = 0.003), 'sports' (mean at baseline: 20, mean at follow-up: 35, crude *p*-value = 0.004, adjusted *p*-value = 0.01), and 'QoL' (mean at baseline: 28, mean at follow-up: 38, crude *p*-value = 0.01, adjusted *p*-value = 0.02), improved significantly 14 weeks after HA injections in the knee (*Figure 4*). The mean NRS pain score at baseline was 7 and improved significantly (crude *p*-value < 0.0001, adjusted *p*-value < 0.0001) to a mean of 4 14 weeks after HA injections (*Figure 4*).

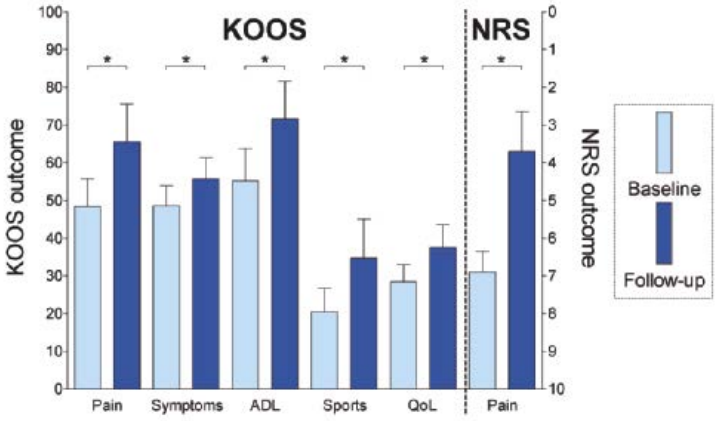

Figure 4: *Bar graphs showing the KOOS subscales and NRS pain at baseline (light blue box) and at follow-up, 14 weeks after HA injections (dark blue box). The bar represents the mean and the whiskers represent the 95% confidence interval for the mean. HA: hyaluronic acid injections. ADL: activities of daily living, sports: sport and function, and QoL: knee-related quality of life. *: p-values adjusted using Holm's method <0.05.*

DISCUSSION

Because of the lack of established DMOADs for early stage knee OA, intra-articular viscosupplementation with HA has become a frequently used treatment for reducing symptoms and pain in early stage knee OA [145, 146]. Since it was suggested in previous *in vitro* research that HA injections might also have disease-modifying properties by increasing cartilage sGAG content [149-152], the aim of this study was to assess whether improvement in cartilage structural composition is detected using dGEMRIC 14 weeks after 3 weekly injections with HA in patients with early stage knee OA.

Outcomes of dGEMRIC in the medial compartment of the knee were lower compared to the lateral compartment at baseline, indicating more structural damage in the medial knee compartment. T1 relaxation times in both knee compartments were lower compared to previously published dGEMRIC T1 relaxation times acquired at 3.0 Tesla in healthy subjects [94, 163, 164], indicating sGAG loss from the cartilage in our early stage OA patients. The outcomes of dGEMRIC are consistent with radiographic findings and our morphological cartilage assessment on MRI with MOAKS and reflect the early stage OA population in which sGAG loss occurs before morphological changes are detectable on radiography or MRI (e.g. using MOAKS). We observed early stage OA in the medial compartment of the knee in 18 of the 20 participants, which is defined as mild to moderate osteophyte formation as the only features on radiography, and only a few participants with partial cartilage damage according to MOAKS, without definite joint space narrowing or bone on bone contact which are signs of advanced or end-stage OA. Based

on these characteristics, we consider our study population suitable to evaluate the potential structural effects of viscosupplementation as a potential DMOAD, since this should be tested in early stages of OA in which disease modification is still possible [13].

At follow-up, 14 weeks after viscosupplementation with HA, no statistically significant change in cartilage sGAG content was detected on dGEMRIC in any of the analyzed anatomical cartilage ROIs compared to the baseline measurements. Outcomes of dGEMRIC showed a trend towards improvement in three of the analyzed cartilage ROIs two of which were the medial and lateral non-weight-bearing cartilage regions of the femoral condyles. This is somewhat unexpected, as one would expect an improvement in cartilage structural composition in the weight-bearing femoral condyles and/or plateaus since those ROIs had lower T1 relaxation times and hence more structural damage at baseline. Moreover, the improvement in T1 relaxation times did not exceed a previously determined threshold of 95 ms which has been shown to represent a clinically relevant improvement in cartilage sGAG content as measured by 3D dGEMRIC of early stage OA knees acquired at 3.0 Tesla [136]. It may be that there are non-significant changes between baseline and follow-up T1 relaxation times which means that the measurements were not the same between the two time points. However, we hypothesized that if the reported clinical effect of viscosupplementation, confirmed by our study, would act through an *improvement* of sGAG content, this would have been detectable using dGEMRIC with the sample size of our study.

We believe there are several possible explanations why we did not observe an increase in cartilage sGAG content by dGEMRIC 14 weeks after viscosupplementation of early stage OA knees. First, cartilage sGAG content and therefore dGEMRIC outcomes might not improve after viscosupplementation if the treatment does not have any disease-modifying effects on articular cartilage. Instead, viscosupplementation may have a primary positive effect on pain and other clinical symptoms of OA. This working mechanism was suggested for HA injections in a recent OARSI review by Zhang *et al*. in which the evidence for available therapies in the treatment of hip and knee OA was re-evaluated and discussed [165].

A second explanation why T1 relaxation times did not increase is that viscosupplementation may *slow down the progression* of OA by preventing the loss of sGAG content rather than *improving* the sGAG content of cartilage (the latter was our hypothesis in this study). This working mechanism of HA was suggested in several *in vitro* studies [166-168], and is supported by the results of recent animal and human studies in which the structural efficacy of HA treatment over time was compared to a control group (non-treatment and placebo) using another quantitative MRI technique (T2 mapping) [169] and cartilage thickness and volume measurements on MRI [170]. However, as it was considered unethical to include a control group by the IRB, we could not compare the

sGAG content 14 weeks after viscosupplementation with the sGAG content of cartilage without viscosupplementation.

A third possible reason that T1 relaxation times may not increase after HA injections is the detection limit and specificity of dGEMRIC to detect (change) in sGAG content of articular cartilage. Minimal changes in sGAG content of cartilage following HA treatment may not be detected using dGEMRIC T1 because, although the technique is highly reproducible in knee OA [136], it is currently unknown to which extent minimal change in sGAG content are detectable using dGEMRIC in humans. dGEMRIC is an indirect measure for cartilage sGAG content and there are no *in vivo* studies, which investigated the sensitivity and specificity of dGEMRIC to measure (small) changes in sGAG content of the extracellular matrix of cartilage. Other drawbacks of dGEMRIC are the long acquisition protocol because of the delay between the contrast administration and MR acquisition and the risk of nephrogenic systemic fibrosis due to contrast administration. In addition to these drawbacks, a recent publication shows that dGEMRIC outcomes might not only represent sGAG content of cartilage, but may also be influenced by collagen orientation which influences diffusion of contrast agent into the extracellular matrix of the cartilage [142] and therefore concluded that dGEMRIC may not be considered sGAG specific. Despite these shortcomings of dGEMRIC, the technique is still considered the best tool available that provides a quantitative measure for cartilage sGAG content in human knee joints.

Finally, the timing of the follow-up measurement in our study could be an explanation why dGEMRIC T1 relaxation times did not improve after viscosupplementation. It may be that the follow-up measurement was either too early or too late after viscosupplementation to detect any changes in cartilage sGAG content caused by the treatment. We chose a 14 weeks follow-up period after viscosupplementation based on a Cochrane review on the efficacy of HA injections as treatment in knee OA [146], in which the maximum clinical benefit of HA injections was reached between 5 and 14 weeks after treatment. It is known that sGAGs are being synthesized within days instead of weeks [171]. Moreover, previous *in vivo* animal research has shown that newly synthesized sGAGs have a turnover time over 100 days [172, 173] and therefore should be still detectable 14 weeks after viscosupplementation. Therefore, we considered our follow-up period of 14 weeks appropriate in relation to our hypothesis. Future research with earlier or extended follow-up measurements might give better insight whether our findings are consistent over time.

In contrast to the results of dGEMRIC, all KOOS subscales ('pain', 'symptoms', 'daily activities', 'sports' and 'quality of life') and the NRS for pain improved significantly 14 weeks after viscosupplementation with HA. These results are in agreement with aforementioned studies [145, 146] in which a significant reduction in patient complaints was observed after HA injections. The relief in patient complaints without an improvement

in cartilage sGAG content might be due to the placebo effect of viscosupplementation [165]. However, the clinical efficacy of HA may also be attributed to a positive effect of viscosupplementation on the viscoelastic properties of the synovial fluid [144] and a positive effect on the synovial membrane, which has been observed histologically in previous clinical studies in OA patients [174-176]. It has been suggested in previous work that this might have anti-inflammatory effects causing less synovitis and therefore less knee complaints since pain and synovitis were recently shown to be closely related in OA patients [22, 177, 178].

In conclusion, the results of this study confirm earlier findings reported in the literature, showing a persisting efficacy of viscosupplementation on symptomatic outcome measures of early stage OA knees 14 weeks after treatment. Outcomes of dGEMRIC, however, did not change after viscosupplementation, indicating no change in cartilage structural composition as an explanation for the improvement of clinical symptoms.

chapter 9

Delayed gadolinium-enhanced MRI of the meniscus (dGEMRIM) in patients with knee osteoarthritis: relation with meniscal degeneration on conventional MRI, reproducibility and correlation with dGEMRIC

J. van Tiel, G. Kotek, M. Reijman, P.K. Bos, E.E. Bron, S. Klein, J.A. Verhaar, G.P. Krestin, H. Weinans, E.H. Oei.

Eur Radiol. 2014 Sep;24(9):2261-70.

ABSTRACT

Introduction

To assess (I) if normal and degenerated menisci exhibit different T1GD on delayed gadolinium-enhanced MRI of the meniscus (dGEMRIM), (II) the reproducibility of dGEMRIM and (III) the correlation between meniscus and cartilage $T1_{GD}$ in knee osteoarthritis (OA) patients.

Materials and Methods

In 17 OA patients who underwent dGEMRIM twice within 7 days, meniscus and cartilage $T1_{GD}$ was calculated. Meniscus pathology was evaluated on conventional MRI. $T1_{GD}$ in normal and degenerated menisci were compared using a student's *t*-test. Reproducibility was assessed using ICCs. Pearson's correlation was calculated between meniscus and cartilage $T1_{GD}$.

Results

A trend towards lower $T1_{GD}$ in degenerated menisci (mean: 402 ms; 95% CI: 359 - 444ms) compared to normal menisci (mean: 448 ms; 95% CI: 423 - 473ms) was observed (p=0.05). Meniscus $T1_{GD}$ ICCs were 0.85-0.90. The correlation between meniscus and cartilage $T1_{GD}$ was moderate in the lateral (r=0.52-0.75) and strong in the medial compartment (r=0.78-0.94).

Conclusion

Our results show that degenerated menisci have a clear trend towards lower $T1_{GD}$ compared to normal menisci. Since these results are highly reproducible, meniscus degeneration may be assessed within one delayed gadolinium-enhanced MRI simultaneously with cartilage. The strong correlation between meniscus and cartilage $T1_{GD}$ suggests concomitant degeneration in both tissues in OA, but also suggests that dGEMRIC may not be regarded entirely sulphated glycosaminoglycan specific.

INTRODUCTION

Knee osteoarthritis (OA) is the most common joint disease in middle-aged and elderly, causing serious morbidity and large socio-economic impact [8, 9, 179, 180]. The disease affects many tissues of the joint, such as subchondral bone, synovium, joint capsule, articular cartilage and the menisci [22]. It has been shown that pathologic changes in the meniscus such as degeneration and tears play an important role in the development of cartilage degeneration in knee OA because pathologic menisci fail to perform their role as shock absorbing tissues in the knee, resulting in more load on the articular cartilage which gives rise to faster degeneration [181, 182]. Conversely, knee OA also leads to damage of the meniscus due to the release of degenerative enzymes and chemokines in the entire OA knee joint [183].

The extracellular matrix of articular cartilage is mainly composed of collagen and proteoglycans (PG) [56, 153, 184]. PGs primarily consist of sulphated glycosaminoglycans (sGAG) [56, 153, 184]. Delayed gadolinium-enhanced magnetic resonance imaging of cartilage (dGEMRIC) is an established quantitative imaging technique that uses the inverse relation between an ionic contrast agent and the amount of sGAG in articular cartilage to measure its biochemical composition and its degradation [93, 95]. Based on the inverse relation of cartilage sGAG content and the contrast agent, cartilage with relatively low sGAG content will have low $T1_{GD}$ relaxation times [65]. Since the extracellular matrix of the meniscus also contains PGs and hence sGAG [184, 185], quantitative analysis of delayed gadolinium-enhanced magnetic resonance imaging of the meniscus (dGEMRIM) has also been proposed as a tool to give insight in the composition of the meniscus in terms of its sGAG content [186, 187]. However, no previous study has assessed if degenerated menisci, similar to articular cartilage in dGEMRIC, exhibit lower $T1_{GD}$ relaxation times compared to morphologically normal menisci. In addition, no previous study has investigated the reproducibility of $T1_{GD}$ of the meniscus in dGEMRIM. The aforementioned information is important to know whether meniscus and articular cartilage degeneration may be analyzed within one gadolinium-enhanced magnetic resonance imaging (MRI) examination and if gadolinium-enhanced MRI provides a robust outcome which can be used in both cross-sectional, as well as longitudinal study designs.

Despite the absolute difference in sGAG content between the meniscus and articular cartilage - the meniscus only contains 10-15% of the amount of sGAG present in the cartilage [55, 153, 184, 188] - Krishnan *et al*. showed that there is a moderate relation between $T1_{GD}$ of the meniscus and of articular cartilage in healthy volunteers and patients with knee complaints who were not diagnosed with OA by their physician [186]. However, the relationship between $T1_{GD}$ of the menisci and articular cartilage has not yet been established in knee OA patients. In OA patients the amount of sGAG in both tissues is known

to be diminished during disease progression [56, 181, 185], which may cause a difference in contrast uptake in both tissues compared to non-OA subjects.

The aims of the current study were: (I) to assess if menisci, identified as normal or degenerated on conventional MRI, also exhibit different $T1_{GD}$ relaxation times on dGEMRIM, (II) to assess the reproducibility of $T1_{GD}$ of the meniscus in dGEMRIM and (III) to assess the correlation between $T1_{GD}$ of the meniscus and the articular cartilage in knee OA patients.

MATERIALS AND METHODS

Participants

For this study we used delayed gadolinium-enhanced MRI data of patients included in a prospective study in which the reproducibility of dGEMRIC was assessed. The 17 patients included in this study underwent dGEMRIC twice (test and retest) within a seven day interval. All analyses of this study, except for the reproducibility analysis of the meniscus, were performed on the datasets from the first dGEMRIC examination. The data were acquired between March and September 2011. Written informed consent was obtained from all participants and the study was approved by the IRB (Medical Ethical committee of the Erasmus MC, protocol number MEC-2010-088).

The inclusion criteria were: participants > 18 years, knee pain > 3 months, severity of knee pain > 2 out of 10 on a numeric rating scale at the time of inclusion [117], and radiographic knee OA with a Kellgren and Lawrence grade of 1 or 2 (doubtful or definite osteophyte formation without joint space narrowing) [28]. Exclusion criteria were: absolute and relative contra-indications to undergo MRI, a glomerular filtration rate < 60 ml/min, a history of previous reactions to contrast agent, significant co-morbidities in the lower extremity of the index knee joint (e.g. severe hip OA, neurologic diseases or muscular diseases causing a disability of the joint) which preclude exercising after the contrast administration, or knee surgery in the index knee < 1 year ago.

Acquisition of delayed gadolinium-enhanced and conventional MRI

Before acquisition of the delayed gadolinium-enhanced and conventional MR images, a double dose (0.2 mmol/kg) of Magnevist® (Bayer Schering Ag, Berlin, Germany) was administered intravenously. After injection of the contrast agent, the participants cycled for 10 minutes on a home trainer with a constant speed to promote contrast distribution into the articular cartilage [95]. Approximately 90 minutes after the contrast injection, the delayed gadolinium-enhanced scan was acquired first, followed by the conventional MR images.

MR imaging was performed on a 3.0 Tesla MRI scanner (Discovery MR750, General Electric Healthcare, Milwaukee, USA) using a custom-made 3-channel knee coil (Flick Engineering Solutions B.V., Winterswijk, The Netherlands). The delayed gadolinium-enhanced MR scanning protocol consisted of a 3D inversion recovery fast spoiled gradient-echo sequence which was acquired with five different inversion times (TI): 2100; 800; 400; 200 and 100 ms [94]. The other scanning parameters were the same for all five acquisitions and are shown in (*Table 1*).

Sequence	dGEMRIC	Proton-density-weighted	Proton-density-weighted	T2-weighted
Plane	Sagittal	Sagittal	Axial	Coronal
Imaging mode	3D	2D	2D	2D
Sequence	IR SPGR	FSE	FSE	FSE
Matrix (frequency)	256	416	416	320
Matrix (phase)	230	256	352	256
FOV (mm)	150	150	150	150
Slice thickness/gap (mm/mm)	3.0/0.0	3.0/0.0	2.0/0.0	3.0/0.0
TI (ms)	2100 / 800 / 400 / 200 / 100	N.a.	N.a.	N.a.
TE (ms)	1.5	27	27	70
TR (ms)	3.9	2250	2250	5000
Flip angle (°)	15	90	90	90
Bandwidth (Hz/pixel)	244	244	244	244
Number excitations averaged	1	1	1	1
Fat saturation	N.a.	N.a.	N.a.	Yes
Number of slices	36	36	32	20
Acquisition time (min)	14	2	2	4

Table 1: *MRI protocol parameters. FOV: field of view. FSE: fast spin-echo. IR SPGR: inversion recovery spoiled gradient-echo. N.a.: not applicable. TE: echo time. TI: inversion time. TR: repetition time*

Additionally, three conventional MR sequences were acquired consisting of a sagittal and axial fast spin echo (FSE) proton-density-weighted and a coronal FSE T2-weighted sequence with fat suppression (*Table 1*). On these images, evaluation of the morphology and signal intensity of the meniscus was performed.

Analysis of delayed gadolinium-enhanced MRI

Using Matlab (R2011a, The MathWorks, Natick, USA), two regions of interest (ROIs) in the articular cartilage and two ROIs in the meniscus were drawn on the images from the

delayed gadolinium-enhanced MR exam acquired with TI=2100 ms by a musculoskeletal imaging researcher with four years of experience. The ROIs were drawn on three consecutive images through the lateral and medial tibiofemoral joint (central slice and one adjacent slice on each side) (*Figure 1*). We chose to use the three central slices since these represent approximately 1 cm of the weight-bearing tibiofemoral joint which is mostly affected by OA. The most central slices through the medial and lateral tibiofemoral compartment was selected using co-localization on the sagittal, coronal and axial conventional MR images by identifying the sagittal slice with the most caudal point of the femoral condyle on it. Because of the use of our dedicated knee coil, all knees were positioned in the same way (10 degrees of flexion in the knee joint) and by acquiring two sets of localizer images we were able to angulate all planes to achieve a consistent slice selection in all participants. The meniscus ROIs were drawn on the same slices as the cartilage ROIs and consisted of the anterior horn of the meniscus (aMEN) and the posterior horn of the meniscus (pMEN) (*Figure 1*).

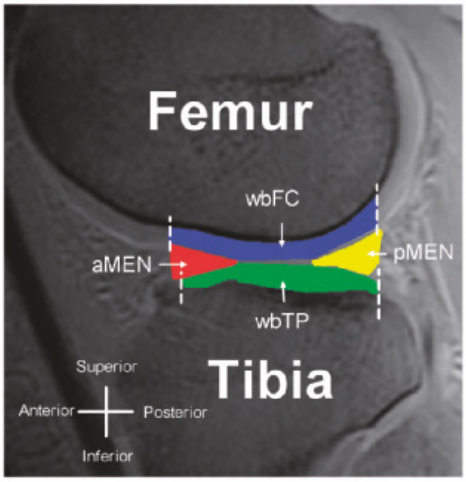

Figure 1: *Representation of the two cartilage and two meniscus ROIs in which the $T1_{GD}$ relaxation time was calculated in three consecutive slices in each compartment of the tibiofemoral joint (lateral side shown in this example). wbFC (blue): weight-bearing cartilage of the femoral condyle. wbTP (green): weight-bearing cartilage of the tibial plateau. aMEN (red): anterior horn of the meniscus. pMEN (yellow): posterior horn of the meniscus.*

During MR acquisition, patient motion might occur which may cause errors in the outcomes of quantitative analyses. Image registration, however, can correct for patient motion [85, 123]. To correct for patient motion, we used an in-house developed registration and $T1_{GD}$-fitting algorithm that was published and used previously [123, 136, 189]. With this tool, first, all images with different TI values were registered to the TI=2100 ms images for both scans (test and retest) of each patient. Next, the retest examination was registered to the test examination based on the images with TI=2100 ms, and the images with other TIs of the retest examination were transformed accordingly. Automated registration of the retest to the test scan eliminates subjective visual slice matching and

also eliminates the need to manually outline the meniscus ROIs on the retest scan. All Details on the registration settings can be found in [123].

For the registered datasets, $T1_{GD}$ maps were estimated using a maximum likelihood fit in each meniscus ($T1_{GD}$ maps of the registered tibia plateau) and cartilage ($T1_{GD}$ maps of registered femoral condyle and tibial plateau) ROIs, the weighted $T1_{GD}$ for each ROI was calculated. By using the weighted $T1_{GD}$ the outcomes are less affected by possible outlier $T1_{GD}$ within the ROIs [123]. Finally, as proposed by Tiderius *et al.*, $T1_{GD}$ was corrected for the participants' body mass index (BMI) since this is a potential source of dose bias of the administered contrast agent [137].

The weighted, BMI-corrected, $T1_{GD}$ relaxation times for each ROI (meniscus and cartilage) were averaged over the three consecutive MR images. Thus, for each patient, eight $T1_{GD}$ measurements from 4 meniscus and 4 cartilage ROIs were obtained for the test and retest examination.

Analysis of meniscus pathology

On the conventional proton-density and T2-weighted MRI sequences, we evaluated four different meniscal regions (anterior and posterior half or the medial and lateral meniscus, each including a part of the meniscal body) for the presence or absence of meniscal pathology. This analysis included all slices on which the specific meniscal region was visible (i.e. more than the three central slices on which dGEMRIM analysis was performed).

If no pathology was observed (*Figure 2A*), menisci were classified as normal. Menisci were evaluated for meniscal degeneration indicated by intrameniscal signal abnormali-

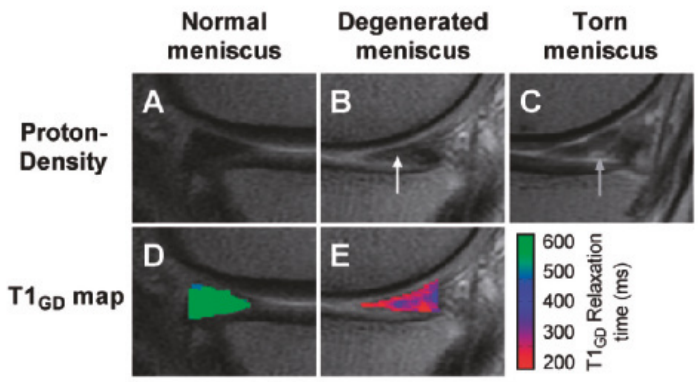

Figure 2: *Top layer (A-C): examples of proton-density images of a normal, degenerated and torn meniscus. A: morphologically normal, B: degenerated (intrameniscal signal abnormalities, white arrow) and C: torn (gray arrow) meniscus on sagittal conventional proton-density-weighted MR images. Bottom layer (D,E): proton-density images with $T1_{GD}$ color overlay of the morphologically normal and degenerated menisci (D, E). No $T1_{GD}$ color overlay of a torn meniscus is presented because those were excluded for all analysis for reasons stated in the materials and methods section.*

ties not reaching the articular surface [190,191] and the presence of tears indicated by signal abnormalities extending to the articular surface (*Figure 2BC*).

Because we aimed to study early degeneration of the meniscus, we excluded meniscus ROIs with tears from our analysis since we consider meniscal tears either an advanced stage of meniscus pathology or of traumatic etiology. In addition, meniscal tears might fill with contrast agent directly from the joint cavity, causing erroneously low $T1_{GD}$ relaxation times.

All MR examinations were read by an experienced musculoskeletal radiologist (EO).

Statistical analysis

We tested our data for normality and equal variance using the Kolmogorov-Smirnov and Levene's test. The outcomes of these tests showed normality and equal variance of our data. For each cartilage and meniscus ROI, we calculated the mean $T1_{GD}$ and its 95% confidence interval (95%CI) in the first MR examination.

To assess if $T1_{GD}$ differs between menisci identified as morphologically normal or degenerated on conventional MRI, we compared the $T1_{GD}$ of normal and degenerated menisci using a student's *t*-test.

To examine the reproducibility of $T1_{GD}$ of the meniscus, we calculated the intraclass correlation coefficient (ICC) measuring the absolute agreement in a two-way random effects model in each meniscus ROI [124]. We did not investigate the reproducibility of cartilage $T1_{GD}$, since this was already shown to be excellent in early stage OA patients [136].

To study the relation between $T1_{GD}$ in the meniscus and the articular cartilage, we calculated the Pearson's correlation coefficients between aMEN and pMEN and wbFC and wbTP $T1_{GD}$ in both tibiofemoral compartments.

All analyses were performed using SPSS 20.0 (SPSS Inc., Chicago, IL, USA). *P*-values <0.05 were considered to be statistically significant.

RESULTS

Participants

The mean age of the 17 participants (seven women, five left knee joints) was 50 (± 10) years and their mean BMI was 30 (± 5) kg/m^2. There were no differences in age (p=0.85) and BMI (p=0.20) between the participants with morphologically normal and degenerated menisci. Two participants had previous meniscal surgery in their index knee. In both cases the posterior meniscal horn (one lateral and one medial) was repaired and partially removed because of a tear. Two patients had their anterior cruciate ligament reconstructed and one patient had a high tibial osteotomy more than one year before inclusion.

On radiography, 11 participants had early stage OA (Kellgren and Lawrence grade 1 or 2) in the medial tibiofemoral compartment [28]. Six participants had early OA in both the medial and lateral knee compartments. No isolated lateral OA was observed on radiography in any of the included participants.

Analysis of meniscus pathology

A total of 68 meniscus ROIs were evaluated for degeneration and tears on the routine MRI sequences (4 meniscus ROIs in 17 patients). A total of 15 meniscus regions in 9 participants were diagnosed with degenerative signal abnormalities: 4 aMEN and 6 pMEN ROIs in the lateral compartment and 5 pMEN ROIs in the medial compartment. A total of 42 menisci were scored as normal on conventional MRI.

Meniscal tears were observed in 11 meniscal regions in 9 participants. 10 of which were located in the medial compartment (9 in the pMEN and one in the aMEN) and one was present in the pMEN in the lateral compartment. These menisci were excluded from all analyses as mentioned before.

Analysis of delayed gadolinium-enhanced MRI

$T1_{GD}$ relaxation time in the meniscus ROIs ranged from 421 to 432 ms and from 489 to 607 ms in the cartilage ROIs (*Table 2*). The $T1_{GD}$ in the medial tibiofemoral compartment of the cartilage was significantly lower than in the lateral compartment (p=0.004), whereas there was no such regional difference observed for the meniscal ROIs (p=0.77) (*Table 2*).

Cartilage / Meniscus ROI (n)	**$T1_{GD}$ (95% CI)**
Medial tibiofemoral compartment	
Weight-bearing femoral condyle (n=17)	489 (443 - 536) ms
Weight-bearing tibial plateau (n=17)	520 (466 - 574) ms
Anterior meniscus (n=16)	423 (372 - 475) ms
Posterior meniscus (n=8)	430 (355 - 506) ms
Lateral tibiofemoral compartment	
Weight-bearing femoral condyle (n=17)	542 (508 - 578) ms
Weight-bearing tibial plateau (n=17)	607 (551 - 662) ms
Anterior meniscus (n=17)	432 (402 - 462) ms
Posterior meniscus (n=16)	421 (394 - 449) ms

Table 2: *Mean T1GD relaxation times in the meniscus and articular cartilage. n: number of regions analyzed (torn menisci were excluded from our analyses). 95% CI : 95% confidence interval*

Analysis of T1GD in normal and degenerated menisci

$T1_{GD}$ relaxation time of morphologically normal menisci on conventional MRI (n=42) was 448 ms with a 95%CI ranging from 423 – 473 ms. We observed a trend towards lower $T1_{GD}$ relaxation time in degenerated menisci (n=15, mean: 402 ms, 95%CI ranging from 359 – 444 ms) (*p*=0.05) (*Figure 2DE and Figure 3*).

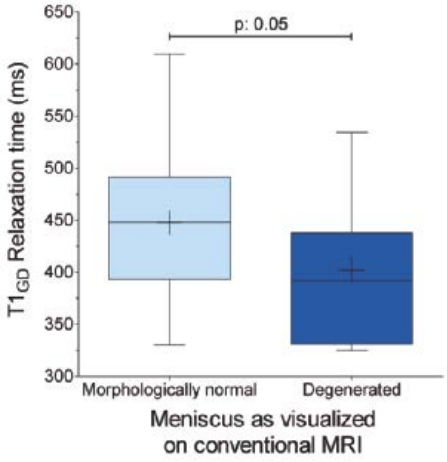

Figure 3: *Boxplots showing $T1_{GD}$ relaxation time of morphologically normal (n=42) versus degenerated menisci (n=15) as visualized on conventional MRI. Whisker represents the 5th - 95th percentile. The + represents the mean $T1_{GD}$.*

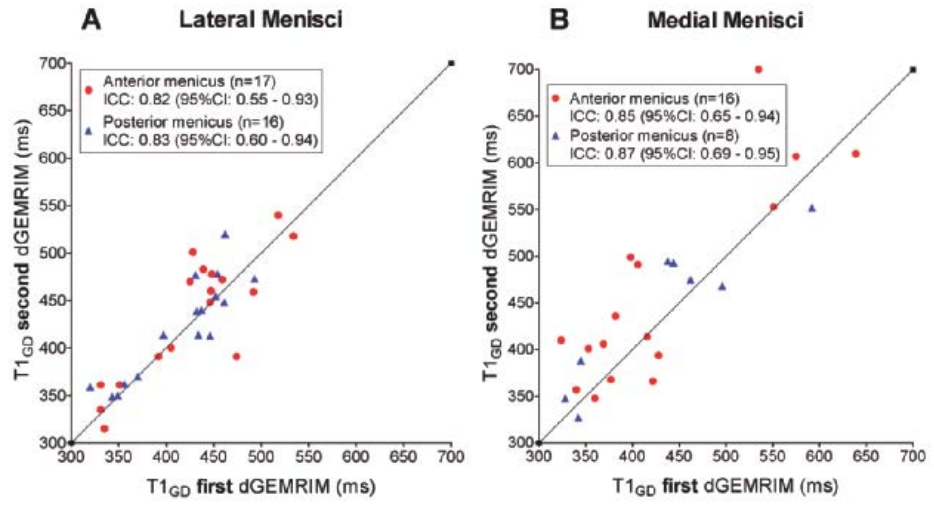

Figure 4: *Scatter plots of the first and second dGEMRIM of all patients. Red circles represent anterior menisci and blue triangles represent posterior menisci. A: lateral menisci. B: medial menisci. The black line represents the relation x=y (perfect reproducibility). n: number of regions analyzed (torn menisci were excluded from our analyses). ICC: intraclass correlation coefficient. 95% CI: 95% confidence interval.*

Reproducibility of meniscus T1GD

The reproducibility of meniscus $T1_{GD}$ relaxation times of dGEMRIM, expressed as ICCs together with the 95%CIs, is shown in *Figure 4*. The reproducibility was good with ICC values > 0.80 [124] in all meniscus ROIs (n=17 for the aMEN and n=16 for the pMEN in the lateral compartment, n=16 for aMEN and n=8 for pMEN in the medial compartment).

Correlation between T1GD of meniscus and cartilage

$T1_{GD}$ relaxation times of the meniscus correlated moderately to strongly with the $T1_{GD}$ relaxation times of the articular cartilage (range of Pearson's correlation coefficients: 0.52 - 0.94, *Table 3*). The correlation in the medial tibiofemoral compartment was stronger (range of correlation coefficients: 0.78 - 0.94, *Table 3*) compared to the lateral compartment of the knee (range of correlation coefficients: 0.52 - 0.75, *Table 3*). Examples of a meniscus and articular cartilage with high and low $T1_{GD}$ relaxation times in the medial knee compartment are shown in *Figure 5*.

	r (95% CI)	
Cartilage ROI	**Meniscus ROI**	
Medial compartment	Anterior (n=16)	Posterior (n= 8)
Weight-bearing femoral condyle	0.94 (0.84 - 0.98)	0.78 (0.17 - 0.96)
Weight-bearing tibial plateau	0.87 (0.66 - 0.95)	0.78 (0.18 - 0.96)
Lateral compartment	Anterior (n=17)	Posterior (n=17)
Weight-bearing femoral condyle	0.75 (0.43 - 0.91)	0.66 (0.27 - 0.87)
Weight-bearing tibial plateau	0.52 (0.05 - 0.80)	0.67 (0.27 - 0.87)

Table 3: *Correlation between meniscus and articular cartilage $T1_{GD}$ relaxation times. n: number of regions analyzed (torn menisci were excluded from our analyses). r: Pearson's correlation coefficients. 95% CI: 95% confidence interval.*

DISCUSSION

dGEMRIC is a frequently used technique to measure cartilage biochemical composition based on the amount of sGAG in the cartilage [93, 95]. Since the extracellular matrix of the meniscus also contains sGAG, dGEMRIM could give insight in biochemical composition of the meniscus tissue [186, 187]. Little research on dGEMRIM in healthy and pathologic menisci, however, has been performed yet.

The first aim of our study was to assess if menisci, identified as normal or degenerated on conventional MRI, also exhibit different $T1_{GD}$ relaxation times on dGEMRIM. We observed a clear trend towards lower $T1_{GD}$ in menisci identified as degenerated on conventional MRI compared to morphologically normal menisci, indicating more

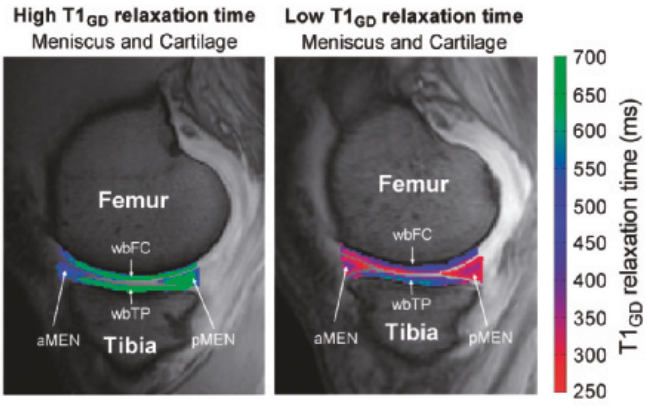

Figure 5. *Representative images with a meniscus and cartilage color maps showing relatively high $T1_{GD}$ (left: 55 year old male, Kellgren and Lawrence grade 1 and a morphologically normal meniscus on conventional MRI) and relatively low $T1_{GD}$ (right: 61 year old female, Kellgren and Lawrence grade 2 and a degenerated medial meniscus on conventional MRI) relaxation times in both tissues. wbFC: weight-bearing cartilage of the femoral condyle. wbTP: weight-bearing cartilage of the tibial plateau. aMEN: anterior horn of the meniscus. pMEN: posterior horn of the meniscus.*

gadolinium-enhancement in degenerated menisci on dGEMRIM. This result suggests that, similar to dGEMRIC, low $T1_{GD}$ in dGEMRIM may possibly be used as an indicator of meniscal degeneration, for example if no conventional MR images are available to identify meniscus degeneration in a research or clinical setting. In addition, it may be useful to assess both articular cartilage as well as meniscus degeneration within one delayed gadolinium-enhanced MR examination. This complementary information about both tissues might be useful for orthopedic surgeons to decide which treatment is indicated for individual patients since it has been shown that meniscus and cartilage quality are important predictors of clinical outcome after treatment of intra-articular pathology in the knee [192, 193].

The second aim of our study was to assess the reproducibility of $T1_{GD}$ of the meniscus in dGEMRIM. The results of our study demonstrate that the reproducibility of individual meniscus ROIs is good, regardless of the anatomical location within the knee joint. Our reproducibility results are similar to those of a previous study assessing the reproducibility 3D dGEMRIC at 3T in early stage OA (ICCs ranging between 0.87 – 0.95) [136], and indicates that dGEMRIM yields robust $T1_{GD}$ relaxation times of the meniscus and can thus be used in longitudinal study designs.

The third aim of our study was to assess the correlation between $T1_{GD}$ of the meniscus and the articular cartilage in patients with early stage knee OA. $T1_{GD}$ of the meniscus and cartilage were moderately to strongly correlated, indicating concurrent degeneration of both tissues in knee OA. The correlation in the medial compartment was stronger compared to the lateral compartment, which might be caused by the absence of lateral

OA in 11 of the 17 included participants. The strong correlation between meniscus and cartilage tissues we observed in our study is in agreement with previous research in which semi-quantitatively analyzed whole joint assessment of the knee showed an association between meniscal degeneration and cartilage loss in OA patients with a Kellgren and Lawrence grade > 2 [181]. In addition, Zarins *et al.* also found a strong correlation between quantitatively analyzed T1rho- (MRI measure for PG content [68]) and T2- (MRI measure for collagen content [194]) maps of meniscus and cartilage in OA patients [195]. Concurrent degeneration of the meniscus and cartilage in knee OA might also explain that the strength of the correlation we found between meniscal and cartilage $T1_{GD}$ is stronger (Pearson's correlation coefficients > 0.78 in the medial tibiofemoral knee compartment) than reported by Krishnan *et al*. who evaluated the correlation between $T1_{GD}$ in menisci and cartilage of healthy volunteers and patients with knee complaints who were not diagnosed with OA by their physician (Pearson's correlation coefficients ranging from 0.37 - 0.57 in the medial compartment) [186].

Since the sGAG constitutes only 1-2% of the total weight of the meniscus compared to 5-10% for articular cartilage [55, 153, 184, 188], it is questionable if sGAG is the only composite of the meniscus determining contrast influx into the meniscus. Li *et al.* analyzed delayed gadolinium-enhanced MRI acquired using both an ionic (inversely related to the sGAG content) and a non-ionic (no known interaction with sGAG content) contrast agent in the meniscus in patients with knee OA and healthy volunteers [196]. They observed significant differences in meniscus $T1_{GD}$ between OA patients and healthy volunteers for both ionic and non-ionic contrast agents, suggesting that sGAG content does not dominate contrast influx into the meniscus. Therefore, they concluded that contrast influx into the meniscus is rather based on the integrity of the collagen network of the meniscus. This result, combined with the strong correlation between $T1_{GD}$ in the meniscus and cartilage we found in the current study, leads to the hypothesis that the amount of sGAG is not the only composite of articular cartilage that determines ionic contrast influx into it in dGEMRIC. In another study, Li *et al.* also performed the aforementioned comparison between ionic and non-ionic contrast influx into OA cartilage and healthy cartilage [197]. They concluded that, in addition to the amount of sGAG, integrity of the cartilage collagen network also partially influences contrast influx into cartilage in dGEMRIC. This conclusion is supported by recent *in vitro* studies investigating ionic contrast diffusion into articular cartilage in dGEMRIC [142, 198, 199]. Furthermore, in a recent *ex vivo* study in which diffusion of an ionic CT contrast agent into cartilage (inverse relation between contrast agent and sGAG content of cartilage, thus similar to dGEMRIC) was investigated, it was also shown that the composition of the cartilage extracellular matrix influences ionic contrast influx into articular cartilage [200]. Therefore, the results of our current study, as well as those of others indicate that dGEMRIC should be regarded sGAG sensitive as advocated by Bashir *et al*. [65] and Watanabe *et al*. [91], but

that its specificity for sGAG is questionable. Therefore, outcomes of dGEMRIC must be interpreted with caution until future studies have evaluated the sGAG sensitivity and specificity of *in vivo* dGEMRIC.

The lack of a significant difference between normal and degenerated menisci may be caused by the design of our study. We analyzed delayed gadolinium-enhanced MR data of 17 early stage OA patients of which not all turned out to have meniscus degeneration, which may have caused insufficient statistical power in our analyses. Another limitation of our study is that conventional MR was acquired after intravenous contrast administration. However, we expect that this did not interact with the morphological evaluation of the menisci that was performed exclusively on proton-density and T2-weighted images, which are typically not, influenced by contrast agent. In addition, it is theoretically possible to divide the meniscus into a peripheral and central region. However, because of the relatively low in-plane spatial resolution of the MR images on which the ROI segmentation was performed, we considered differentiating between peripheral and central ROIs of the meniscus unreliable. Finally, we used dGEMRIC data in which some of the parameters of the MRI (e.g. contrast agent dose, delay between contrast administration and MR acquisition, and acquired TIs) were optimized for cartilage imaging and may therefore not be optimal for analysis of the meniscus. Especially the delay between contrast administration and MR acquisition is relatively short compared to Mayerhoefer *et al.* who suggest a delay of 2,5 – 4,5 hours [187]. However, we consider it more practical to use a single MRI protocol which can be used to analyze both meniscus and cartilage tissue within one MR examination since both are known to play a role in the development of knee OA [183].

Future studies using dGEMRIM should be conducted to further investigate its accuracy to detect meniscus degeneration before morphological or signal changes appear on conventional MRI. Although our results are promising, the relation between low $T1_{GD}$ as measure of meniscus compositional change should be validated against biochemical analyses and histology of meniscus composition. In addition, including a wider range of Kellgren and Lawrence grades (0 – 4 instead of only grade 1 and 2 as in the current study) could provide valuable information regarding the degree of degeneration of the meniscus in various stages of OA. Such studies could also investigate if torn menisci can be assessed for compositional changes using dGEMRIM by comparing $T1_{GD}$ outcomes of torn menisci against normal and degenerated menisci as well as to biochemical assays and histology. Future research might also benefit from using a combination of quantitative MRI techniques, e.g. delayed gadolinium-enhanced MRI and T2-, T1rho- and T2*-mapping which have been previously used to analyze meniscus composition [201, 202] since this might offer additional perspectives on the development of meniscus degeneration in knee OA in particular using MRI techniques that do not require a contrast agent.

In conclusion, the results of the current study show that degenerated menisci have a clear trend towards lower $T1_{GD}$ on dGEMRIM compared to normal menisci. Since these results are highly reproducible, meniscus degeneration may be assessed within one delayed gadolinium-enhanced MR examination simultaneously with articular cartilage. The strong correlation between meniscus and cartilage $T1_{GD}$ suggests concomitant degeneration in both tissues in OA, but also suggests that dGEMRIC may not be regarded entirely sGAG.

Part 2

CT based quantitative imaging biomarkers of cartilage sulphated glycosaminoglycan content

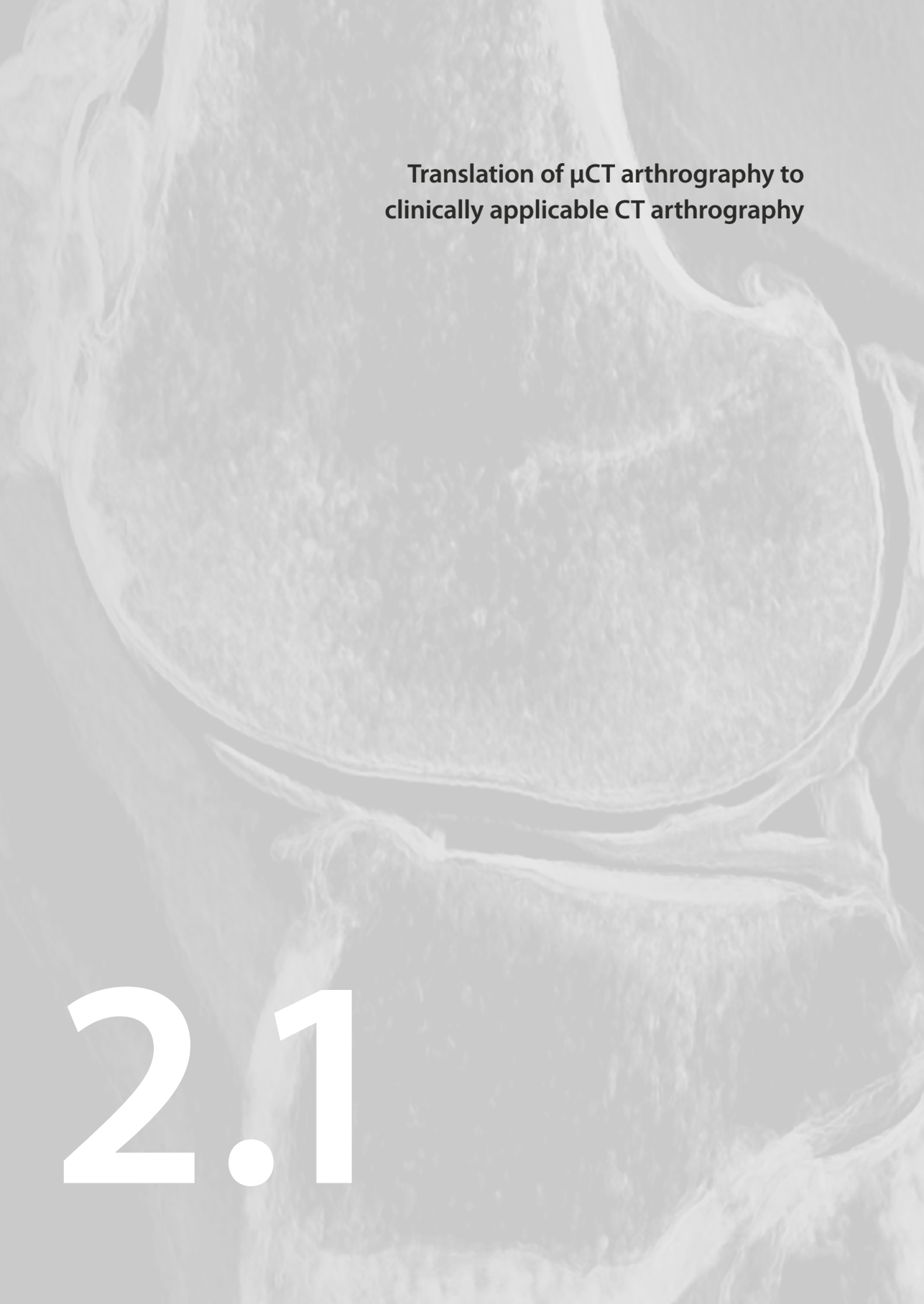

Translation of µCT arthrography to clinically applicable CT arthrography

2.1

Chapter 7

Clinically applied CT arthrography to measure the sulphated glycosaminoglycan content of cartilage

J. van Tiel, M. Siebelt, J.H. Waarsing, T.M. Piscaer, M. van Straten, R. Booij, M.L. Dijkshoorn, G.J. Kleinrensink, J.A. Verhaar, G.P. Krestin, H. Weinans, E.H. Oei.

Osteoarthritis Cartilage. 2011 Oct;19(10):1183-9.

ABSTRACT

Introduction

Similar to delayed gadolinium enhanced MRI of cartilage, it might be possible to image cartilage quality using CT arthrography (CTa). This study assessed the potential of CT arthrography as a clinically applicable tool to evaluate cartilage quality in terms of sulphated glycosaminoglycan content (sGAG) and structural composition of the extracellular matrix (ECM).

Materials and Methods

Eleven human cadaveric knee joints were scanned on a clinical CT scanner. Of each knee joint, a regular non-contrast CT (ncCT) and an ioxaglate injected CTa scan were performed. Mean X-ray attenuation of both scans were compared to identify contrast influx in seven anatomical regions of interest (ROI). All ROIs were rescanned with contrast-enhanced μCT, which served as the reference standard for sGAG content. Mean X-ray attenuation from both ncCT and CTa were correlated with μCT results and analyzed with linear regression. Additionally, residual values from the linear fit between ncCT and μCT were used as a covariate measure to identify the influence of structural composition of cartilage ECM on contrast diffusion into cartilage in CTa scans.

Results

CTa resulted in higher X-ray attenuation in cartilage compared to ncCT scans for all anatomical regions. Furthermore, CTa correlated excellent with reference μCT values (sGAG) ($R=0.86$; $R^2=0.73$; $p<0.0001$). When corrected for structural composition of cartilage ECM, this correlation improved substantially ($R=0.95$; $R^2= 0.90$; $p<0.0001$).

Conclusion

Contrast diffusion into articular cartilage detected with CTa correlates with sulphated glycosaminoglycan content and to a lesser extent with structural composition of cartilage ECM. CTa may be clinically applicable to quantitatively measure the quality of articular cartilage.

INTRODUCTION

The current reference standard for osteoarthritis (OA) staging is the Kellgren and Lawrence score based on knee radiography [28]. However, this technique is not sensitive enough to detect OA at an early stage. Sulphated glycosaminoglycan (sGAG) is a key molecule in articular cartilage and its content is an indicator of cartilage health [153]. Loss of sGAG from the articular cartilage is a hallmark of early OA and occurs well before OA is detected radiographically [56, 116].

Micro computed tomography (μCT) used together with a negatively charged contrast agent (ioxaglate) is a well-established technique to image sGAG-distribution in cartilage [78, 203, 204]. The technique is comparable to delayed gadolinium enhanced magnetic resonance imaging of cartilage (dGEMRIC) [64, 65, 93, 205, 206]. Previous *in vitro* work has shown that there is a clear inversed relationship between the amount of ioxaglate in the cartilage measured with μCT and the negatively charged sGAG content of the cartilage measured with biochemical essays (R^2 = 91-94%) [78, 203], and histology (R^2 = 77%) [79]. *In vivo* research in small animals has also demonstrated that μCT arthrography is able to accurately measure changes in cartilage quality [80, 81].

In humans, CT arthrography (CTa) using intra-articularly injected contrast agent is an established clinical technique for imaging of knee abnormalities [82, 83]. However, it is solely used for detection of morphologic derangements rather than assessment of cartilage sGAG content. In this cadaver study we determined whether it is possible to quantitatively measure the sGAG content of human articular cartilage with a clinical CT system, after intra-articular injection of a contrast agent. We also investigated to what extent the contrast influx into cartilage is influenced by the structural composition of the extra-cellular matrix (ECM).

MATERIALS AND METHODS

Cadaver specimens

Thirteen cadaveric lower extremities from eleven individuals who had donated their bodies to science (seven female, four male; mean age at death 74 years, age range at death 30 - 96 years) were available. All extremities were freshly frozen at -20ºC until start of the experiment. Prior to first imaging, all specimens were slowly defrosted in a cooled environment (7ºC) for 5 days. All extremities were at room temperature during imaging.

Acquisition and post processing of non-contrast CT and CT arthrography data

Non-contrast CT (ncCT) was performed of all knee joints using a second generation dual source multidetector spiral CT scanner (SOMATOM Definition Flash, Siemens Healthcare AG, Erlangen, Germany) with a tube voltage of 80kV and an effective mAs-value of 3140. Scan time per ncCT was approximately 30 seconds per scan. All specimens were scanned in the standard anatomic axial plane. All scans were reconstructed with an effective slice thickness of 0.75 mm and a sharp reconstruction kernel (B75s). Multiplanar reconstruction was performed (image pixel size 0.265mm) (*Figure 1A-C*).

Immediately after ncCT, 20ml of 30% ioxaglate solution (diluted in saline) (Hexabrix 320, Mallinckrodt, Hazelwood, MO, USA) [83] was injected intra-articularly using a 18 gauge needle. All knees were flexed (~120°) and extended (~0°) for 5 minutes in order to achieve optimal distribution of the contrast agent throughout the joint. Ten minutes after contrast injection, all knees were rescanned using the same CT scanner, scanning parameters (30 seconds/scan), and reconstruction methods (*Figure 1D-F*).

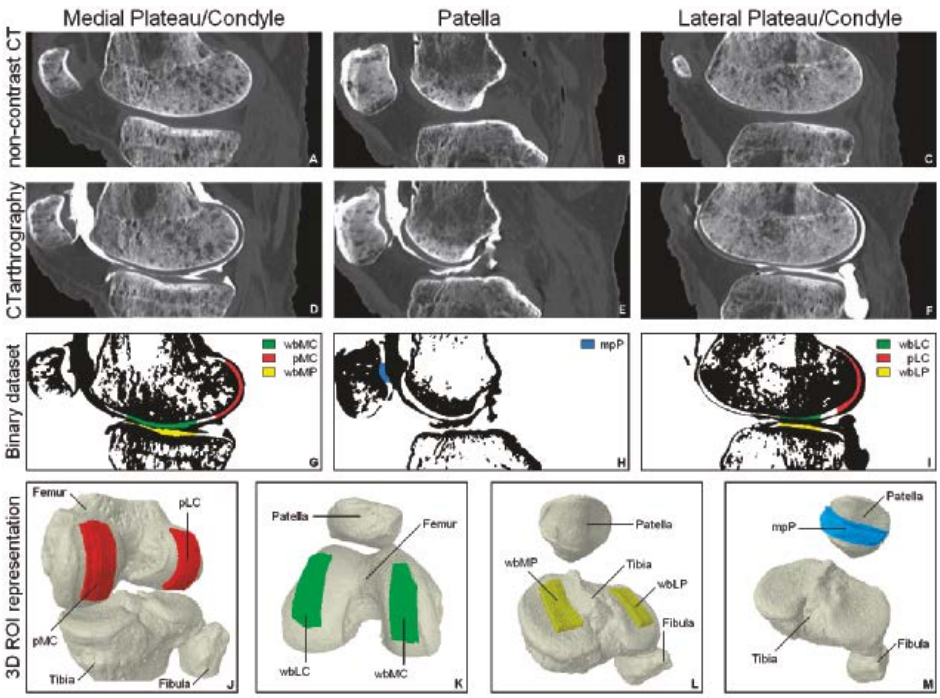

Figure 1: *Representative sagittally reconstructed images of a knee joint from non-contrast CT (ncCT) (A-C) and after intra-articular contrast injection for CT arthrography (CTa) (D-F), after segmentation into a binary dataset showing the definition of the regions of interest. (G-I), and a 3D representation of all seven analyzed ROIs (J-M): weight-bearing medial and lateral condyle (wbMC/wbLC; posterior medial and lateral condyle of the femur (pMC/pLC); weight-bearing medial and lateral plateau of the tibia (wbMP/wbLP); mid portion of patellar cartilage (mpP).*

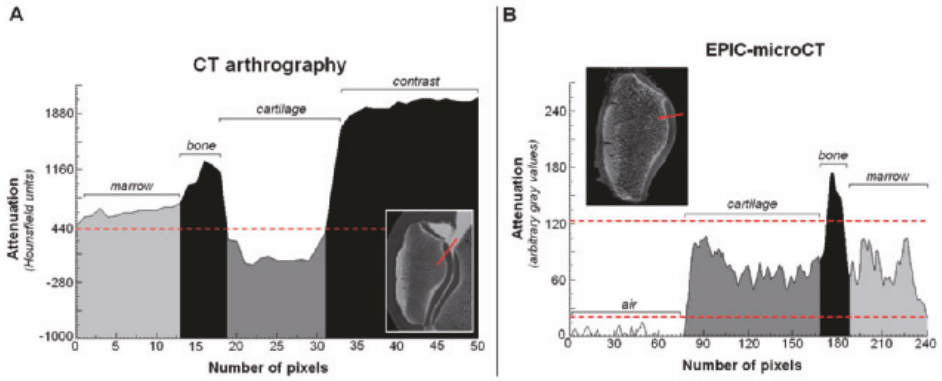

Figure 2: *Profile line through different structures (red line in insert) of both CT arthrography (A) and EPIC-microCT (B). On the x-axis subsequent pixels in the profile line are represented, the y-axis indicates the attenuation values of these pixels. With the red dotted line, we have visualized the level of our selected thresholds per technique (CT arthrography <430 Hounsfield units; EPIC-microCT >25 and <125 gray values).*

All scans were converted into binary datasets using one fixed attenuation threshold (430 Hounsfield units) that was selected visually to render the best possible segmentation of cartilage in all datasets (*Figure 1G-I*, *Figure 2*) [80]. Using analysis software (Skyscan, Kontich, Belgium), per knee seven regions of interest (ROIs) were manually defined. Each cartilage ROI extended over 40 contiguous sagittal slices. These cartilage ROIs consisted of the central weight-bearing area of both medial and lateral femoral condyles (wbMC and wbLC), the posterior non-weight bearing area of both femoral condyles (pMC and pLC), both weight-bearing medial and lateral tibial plateaus (wbMP and wbLP) and the mid-portion of patellar cartilage (mpP) (*Figure 1G-M*). Anterior margins of the weight-bearing femoral condyles and tibial plateaus were defined at the level of the posterior aspect of the anterior meniscal horn. The posterior margins were defined at the level of the anterior aspect of the posterior meniscal horn. The posterior non-weight bearing femoral condyle ROI extended backward from the level of the dorsal margin of the posterior meniscal horn. We calculated the mean X-ray attenuation of cartilage in these ROIs on non-contrast and contrast-enhanced clinical CT scans.

Equilibrium partitioning of an ionic contrast agent using (EPIC-)µCT

Because EPIC-µCT has shown strong correlation with cartilage sGAG content, we selected this as our reference test for sGAG content of cartilage [78, 79, 203]. In EPIC-µCT an equilibrium-state exists between sGAG and contrast agent after a long incubation period. Due to the equilibrium, structural composition of the cartilage ECM [199] does not influence the interaction between contrast and sGAG content of cartilage [79].

After CTa, the knee joints were dissected into five parts: both medial and lateral femoral condyles, both medial and lateral tibial plateaus and the patella. Soft tissue was

removed to a maximal extent, without harming cartilage integrity. In order to achieve equilibrium between the contrast agent and sGAG in cartilage, all dissected specimens were incubated in an ioxaglate contrast solution for 24 hours at room temperature [207-209]. It is advocated to use the highest possible concentration of contrast, allowing best cartilage segmentation to achieve highest sensitivity for changes in sGAG content [79, 204]. We used a 20% solution of ioxaglate, which resulted in the best cartilage segmentation at the air/cartilage and bone/cartilage interfaces.

EPIC-μCT was performed on a μCT scanner (Skyscan1076, Skyscan, Kontich, Belgium). The following scan settings were used: isotropic voxel size of 35 μm; a voltage of 55 kV; a current of 181 mA; field of view 68 mm; a 0.5 mm aluminum filter; 198° with a 0.4 degree rotation step. Scanning time per specimen was 6 - 10 hours, depending on the size of the specimen (condyle, plateau or patella) which was scanned. A plastic foil was wrapped around the specimen to avoid dehydration. All scans were performed using the same settings and all data were reconstructed identically.

Using Skyscan analysis software, these datasets were segmented using a fixed attenuation threshold between air (25 gray value) and subchondral bone (120 gray value) that was selected visually for the best segmentation result in all datasets. In all segmented μCT datasets, similar ROIs of the cartilage regions corresponding with ROIs of the clinical CTa were drawn and the mean X-ray attenuation was calculated again. These μCT based mean attenuation values were used as the reference for sGAG content against which the attenuation values on ncCT and CTa were compared.

Contrast diffusion influenced by structural composition of cartilage ECM

An important difference between the μCT and CTa scans is that with μCT scanning, the contrast agent and sGAG are partitioned at equilibrium. However, the principle of CTa is dependent on a diffusion process before equilibrium, which is influenced by the electrostatic interaction between sGAG and ioxaglate [81]. Therefore, measurements from non-equilibrium CTa are also influenced by other factors than sGAG content alone[207-209]. In particular, so-called tissue dragging influences the interaction between contrast and sGAG [210, 211]. A high tissue drag results from an intact collagen network and is predominantly present in the top layers of healthy cartilage where collagen is densely packed parallel to the cartilage surface and acts as a barrier membrane [212, 213]. Consequently, contrast diffusion goes slowly in regions with high tissue drag. When collagen is structurally impaired, e.g. in OA, tissue dragging diminishes and more contrast penetrates in comparison to healthy cartilage due to a higher diffusion rate.

In non-contrast CT, X-ray attenuation of cartilage results only from initial dissimilarities in cartilage composition (e.g. collagen, sGAG and water content). Together with the information on sGAG content from μCT, the influence of this structural composition of the cartilage on CTa outcome was further investigated using statistical models.

Statistical analysis

To assess if the influx of contrast agent into the cartilage could be detected, we compared the attenuation values per anatomical region between ncCT and CTa scans with paired student's t-tests. To evaluate to what extent the attenuation values represented sGAG content, we fitted linear regression models of the mean X-ray attenuation values of both the ncCT and CTa to the results of µCT scans for each knee compartment, of which we report the Pearson's correlation coefficients. To test if the correlation with µCT was different between ncCT and CTa, we compared the slopes of both models. These analyses were performed using GraphPad (GraphPad Software Inc., San Diego, USA).

In this study we used thirteen knees from eleven individuals. The use of two knees from one individual could potentially lead to an overestimation of the correlation between µCT and CTa measurements [214, 215]. Exclusion of either one of the knees in the two patients that were scanned bilaterally did, however, not influence the results of our study. Therefore, we did not apply a statistical correction.

Next, we investigated to what extent the influx of contrast was influenced by structural composition of cartilage ECM itself. The spatial variation in X-ray attenuation inside cartilage from ncCT scans is related to both structural composition of cartilage ECM and its sGAG content. Thus, when ncCT attenuation values are fitted to µCT values (representing sGAG content) using linear regression, the residuals, which is that part of the ncCT values which is not explained by µCT, contain information on structural composition independent of sGAG content. When these residuals are subsequently added as a covariable to the linear regression model that relates CTa to µCT values, the contribution of these residuals to the model represent the extent to which the influx of the contrast is influenced by structural composition of the cartilage ECM, independent of sGAG content. These analyses were performed using SPSS (SPSS Inc., Chicago, USA). All p-values < 0.05 were considered to be statistically significant.

RESULTS

Cadaver subjects

After CT scanning, three extremities were excluded from the study due to clearly visible calcifications inside the cartilage. Thus, a total of ten cadaveric knee joints from nine individuals were included in the analysis (six female, three male; mean age at death 69 years; age range at death 30 – 94 years).). Furthermore, 12 cartilage ROIs were not included in our data analysis because of (motion) artifacts during µCT scanning and segmentation errors because of severe cartilage loss [81].

sGAG correlation in ncCT and CTa

Mean X-ray attenuation results showed clear differences between the anatomical cartilage locations and between ncCT and CTa outcomes. In all locations, cartilage attenuation increased significantly after injection of contrast agent (*Figure 3A*).

Cartilage X-ray attenuation in ncCT correlated moderately with µCT (n=57, R=0.45; R^2=0.20; p=0.0003). The correlation between cartilage X-ray attenuation from CTa scans and µCT was strong (n=57, R=0.86; R^2=0.73; p<0.0001) (*Figure 3B*). The slopes of both regression lines were significantly different (p < 0.0001).

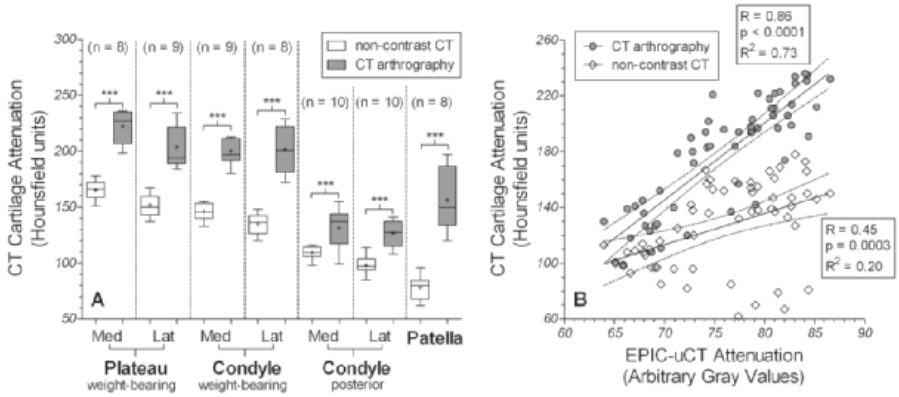

Figure 3: *Contrast diffusion into cartilage. Comparison of cartilage attenuation between non-contrast CT (ncCT) and CT arthrography (CTa) scans. A: Box plot of mean attenuation in cartilage from CT and CTa scans per anatomical region. Boxes range from 25th to 75th percentile, whiskers run from min to max, the horizontal line in the box represents the median and the plus sign shows the mean. B: Correlated results of mean attenuation from EPIC-µCT and clinical CT scans with and without injected contrast for all anatomical regions combined (n = 57). ***: p < 0.0001*

sGAG content per anatomical location

The cartilage attenuation derived from CTa for all separate anatomical compartments correlated strongly with attenuation from µCT (wbMP, wbLP: n=17, R=0.89, R^2=0.79, p<0.0001; wbMC, wbLC, pMC, pLC: n=33, R=0.87, R^2=0.75, p<0.0001; patella: n=8, R=0.89 R^2=0.7P, p=0.003; *Figure 4A-C*). There was a clear trend for all posterior condyle regions to have lower mean attenuation values, indicating that less contrast penetrated this less weight-bearing cartilage. The patellar values were clustered in a different location than the values for the other anatomical regions. When the data was analyzed for the tibiofemoral cartilage, the correlation coefficient was 0.92 (n=49, R^2=0.85, p<0.0001, *Figure 4D*). When all regions (including mpP cartilage) were pooled, the correlation diminished slightly (n=57, R=0.86, R^2=0.73, p<0.0001, *Figure 4E*).

To display the spatial agreement of both techniques, *Figure 5* shows representative images for cartilage attenuation for both CTa and µCT.

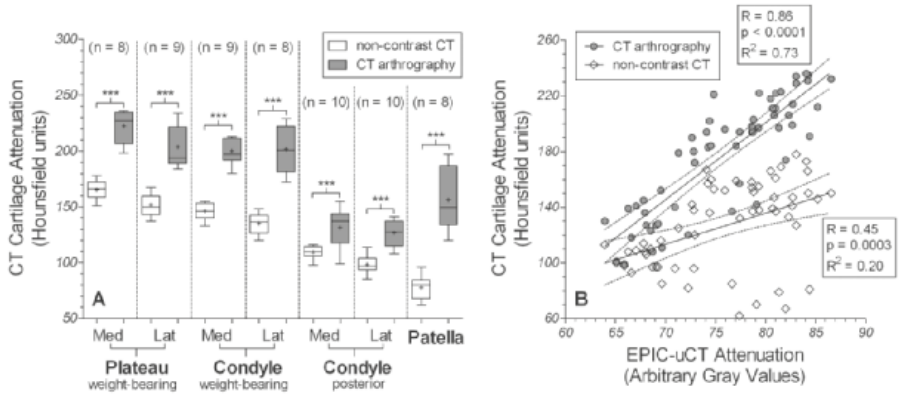

Figure 4: *Correlation plots of mean attenuation from EPIC-µCT and CT arthrography. A: weight-bearing cartilage of medial and lateral plateaus (n=17). B: weight-bearing and posterior cartilage of medial and lateral condyles (n=17). C: mid-portion of patellar cartilage (n=8). D: pooled results for both tibial and femoral compartments (n=49). E: pooled results for all regions of interest (n=57). The dashed lines indicate the 95% confidence interval of the best fit regression line. wbMP: weight-bearing medial plateau, wbMC: weight-bearing medial condyle, pMC: posterior medial condyle, mpP: mid-portion patella, wbLP: weight-bearing lateral plateau, wbLC: weight-bearing lateral condyle, pLC: posterior lateral condyle.*

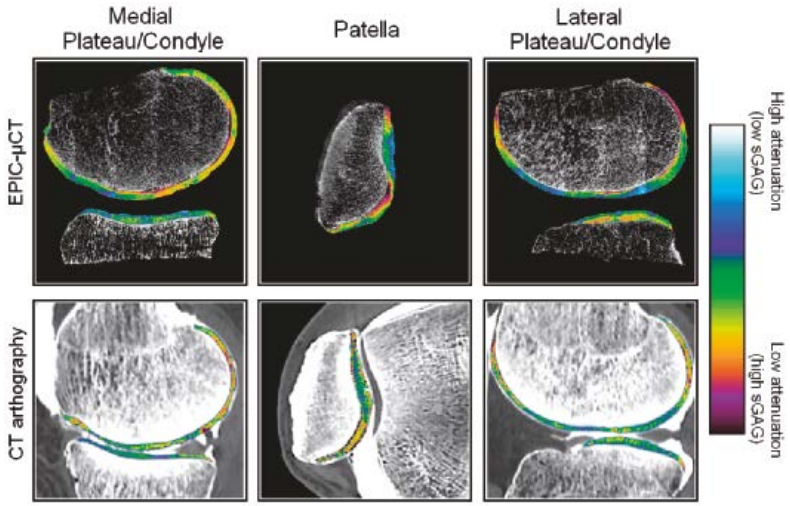

Figure 5: *Images of both EPIC-µCT and CT arthrography. The attenuation of cartilage regions is visualized in color and representative for sGAG content. High levels of attenuation represent a low sGAG-distribution.*

CTa corrected for structural composition of cartilage ECM

Figure 6 shows the results of the additional analysis into the role of structural composition of cartilage ECM for non-equilibrium CTa scans. When residual values from the model that fits µCT to ncCT, which represents structural composition of the ECM independent of sGAG, were added as a covariate to the model that fits µCT to CTa, the correlation coefficient was 0.95 (n=57, R^2=0.90; p<0.0001).

DISCUSSION

Quantitative imaging techniques are of the utmost necessity for development and monitoring of treatment strategies targeted at early OA. Therefore, imaging techniques (e.g. like dGEMRIC) are extensively studied for their capability to measure sGAG content. This cadaver study demonstrates that cartilage attenuation from CTa is influenced by

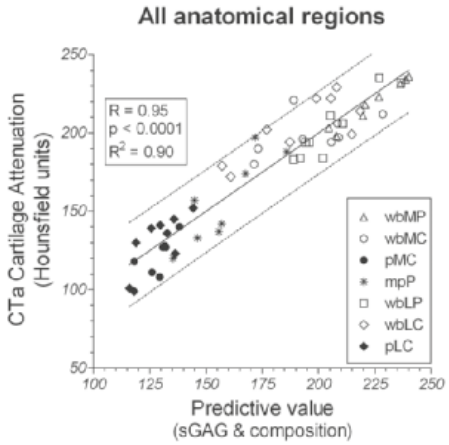

Figure 6: *Predictive CT arthrography value (horizontal axis) based best fitted model from EPIC-µCT (sGAG) and non-contrast CT residuals (cartilage ECM composition) correlated with mean attenuation of CT arthrography (vertical axis) (n=57). The dashed lines indicate the 95% confidence interval of the best fit regression line. wbMP: weight-bearing medial plateau, wbMC: weight-bearing medial condyle, pMC: posterior medial condyle, mpP: mid-portion patella, wbLP: weight-bearing lateral plateau, wbLC: weight-bearing lateral condyle, pLC: posterior lateral condyle.*

ioxaglate diffusion. And intra-articular injection of ionic ioxaglate significantly improved the correlation with the outcome of µCT. These results are similar to previous non-clinical reports [78, 208, 216], supporting our hypothesis that CTa can be used as a quantitative surrogate measure of the cartilage sulphated-glycosaminoglycan content.

Patellar cartilage is known to have a different structural ECM composition [217, 218]. In the µCT and CTa scatter plot the patellar values were located differently than the other anatomical locations. Exclusion of patellar cartilage from our analysis improved the predictive value of CTa for sGAG content (R^2 from 73% to 85%), indicating that structural composition of cartilage ECM influences the outcome of non-equilibrium CTa. When residual ncCT values representing structural composition of cartilage ECM were combined with µCT (sGAG content) as a predictive value for CTa, the R^2 values from the model fit to CTa increased from 73% to 90%. This improvement indicates to what extent contrast diffusion into cartilage is influenced by structural composition of cartilage ECM. In clinical practice, a correction for different contrast diffusion rates

cannot be calculated, since a reference standard for sGAG like EPIC-μCT is not available in clinical practice. Therefore, cartilage X-ray attenuation from CTa does not solely resemble sGAG content, but reflects a quality measure of cartilage, which also concerns the structural integrity of the ECM.

Despite these encouraging results, there are limitations of CTa that need to be addressed. For example, the intra-articular injection introduces the risk of infection and also increases the risk of patient complaint of knee pain after injection. Furthermore, the high concentrations of ioxaglate used in this study, could influence cartilage electro-mechanical properties [219].

CTa is best applied in early stages of OA, because with severe sGAG loss in advanced stages of OA segmentation errors will occur [81]. Usually, early OA progression develops in relatively young patients and obviously the main concern with (repetitive) CT scans at a younger age is radiation exposure. The total dose of the scanning protocol in this study (~2 mSv) was ten times higher in comparison to previously defined radiation doses of routine knee CT scans (~0.2 mSv) [220]. More research is needed to determine whether the same correlation with sGAG content can be measured if radiation dose is reduced.

MRI uses no ionizing radiation and during the last years, has seen a rapid improvement with several newly developed MR-based imaging techniques to measure articular cartilage quality (e.g. dGEMRIC, Na^{23} mapping, T2 mapping, and T1rho [154, 221]. Thanks to the more widespread availability of 3.0 Tesla MR systems and the development of novel MRI sequences (e.g. Ultrashort TE [222], SSFP [223], UTE T2* [224], and DENSE-FSE [225]), relatively fast MR scans can be acquired with high in plane resolution for (semi)quantitative cartilage imaging in OA research. However, these techniques still have several limitations: relative (e.g. claustrophobia) or absolute (e.g. pacemaker) contraindications for patients to undergo MRI, relatively low spatial resolution, and costs [226]).

Given our results in relation to previously reported outcomes of *in vivo* μCT arthrography studies in small animals with an intact circulation [80, 81], we believe that CTa may be able to measure cartilage quality in human patients in a clinical setting. CT has a short scanning time (~30 seconds), generates images with a high isotropic resolution. Therefore, CT techniques may be a valuable alternative to MR techniques, but more research is needed for this technique to find its place in clinics and research.

In our opinion, research should first focus on optimizing the CTa protocol for clinical use. The reproducibility of CTa measurements should be evaluated in an *in vivo* environment in which all factors that influence CTa outcomes are present (intact circulation, muscle tension, joint capsule strength, etc.). Future studies could also focus on the fact that recent *in vitro* studies indicate that X-ray attenuation of cartilage can predict certain biomechanical properties such as compressive stiffness [216]. Our finding that CTa outcome is influenced by sGAG and structural composition of cartilage ECM could be used to predict the biomechanical function of articular cartilage with CT.

In conclusion, the results of this cadaver study demonstrate the proof-of-principle that CTa is able to measure cartilage quality in human knee joints. A wide implementation of this quantitative analysis of articular cartilage may detect early changes in OA patients and may contribute to the development of new treatment strategies.

Chapter 8

CT arthrography of the human knee to measure cartilage quality with low radiation dose

J. van Tiel, M. Siebelt, J.H. Waarsing, T.M. Piscaer, M. van Straten, R. Booij, M.L. Dijkshoorn, G.J. Kleinrensink, J.A. Verhaar, G.P. Krestin, H. Weinans, E.H. Oei.

Osteoarthritis Cartilage. 2012 Jul;20(7):678-85.

ABSTRACT

Introduction

Recently, CT arthrography (CTa) was introduced as a possible technique to quantitatively measure cartilage quality in human knees. This study investigated whether this is also possible using lower radiation dose CT protocols. Furthermore, we studied the ability of (lower radiation) CTa to distinguish between local sGAG content differences.

Materials and Methods

Of ten human cadaveric knee joints, six CT scans using different radiation doses (81.33-8.13mGy) were acquired after intra-articular ioxaglate injection. The capability of CTa to measure overall cartilage quality was determined in seven anatomical regions of interest (ROIs), using EPIC-μCT as reference standard for sGAG content. To test the capability of CTa to spatially distinguish between local differences in sGAG content, we calculated the percentage of pixels incorrectly predicted as having high or low sGAG content by the different CTa protocols.

Results

Low radiation dose CTa correlated well with EPIC-μCT in large ROIs ($R=0.78;R^2=0.61;p<0.0001$). CTa can also distinguish between high and low sGAG content within a single slice. However, the percentage of incorrectly predicted quality pixels increases (from 35% to 41%) when less radiation is used. This makes is hard or even impossible to differentiate between spatial differences in sGAG content in the lowest radiation scans.

Conclusion

CTa acquired using low radiation exposure, comparable to a regular knee CT, is able to measure overall cartilage quality. Spatial sGAG distribution can also be determined using CTa, however for this purpose a higher radiation dose is necessary. Nevertheless, radiation dose reduction makes CTa suitable for quantitative analysis of cartilage in clinical research.

INTRODUCTION

The current reference standard for grading the severity of osteoarthritis (OA) in the knee is the radiography based Kellgren and Lawrence score [28]. This technique is, however, not sensitive enough to detect or follow OA at an early stage of the disease because it only indirectly visualizes the cartilage and is not able to (semi)quantitatively measure cartilage quality [33]. Therefore, sophisticated magnetic resonance imaging (MRI) imaging techniques have been developed which can qualitatively measure cartilage quality in terms of the sulphated glycosaminoglycan (sGAG), collagen or sodium content of articular cartilage [116, 154, 155].

Recently, it has been shown that CT arthrography of the knee (CTa) is able to measure overall cartilage quality in large anatomical cartilage regions in human cadaveric knees [200]. Similar to micro CT (μCT) arthrography in small animals [80, 81] and delayed gadolinium enhanced MRI of cartilage (dGEMRIC) in humans [65, 95, 227], this technique uses the inversed relationship between a negatively charged contrast agent (ioxaglate) and the sGAG content of cartilage.

The reported CTa protocol has a CT-Dose Index (CTDIvol) of 81.33 mGy per CTa scan, which poses a limitation on this technique [220]. Therefore, the radiation dose must be reduced before CTa can be used in clinical research. The use of less radiation to acquire CT scans results however, in an increase of noise in the reconstructed CT images. This increase of noise may influence the measured X-ray attenuation values and therefore interfere with the capability of measuring quality of cartilage using CTa.

Therefore, we designed a cadaver study with the purpose to investigate the effect of radiation dose reduction of CTa on its ability to measure articular cartilage quality in large cartilage regions. We also assessed the capability of CTa to distinguish between spatial high and low sGAG content of cartilage on a single slice and the influence of radiation dose reduction on this capability. The latter is of interest because it could enable the use of CTa as a tool to diagnose (focal) cartilage defects and follow the repair in these defects over time.

MATERIALS AND METHODS

Cadaveric knee joints

For this study, we used ten randomly selected cadaveric lower extremities from eight individuals who had donated their bodies to science. All extremities were frozen at -20ºC directly after death. Before the start of the experiment, the specimens were defrosted slowly in a cooled environment (7ºC) for five days. All extremities were at room temperature during imaging procedures.

Acquisition and post processing of CT arthrography data

We injected 20 milliliters of 30% ioxaglate dilution (Hexabrix 320, Mallinckrodt, Hazelwood, MO, USA and saline) intra-articularly in all knee joints, using an 18 gauge needle. After the injection, we flexed (~120°) and extended (~0°) the knee joints for five minutes in order to achieve optimal distribution of the contrast agent throughout the joint cavity. Ten minutes after contrast injection, CTa scans of all knee joints were acquired using a second generation dual source multidetector spiral CT scanner (SOMATOM Definition Flash, Siemens Healthcare AG, Erlangen, Germany) with a tube voltage of 80 kV, an effective mAs value of 3140 mAs, a pitch of 0.35 and a collimation of 32 x 0.6 mm, resulting in a CTDIvol of 81.33 mGy [200]. This protocol will be referred to as maximum dose in this paper. Directly after the first scan, five additional scans were acquired using the same tube voltage (80kV), but with reduced radiation exposures: 1570 mAs (50%), 1256 mAs (40%), 942 mAs (30%), 628 mAs (20%) and 314 mAs (10%) per scan. All knee joints were scanned in the axial plane with a scanning time of 30 seconds per scan. All CT datasets were reconstructed with an effective slice thickness of 0.75 mm and a sharp reconstruction kernel. Multiplanar reconstruction was performed (image pixel size 0.265mm).

Using Skyscan analysis software (Skyscan, Kontich, Belgium), we segmented all CT datasets into binary datasets using one fixed attenuation threshold of 500 Hounsfield units (HU) that was selected because it resulted in the best segmentation of the cartilage [200]. Next, we manually defined seven anatomical cartilage regions of interest (ROIs) in all CT datasets based on the nomenclature and scheme as suggested by Eckstein et al. [120]. Each ROI consisted of 40 consecutive slices covering the central weight bearing area of the cartilage of both the medial and lateral femoral condyles (wbMC and wbLC), the posterior non-weight bearing cartilage area of both femoral condyles (pMC and pLC), both weight bearing medial and lateral tibial plateaus (wbMP and wbLP) and

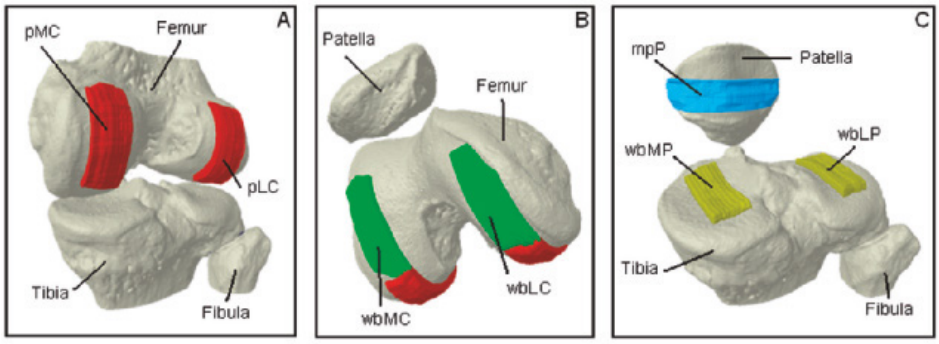

Figure 1: *3D representation of the seven analyzed large cartilage ROIs per knee joint: (A) posterior medial and lateral condyle of the femur (pMC/pLC); (B) weight-bearing medial and lateral femoral condyle (wbMC/wbLC); (C) weight-bearing medial and lateral plateau of the tibia (wbMP/wbLP) and mid portion of patellar cartilage (mpP).*

the mid-portion of the patellar cartilage (mpP) (*Figure 1A-C*). After defining all ROIs, we calculated the mean X-ray attenuation per cartilage ROI on the CTa scans.

Equilibrium partitioning of an ionic contrast agent using µCT

Mean X-ray attenuation values of equilibrium partitioning of an ionic contrast agent using (EPIC)-µCT have a good correlation with the sGAG content of articular cartilage measured with a dimethylmethylene blue essay or quantified with optical density measurements [78, 79, 203]. Therefore, we selected the outcomes of EPIC-µCT in mean X-ray attenuation values as our reference test of sGAG content of articular cartilage.

After CTa, all knee joints were dissected into five parts: the medial and lateral femoral condyles, the medial and lateral tibial plateaus and the patella. Soft tissue was removed to a maximal extent, without harming the integrity of the cartilage. In order to achieve equilibrium between the contrast agent and the sGAG content of the cartilage, all dissected specimens were incubated in an ioxaglate dilution (Hexabrix 320, Mallinckrodt, Hazelwood, MO, USA and saline) for 24 hours at room temperature [207-209]. We used a 20% dilution of ioxaglate, which resulted in the best cartilage segmentation at the air/cartilage and bone/cartilage interfaces [200] .

µCT scans were performed on a Skyscan 1076 *in vivo* µCT scanner (Skyscan, Kontich, Belgium). The following scan settings were used: isotropic voxel size of 35 µm; a voltage of 55 kV; a current of 181 mA; field of view 68 mm; a 0.5 mm aluminum filter; 198° with a 0.4 degree rotation step [200] . Scanning time per specimen was 6 - 10 hours, depending on the size of the specimen (patella, plateau or condyle). A plastic foil was wrapped around the specimen to avoid dehydration during scanning. All scans were performed using the same settings and all data were reconstructed identically.

Using Skyscan analysis software, we segmented the µCT datasets using a fixed attenuation threshold between air and subchondral bone that was selected visually for the best segmentation result in all datasets [200]. In all segmented µCT datasets, seven anatomical ROIs of the cartilage corresponding with ROIs of the CTa were drawn manually and the mean X-ray attenuation per ROI was calculated.

Spatial analysis of cartilage quality

Using commercially available software (Matlab version 7.1, MathWorks, Natick, MA, USA and Multimodality Image Registration using Information Theory (MIRIT), Laboratory for Medical Imaging Research, Leuven, Belgium [228]), all CTa (50%, 40%, 30%, 20% and 10%) and EPIC-µCT datasets were registered using the dataset that was acquired at the maximum dose as reference. Registration of the datasets enabled comparison of corresponding cartilage regions (femoral condyles, tibial plateaus and patellar cartilage) in all CTa scans per knee.

To study the capability of CTa to analyze the spatial distribution of high and low sGAG content in cartilage and the influence of radiation dose reduction on this capability, we used the EPIC-µCT as reference standard for spatial sGAG distribution in cartilage (*Figure 2A*) [78, 79, 203]. Using Skyscan analysis software, we defined an area of high and low sGAG content in the cartilage within a central slice through the medial and lateral tibiofemoral joint and on a central slice of the mid-potion of the patellar cartilage in all CTa datasets (maximum dose, 50%, 40%, etc.) (*Figure 2B-D*). To define these areas (which we will refer to as masks from now on), we used 150 HU as cut-off point between high and low sGAG content of cartilage. We used this number based on the point where the cumulative histogram of all cartilage ROIs used in the spatial analysis of cartilage reaches 50% (*Figure 3*). Next, both masks for sGAG distribution were used as an overlay for cartilage on the registered corresponding EPIC-µCT images (*Figure 2E-F*). Within the masked EPIC-µCT images, we calculated the number of pixels defined as having high

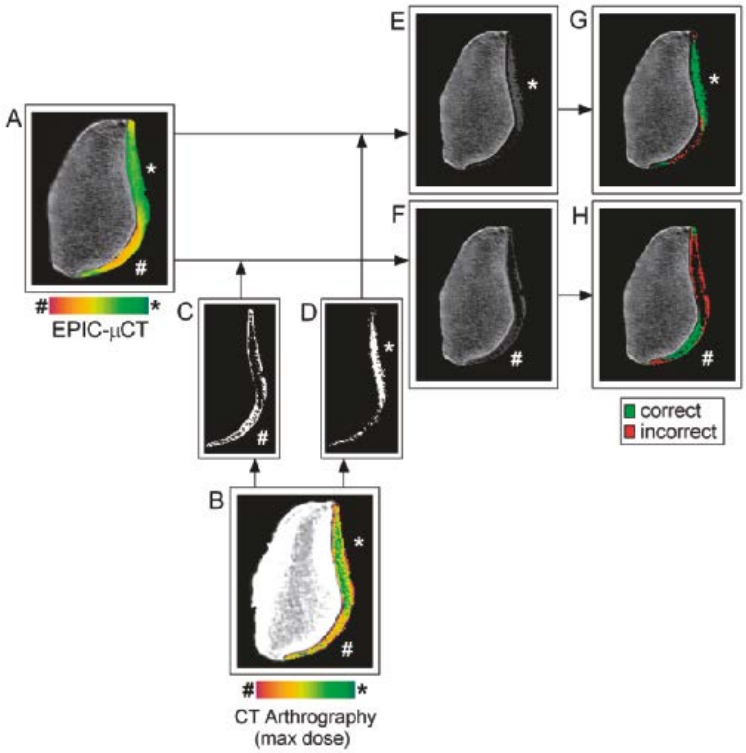

Figure 2: *EPIC-µCT datasets are used as reference for the spatial sGAG distribution of cartilage (A). Using a fixed X-ray attenuation threshold of 150 Hounsfield Units in all CTa datasets (B, only maximum radiation dose shown), a mask for high and low sGAG content was created (C-D). The masks were used as an overlay of EPIC-µCT cartilage (E-F). Within the masked EPIC-µCT images, the number of pixels correctly and incorrectly predicted as having a high and low sGAG content by CTa was calculated (G-H). #: high sGAG content. *: low sGAG content.*

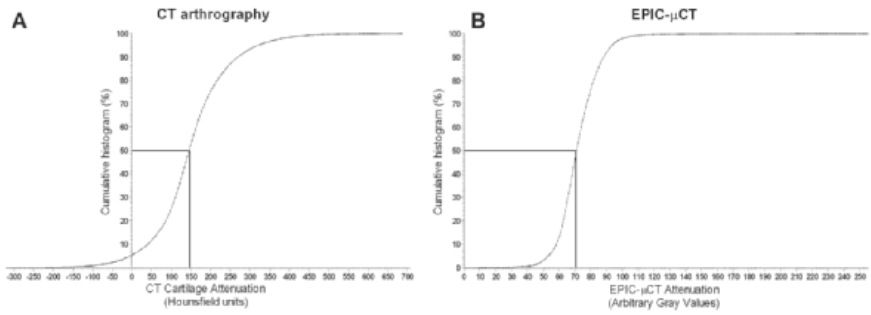

Figure 3: *Cumulative histograms of both CT arthrography (A) and EPIC-µCT (B). On the x-axis the attenuation values in Hounsfield Units (CT arthrography) and gray values (EPIC-µCT), the y-axis indicates the percentage of pixels within the histogram with a certain attenuation value and all attenuation values below that value. With the black line, we have visualized the level of our selected thresholds (50% of the cumulative histogram) per technique as cut-of point between high and low sGAG content of cartilage (CT arthrography 150 Hounsfield Units, EPIC-µCT 70 gray values).*

or low sGAG content by CTa, using a threshold of 70 gray values for EPIC-µCT. This was again based on the cumulative histogram of all cartilage ROIs on the EPIC-µCT images (*Figure 3*). Finally, we calculated the number of pixels which were incorrectly defined as high or low quality by CTa by adding the number of incorrectly defined pixels in both masks, dividing them by the total number of pixels in both masks together and then multiplying them by 100 to obtain the percentage of incorrectly defined pixels (*Figure 2G-H*).

Statistical analysis

In this study we used ten knees from eight individuals. The use of two knees from one individual could potentially lead to an overestimation of the correlation between µCT and CTa measurements [214, 215]. Exclusion of either one of the knees in the two patients that were scanned bilaterally did not influence the results of our study. Therefore, we decided to exclude the bilaterally scanned knees from the analysis.

The correlation between the mean X-ray attenuation values of CTa and the mean X-ray attenuation values of EPIC-µCT was calculated per radiation dose for all cartilage ROIs pooled. Because of the fact that we analyzed seven cartilage ROIs per knee joint and the potential correlation which might already exist within all knee joints itself, we used a linear mixed model to analyze if the correlation coefficients between, CTa outcomes and EPIC-µCT outcomes were statistically significant.

All analyses were performed using GraphPad (GraphPad Software Inc., San Diego, USA) and SPSS version 17.0 (SPSS Inc., Chicago, USA). All p-values < 0.05 were considered to be statistically significant.

RESULTS

Cadaveric knee joints

After CT scanning, four knees were excluded from the study due to clearly visible calcifications in the cartilage and due to the fact that from two individuals two knees were scanned. Thus, a total of six cadaveric knee joints from six individuals were included in the analysis (three female, three male; mean age at death 72 years; age range at death 30 – 94 years). Furthermore, 12 cartilage ROIs were not included in our data analysis because of motion artifacts during µCT scanning and segmentation errors due to severe cartilage loss [81].

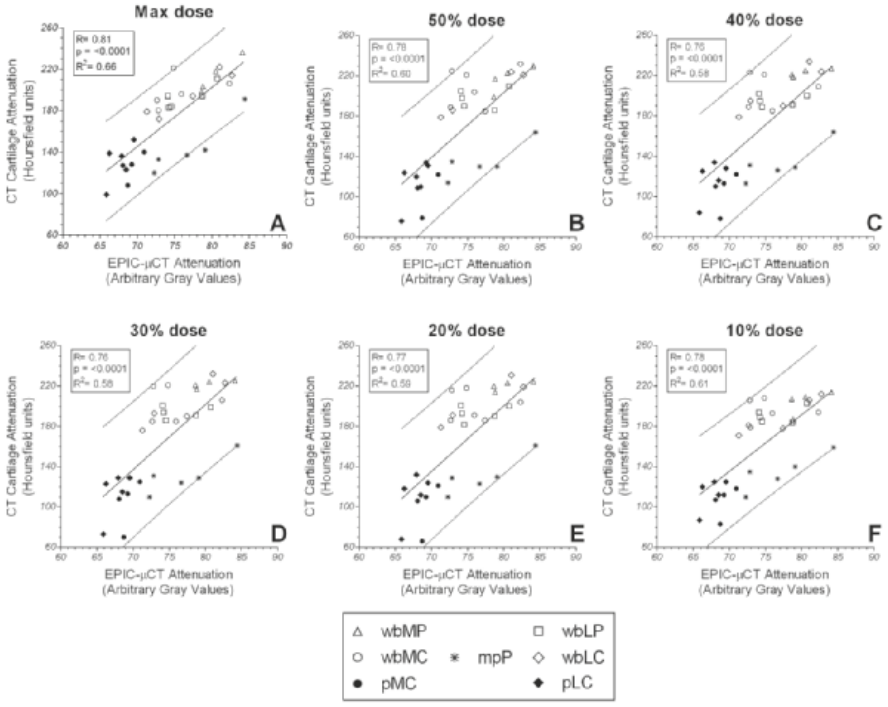

Figure 4: *Correlation plots of mean attenuation from EPIC-µCT and CT arthrography acquired using six different radiation doses. A: maximum radiation dose (n=33); B: 50% of the maximum radiation dose (n=33); C: 40% of the maximum radiation dose (n=33); D: 30% of the maximum radiation dose (n=33); E: 20% of the maximum radiation dose (n=33); F: 10% of the maximum radiation dose (n=33). The dashed lines indicate the 95% confidence interval of the best fit regression line. wbMP: weight-bearing medial plateau; wbMC: weight-bearing medial condyle; pMC: posterior medial condyle; mpP: mid-portion patella; wbLP: weight-bearing lateral plateau; wbLC: weight-bearing lateral condyle; pLC: posterior lateral condyle.*

Correlation of CTa with sGAG content in large anatomical ROIs

Mean X-ray attenuation values of the CTa scans acquired with maximum radiation correlated strongly with the sGAG content of cartilage expressed by EPIC-µCT attenuation values (n=33; R=0.81; R^2=0.66; p<0.0001) (*Figure 4A*). In the analysis of the additional CTa scans with reduced radiation dose, this correlation remained strong when radiation dose was reduced; 50% of the maximum radiation dose (n=33; R=0.78; R^2=0.60; p<0.0001), 40% of the maximum radiation dose (n=33; R=0.76; R^2=0.58; p<0.0001), 30% of the maximum radiation dose (n=33; R=0.76; R^2=0.59; p<0.0001), 20% of the maximum radiation dose (n=33; R=0.77; R^2=0.59; p<0.0001), and 10% of the maximum radiation dose (n=33; R=0.78; R^2=0.61; p<0.0001) radiation dose per scan was used (*Figure 4B-F*).

Spatial analysis of cartilage quality

The number of pixels that were incorrectly defined as having high or low sGAG content by CTa was lowest in the CTa scan acquired using the maximum radiation dose (35% ± 9%) (*Figure 5*). When less radiation was used to obtain CTa, the number of pixels which were incorrectly defined as high and low quality cartilage increased (50% radiation: 37% ± 9%, 40% radiation: 38% ± 9%, 30% radiation: 38% ± 9%, 20% radiation: 39% ± 9%, 10% radiation: 40% ± 9%) (*Figure 5*). The effect of this increase in incorrectly defined pixels on the capability of CTa to distinguish between the spatial distribution of high and low sGAG content of cartilage within a single slice is clearly visible in *Figure 6*.

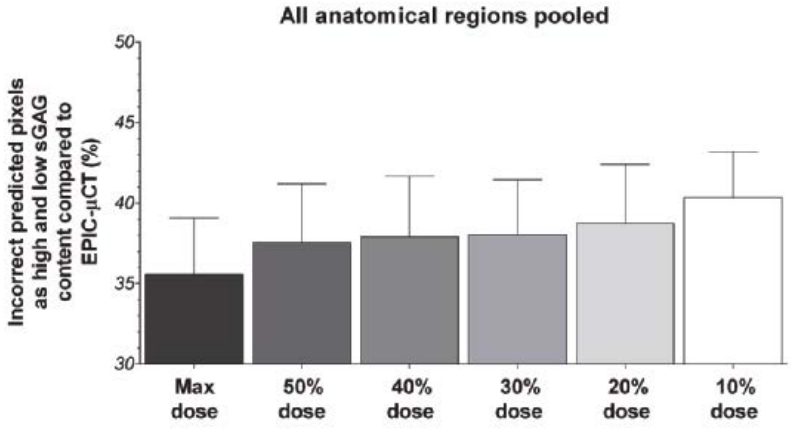

Figure 5: *Bar graphs showing the percentage of pixels incorrectly predicted as high and low sGAG content by the different radiation doses (maximum, 50%, 40%, 30%, 20% and 10% of the maximum dose) used in this study. Whiskers show the 95% confidence interval of the mean.*

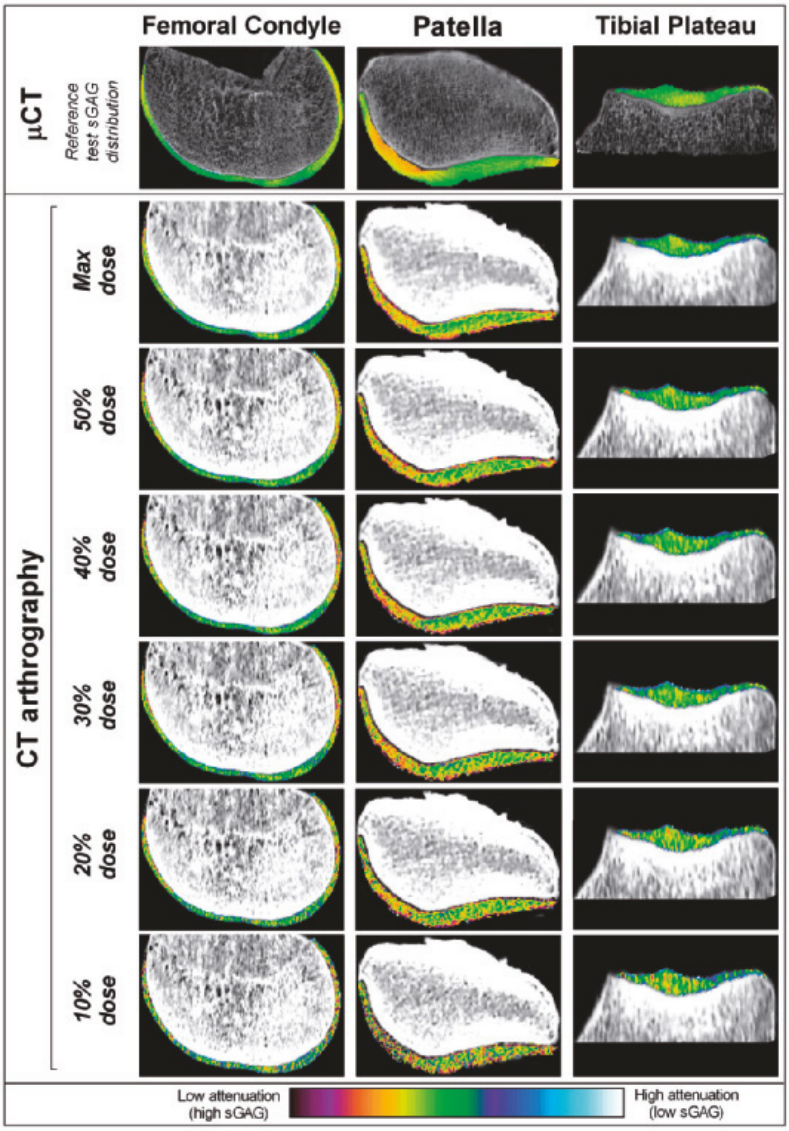

Figure 6: *Registered images of both EPIC-µCT and CT arthrography acquired using different radiation doses (maximum radiation dose, 50%, 40%, 30%, 20% and 10% of the maximum radiation dose) per scan. The attenuation of cartilage regions is visualized in color and representative for the sGAG content of the cartilage. High attenuation values represent low sGAG content and low attenuation values represent high sGAG content.*

DISCUSSION

Recently, CTa was introduced as a non-destructive method to measure cartilage quality in human cadaveric knees [200]. The main aim of the present cadaver study was to assess whether radiation dose reduction influences the ability of CTa to measure cartilage quality. Lowering the ionizing radiation dose of the acquisition protocol is necessary to make CTa suitable and acceptable for use in clinical research in humans. The results of this study demonstrate that mean attenuation values in large anatomical ROIs in CTa acquired with different radiation doses are strongly correlated with the sGAG content of articular cartilage measured with EPIC-μCT. This correlation was similar to previous reported results in cadavers [200] and also similar to previously published *in vitro* results [78, 208, 216]. When the radiation dose used to acquire CT scans was decreased, the correlation between CTa X-ray attenuation values and the sGAG content of cartilage only slightly decreased, but remained good, even if the radiation dose was reduced to approximately 10% of the original dose. The correlation between X-ray attenuation and the reference test for sGAG content remains relatively good because of the fact that the noise in the CT images averages out when calculating the mean X-ray attenuation values in relatively large cartilage ROIs.

The second aim of this study was to assess the capability of CTa to detect local differences in the sGAG content of articular cartilage and to study the effect of radiation dose reduction on this differentiation of cartilage quality within a single slice. The ability to detect local differences in cartilage sGAG content could make CTa applicable as a diagnostic tool for focal cartilage damage instead of a diagnostic arthroscopy. Additionally, it would enable the use of CTa as an imaging tool to measure the effect of cartilage repair therapies (e.g. microfracturing and autologous chondrocyte implantation [14, 126] similar to MRI based techniques like dGEMRIC [111, 114]. Our results demonstrate that, using CTa acquired using the maximum radiation dose, high and low sGAG distribution can be clearly distinguished. An important remark is that the choice of the used thresholds for defining high and low sGAG content within the cartilage based on the pooled cumulative histograms has an arbitrary component. This might introduce an over or underestimation of the capability of CTa to determine local sGAG differences. The increase of noise in the CT image obtained using lowered radiation doses, however, causes an increased percentage of incorrectly defined pixels with high and low sGAG content. In the lowest radiation dose used to obtain CTa, the increased noise even makes it impossible to distinguish differences in sGAG distribution from noise in the CT images.

Based on the results of this study, we suggest using a CTa protocol with a low radiation dose if overall cartilage quality is of interest in clinical research. The lowest radiation dose we used (CTDIvol of 8.13 mGy per scan) is comparable to the dose of a regular CT

scan of the knee (CTDIvol of approximately 8 mGy [220]). In addition to cartilage quality, morphological abnormalities can also be diagnosed using CTa with accuracy comparable to conventional MRI sequences. This was demonstrated in previous research by De Filippo et al. and Vande Berg et al. [82, 229], however, we did not investigate this in the present study. If the spatial distribution of sGAG on a single slice is of interest, we recommend using a higher radiation dose than for overall cartilage quality measurements since decrease in CNR increases the number of incorrectly predicted quality pixels and makes it hard or impossible to differentiate high from low quality cartilage at low radiation dose scans.

Despite the promising results, a limitation of CTa will remain the use of ionizing radiation, because of the risk of predisposing patients to the development of certain cancers by using (repetitive) CT scans [220]. Therefore, MRI based techniques which quantitatively measure cartilage quality (e.g. dGEMRIC, Na^{23} mapping, T2 mapping, and T1rho [154, 155]) remain favorable in a clinical research setting in large cohorts in humans. However, we think that by using a relatively low radiation dose protocol, subgroups of patients in which CTa is favorable of MRI can be identified (e.g. patients with contra-indications to undergo MRI). In addition, CT has also some advantages over MRI (e.g., relative short acquisition time and low costs). Therefore, we expect that low radiation dose CTa can become a complementary technique to MRI based techniques to quantitatively measure cartilage quality in clinical research. In addition to ionizing radiation, other potential limitations of CTa when applied in humans are: the risk of infection and pain due to the intra-articular injection with contrast agent, and the risk of an (allergic) reaction to the contrast agent.

Future research using CTa should focus on implementing and validating CTa in a clinical research setting in humans *in vivo* using a low radiation dose protocol. Filtering the CT data using a low-pass image processing filter will diminish the amount of noise in CT images and might enable the use of even less radiation than suggested in our study. A drawback of using such a filter is, however, the decrease in spatial resolution of the CT images. Another method to lower the radiation dose is the use of an iterative reconstruction algorithm [230, 231] instead of the standard filtered back projection image reconstruction algorithm as used in this study. Because of the high in plane resolution of CT images acquired with multidetector CT scanners, future research could also focus on investigating the potential of CTa to detect subchondral bone changes and changes in cartilage quality simultaneously. Recently, the feasibility of contrast-enhanced peripheral quantitative CT to analyze cartilage and subchondral bone status on a single scan *in vitro* was described [232] and therefore it is of interest to test this as well as *in vivo* using CTa.

In conclusion, CTa acquired using a low radiation dose is able to measure overall articular cartilage quality throughout the whole human knee with a radiation dose

comparable to a regular CT scan of the knee. Spatial sGAG distribution assessment is also possible using CTa, however for this purpose a higher radiation dose is necessary. Nevertheless, due to the reduction in radiation dose, CTa might be implemented as a non-destructive tool to quantitatively measure articular cartilage in clinical research.

Validation of CT arthrography as imaging biomarker in human osteoarthritis research

2.2

Chapter 6

Quantitative in vivo CT arthrography of the human osteoarthritic knee to estimate cartilage sulphated glycosaminoglycan content: correlation with ex-vivo reference standards

J. van Tiel, M. Siebelt, M. Reijman, P.K. Bos,
J.H. Waarsing, A.M. Zuurmond, K. Nasserinejad,
G.J. van Osch, J.A. Verhaar, G.P. Krestin,
H. Weinans, E.H. Oei.

Osteoarthritis Cartilage. 2015. Revision submitted

ABSTRACT

Introduction

Recently, computed tomography arthrography (CTa) was introduced as quantitative imaging biomarker to estimate cartilage sulphated glycosaminoglycan (sGAG) content in human cadaveric knees. The aim of the present study was to assess the correlation between in vivo CTa in human knees with osteoarthritis (OA) and ex vivo reference standards for sGAG and collagen content.

Materials and Methods

In this prospective observational study 11 knee OA patients underwent CTa before total knee replacement (TKR). Cartilage CTa X-ray attenuation was determined in 6 anatomical regions of interest. Femoral and tibial cartilage specimens harvested during TKR were scanned using equilibrium partitioning of an ionic contrast agent with micro-CT (EPIC-μCT), which served as reference standard for sGAG. Next, cartilage sGAG and collagen content were determined using dimethylmethylene blue (DMMB) and hydroxyproline assays. The correlation between CTa X-ray attenuation, EPIC-μCT X-ray attenuation, sGAG content and collagen content was assessed.

Results

CTa X-ray attenuation correlated well with EPIC-μCT (r=0.76, 95% confidence interval (95%CI) 0.64 to 0.85). CTa correlated moderately with the DMMB assay for sGAG content (r=-0.66, 95%CI -0.87 to -0.49) and to lesser extent with the hydroxyproline assay for collagen content (r=-0.56, 95%CI -0.70 to -0.36).

Conclusion

Outcomes of CTa applied in vivo in human OA knees correlates well with sGAG content. Outcomes of CTa also slightly correlate with cartilage collagen content. However, since outcomes of CTa are mainly sGAG dependent, CTa may be suitable as quantitative imaging biomarker to estimate cartilage sGAG content in future clinical OA research.

INTRODUCTION

Knee osteoarthritis (OA) is the most common joint disease in middle-aged and elderly, causing serious morbidity and large socio-economic impact [8, 9]. Since no definitive treatment options other than joint replacement surgery in end stage OA are available, research focuses on development of disease-modifying osteoarthritis drugs (DMOADs) which may be effective in early OA, for example by improving cartilage biochemical composition [13, 128].

To non-invasively monitor effectiveness of these novel interventions on cartilage biochemical composition, imaging techniques are essential. Therefore, quantitative imaging assessing important cartilage composites i.e. sulphated glycosaminoglycan (sGAG) and collagen, became of interest [129] .

Most imaging techniques applied in clinical research are magnetic resonance imaging (MRI) based, e.g. delayed gadolinium-enhanced MRI of cartilage (dGEMRIC) for analyzing sGAG content [93] and T2-mapping for analyzing collagen content [233]. Computed tomography (CT) based techniques have also been developed, but are mainly applied in *in vitro* or animal research. Examples are: equilibrium partitioning of an ionic contrast agent using micro-CT (EPIC-µCT) and µCT arthrography estimate sGAG content [78-81, 203, 234, 235].

Recently, a clinically applicable protocol for CT arthrography (CTa) was introduced as a potential alternative technique to MRI based estimate of cartilage biochemical composition [200]. *Ex vivo* CTa in human cadaveric knee joints was shown to be a quantitative imaging biomarker cartilage sGAG content by exploiting its inverse relation with an ionic contrast agent similar to dGEMRIC [200]. However, outcomes of CTa were also dependent on integrity of the collagen network of cartilage, which influences the speed of contrast influx into cartilage [200]. Although CTa was already applied *in vivo* by comparing its outcomes to dGEMRIC and cartilage morphology observed during arthroscopy [236, 237], these studies did not assess the correlation between CTa and reference standards for cartilage biochemical composition and were not performed in knee OA patients which constitute an important target population for quantitative imaging techniques for cartilage composition.

The aim of this study was to assess the correlation between *in vivo* CTa in human knees with OA and *ex vivo* reference standards for sGAG and collagen content.

MATERIALS AND METHODS

Study design and participants

For this prospective observational study, conducted between October 2012 and December 2013, all consecutive patients scheduled for total knee replacement (TKR) at our institution were approached.

The inclusion criteria were: age ≥ 18 years and radiographic knee OA with asymmetric distribution and a maximum of grade 1-2 (doubtful or definite osteophyte formation without definite joint space narrowing) according to the Kellgren & Lawrence (KL) grading system [28] in the least affected tibiofemoral compartment. We chose to include only these patients to be sure that we captured a relatively wide range of cartilage quality and therefore also sGAG content of the articular cartilage. Exclusion criteria were: glomerular filtration rate < 60 ml/min, previous reactions to CT contrast agent and co-morbidities in the ipsilateral lower extremity precluding exercise after contrast administration.

We performed a power analysis in which we used the Fisher transformation [238] to assess the number of measurements needed to establish a correlation coefficient of at least 0.7 (considered a good correlation [239]) with a predefined 95% confidence interval (95%CI) width of 0.5 - 0.9, and found that 25 measurements would be needed. Since six measurements are performed per participant, three participants would be enough for our study. Because we considered this number very low, we decided to include at least 10 participants (60 measurements for the correlation analyses) until the end date of the study (December 2013).

The study was approved by the institutional review board of our institution (MEC-2012-218) and written informed consent was obtained from all participants.

Acquisition of CT arthrography

CTa was performed four weeks before TKR. This time window was chosen to allow detection of infection caused by the intra-articular injection well before surgery. Patients were positioned in a supine position and after disinfection, 15 ml 30% ioxaglate (Hexabrix 320, Mallinckrodt, Hazelwood, USA) and 70% 1% phosphate buffered saline (PBS) solution was injected intra-articularly using a 21 gauge needle [200] and a superolateral approach [160]. We first aspirated synovial fluid from the knee in order to confirm that the needle was positioned in the knee joint and to ensure that we could inject the 15 ml of contrast dilution while minimizing further dilution due to extensive joint effusion. To promote contrast distribution throughout the joint, participants actively exercised their knee for two minutes over the full possible range of motion immediately after the injection.

Ten minutes post-injection, CT in the axial plane was acquired using a dual-source multidetector spiral CT scanner (SOMATOM Definition Flash, Siemens Healthcare AG, Germany). We used a tube voltage of 80 kV, units of current of 3140 mAs, pitch of 0.35

and collimation of 32 x 0.6 mm [200]. Scan time was approximately 30 seconds. These parameters resulted in an effective radiation dose of 0.4 millisievert (mSv) and an effective skin dose of 120 milligray (mGy) which is well below the threshold of 1000 mGy above which deterministic effects on the skin are expected [240].

All scans were reconstructed in the sagittal plane with an effective slice thickness of 0.75 mm and a sharp reconstruction kernel. Multiplanar reconstruction was performed resulting in an image voxel size of 0.265 by 0.265 mm, e.g. an in-plane resolution of 512 x 512 voxels.

Analysis of CT arthrography

Reconstructed datasets were segmented into binary datasets using a local attenuation threshold algorithm (3D-Calc, Skyscan, Kontich, Belgium) (*Figure 1A-D*) [81, 241] . These binary datasets (*Figure 1C-D*) were used to manually draw six cartilage regions of interest

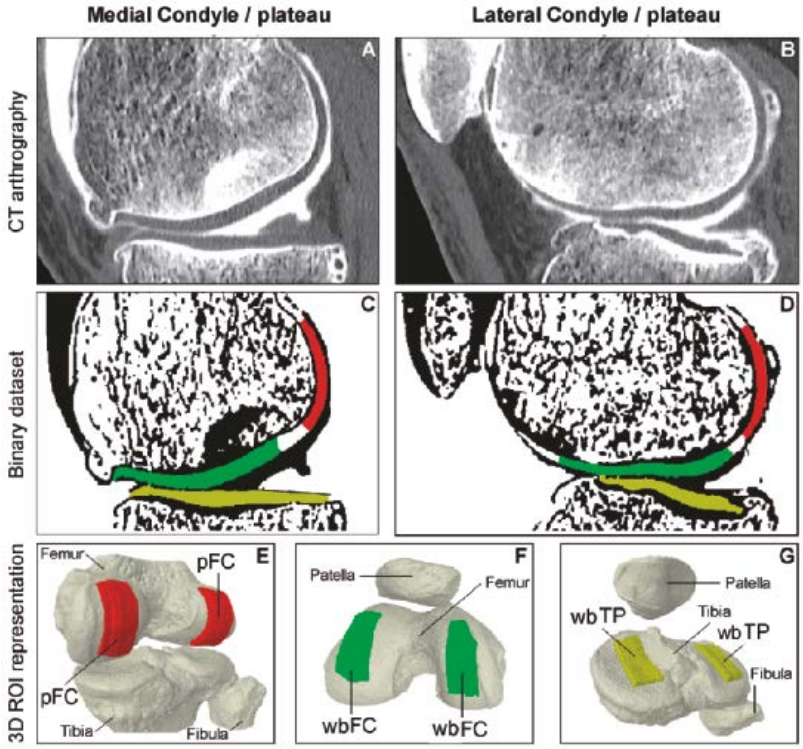

Figure 1: *Regions of interest in CTa and EPIC-µCT datasets. Representative sagittally reconstructed images of a medial and lateral compartment of a knee joint which underwent CTa (A-B). After segmentation into a binary datasets, the different regions of interest are shown in 2D (C-D) and in a 3D representation: the posterior non-weight-bearing cartilage of the femoral condyles (pFC) (E), the weight-bearing cartilage of the femoral condyles (wbFC) (F) and the weight-bearing cartilage of the tibial plateaus (wbTP) (G). After image registration, the same ROIs were analyzed in EPIC-µCT datasets.*

(ROIs): posterior non-weight-bearing femoral cartilage (pFC) (*Figure 1E*), weight-bearing femoral cartilage (wbFC) (*Figure 1F*) and weight-bearing tibial cartilage (wbTP) of the medial and lateral tibiofemoral compartment (*Figure 1G*). Each ROI consisted of 40 contiguous slices and was manually drawn by a researcher with four years of experience in musculoskeletal imaging (JvT) using CT Analyser software (Skyscan, Kontich, Belgium). In each ROI, mean cartilage X-ray attenuation was calculated using CT Analyser.

Harvesting of cartilage and acquisition of EPIC-µCT

During TKR, weight-bearing and non-weight-bearing femoral cartilage and weight-bearing tibial cartilage with adjacent subchondral bone were harvested, stored in saline and transported directly to the laboratory.

We used EPIC-µCT as reference standard for cartilage sGAG content since its outcomes have a good correlation with cartilage sGAG content [78, 79, 203]. Similar to CTa, EPIC-µCT provides information on sGAG distribution of cartilage within the entire cartilage volume, allowing analysis of articular cartilage regions exactly matching the cartilage ROIs analyzed with CTa.

Between 30 minutes and 1 hour after surgery, all specimens were removed from the saline and incubated in ioxaglate solution for 24 hours at room temperature [207-209]. A 20% ioxaglate with 80% PBS 1% solution was used since this results in optimal cartilage segmentation at the air/cartilage and bone/cartilage interfaces [200]. The contrast solution also contained Ethylenediaminetetraacetic acid (EDTA) (Sigma Aldrich, St Louis, USA) and protease inhibitors (Roche, Basel, Switzerland) to prevent sGAG removal from the specimen during incubation.

EPIC-µCT was performed using a Skyscan 1076 (Skyscan, Kontich, Belgium) with the following scan settings: isotropic voxel size of 35 µm; voltage of 95 kV; current of 100 mA; field of view 68 mm with a 1.0 mm aluminum / 0.25 mm copper filter over 198° with a 0.36 degree rotation step. Plastic foil was wrapped around the specimen to avoid dehydration during scanning. Depending on the size of the specimen, scan time was 0.5 – 1.5 hours. The datasets were reconstructed identically using NRecon software (Skyscan, Kontich, Belgium).

Analysis of EPIC-µCT

To enable comparison of corresponding cartilage regions, EPIC-µCT datasets were registered to CTa datasets with Multimodality Image Registration using Information Theory (MIRIT, University of Leuven) [228]. This automated registration algorithm uses a rigid transformation model (translations and rotations) and uses mutual information as a similarity measure for the registration of the µCT datasets to the CT datasets. Next, using CT Analyser software, datasets were segmented into binary datasets using a previously determined fixed attenuation threshold (25 gray values for air and 120 gray

values for subchondral bone) [200]. In the segmented µCT datasets, cartilage ROIs corresponding with ROIs of CTa were drawn and mean X-ray attenuation was calculated.

Biochemical cartilage analyses

After acquisition of EPIC-µCT, four (posterior femoral cartilage), six or eight (weight-bearing femoral and plateau cartilage based on the size) full thickness cartilage explants of 6 mm diameter were taken using a biopsy punch from standardized locations corresponding with cartilage of the ROIs analyzed with CTa and EPIC-µCT. Location and number of cartilage explants were chosen to ensure representative cartilage samples in each ROI.

Since ioxaglate used for EPIC-µCT might interact with biochemical assays (pilot tests, data not shown), explants were washed at room temperature for 24 hours in 1% PBS. During washing, EDTA and protease inhibitors were added to prevent sGAG loss from cartilage. Next, explants were cut in halves and stored separately in airtight tubes at -20 °C together with the washing solution.

Before biochemical analyses were performed, explants were thawed at room temperature. One half of each explant was digested in papain solution containing 250 µg/ml papain and 5 MM l-cytein HCl overnight at 60 ºC. sGAG content in cartilage and in the washing solution of the matching explant was quantified with the 1,9dimethylmethylene blue (DMMB) dye binding assay at pH 3 described by Farndale *et al.* [138]. Absorption ratios at 540nm and 595 nm were used to calculate sGAG content using chondroitin sulphate (Sigma Aldrich, St Louis, USA) as standard. Total sGAG content in explant and washing solution was calculated to correct for possible loss of sGAG during washing.

The other half of each explant was used to quantify collagen content based on the hydroxyproline content according to Bank *et al.* [139]. Samples were digested with alpha-chymotrypsin followed by a papain solution and digests were hydrolyzed with equal volumes 12M HCl at 95 ºC overnight. Samples were then dried and re-dissolved in water. Hydroxyproline content was measured using a colorimetric method with chloramine-T and dimethylaminobenzaldehyde as reagents and hydroxyproline as standard (Merck, Darmstadt, Germany) at extinction 570 nm. Values of degraded and intact collagen content were summed, resulting in total collagen content per explant.

Next, for each ROI four to eight explants were used to calculate the mean sGAG and collagen content by averaging the content of the explants taken from that specific ROI. The mean sGAG and the mean collagen content of a specific cartilage ROI could then be correlated with the mean CT and µCT attenuation in the matching ROI.

Statistical analysis

To assess the correlation between CTa and reference tests (EPIC-μCT, sGAG content and collagen content), a four-dimensional multivariate mixed-effects model was applied. In this model, it is assumed that the CTa and the reference tests are multivariately normally distributed (i.e. $Y \sim N_4(\mu,\Sigma)$, where Y = (CTa, EPIC-μCT, sGAG content, collagen content); μ and Σ are the mean vector (i.e. $\mu = (\mu_1 = CTa, \mu_2 = EPIC\text{-}\mu CT, \mu_3 = sGAG\ content, \mu_4 = collagen\ content)$) and covariance matrix of these variables, respectively. To take into account potential intrinsic correlation between outcomes of different ROIs within one participant, a random intercept was included in the model (e.g. $\mu_{1,i,j.} = \beta_1 + b_{1,J}$; i = 1, … , 11, j; j= 1, …, 62).

Pearson's correlation coefficients of CTa and each reference test were extracted from the results of this model. For each Pearson's correlation coefficient the 95%CI was calculated. To assess goodness-of-fit, we used an omnibus posterior predictive check (PPC) [242]. We computed a Bayesian p-value with extreme values of this p-value (e.g., < 0:05 or > 0:95) indicating a poor fit of the model to the data [242].

To assess if the correlation coefficients calculated within the model were significantly different, we calculated the contour probability of the correlations. For these values, similar to the Bayesian p-value, extreme values, i.e. <0.05 or >0.95, indicate that there is a statistically significant difference between two correlation coefficients [243]. These analyses were performed using a Bayesian approach with Markov chain Monte Carlo (McMC) sampling using WinBugs [140].

RESULTS

Participants

Fourteen patients were included. Two participants were excluded because their TKR was postponed after inclusion, in one participant ioxaglate was injected extra-articularly and four cartilage specimens (two weight-bearing cartilage specimens of the medial tibial plateau, one posterior non-weight-bearing cartilage specimen of the lateral femoral condyle and one weight-bearing cartilage specimen of the medial femoral condyle) were severely damaged during surgery and were therefore excluded from the analysis. Therefore, results are based on data of 11 participants (5 women and 6 men, 7 left and 4 right knees).

The mean age with standard deviation was 64 ± 7 years and their mean body mass index with standard deviation was 33 ± 6 kg/m^2. The KL grades in the medial tibiofemoral compartments were 3 or 4 in seven participants and 1 or 2 in four participants. KL grades in the lateral tibiofemoral compartments were 1 or 2 in nine participants and 3 in two participants. We did not observe any adverse reactions related to the intra-articular contrast injections.

Correlation of CTa, EPIC-µCT and biochemical cartilage analyses

For the applied four-dimensional mixed-effects model, the Bayesian p-value of the PPC was 0.52, which indicates that the model assumptions appear to be satisfied.

Mean CTa X-ray attenuation in all femoral and tibial cartilage ROIs correlated well with attenuation of EPIC-µCT (r=0.76, 95%CI 0.64 to 0.85; *Figure 2A*). When each ROI was analyzed separately, the range of correlation coefficients between outcomes of CTa and EPIC-µCT was 0.75 to 0.80.

The correlation between CTa and sGAG content measured using the DMMB assay was moderate (r=-0.66, 95%CI -0.87 to -0.49; *Figure 2B*). A range of -0.75 to -0.60 was observed for the correlation coefficients between X-ray attenuation of CTa and sGAG content in all separate cartilage ROIs.

The correlation between outcomes of CTa and collagen content measured using the hydroxyproline assay was also moderate (r=-0.56, 95%CI -0.70 to -0.36; *Figure 2C*). Here, a range of correlation coefficients from -0.56 to -0.51 was obtained for each separate ROI.

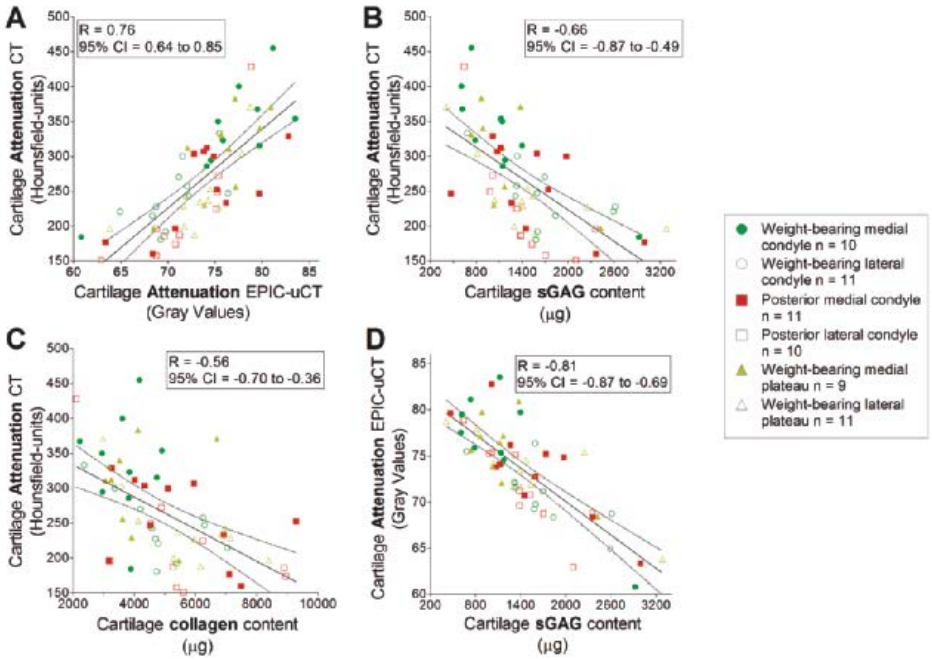

Figure 2: *Correlation plots of CTa, EPIC-µCT and ex vivo reference standards for sGAG and collagen content of articular cartilage. Correlation plots of mean attenuation of CTa in all anatomical ROIs with EPIC-µCT attenuation (A), sGAG content of the cartilage measured with DMMB assay (B), collagen content of the cartilage measured with hydroxyproline assay (C) and mean attenuation of EPIC-µCT and sGAG content measured with DMMB assay (D). The dashed lines indicate the 95% confidence interval of the Pearson's correlation coefficient.*

Mean EPIC-µCT outcomes and sGAG content measured using the DMMB assay correlated well (r=-0.81, 95%CI -0.87 to -0.69; *Figure 2D*). The range of correlation coefficients for each separate ROI was -0.82 to -0.75.

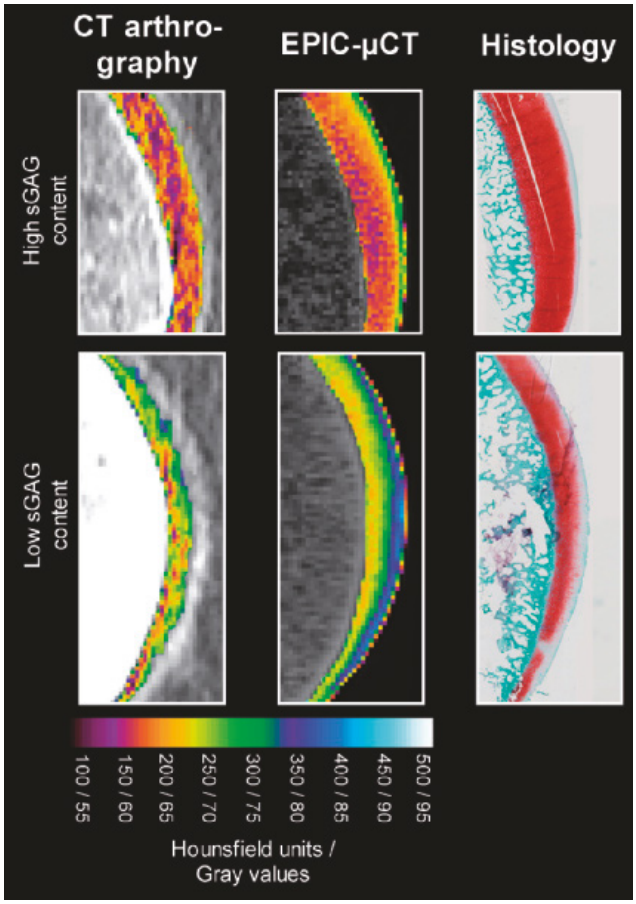

Figure 3: *Cartilage sGAG content estimated using CTa, EPIC-µCT and histology. Representative images of matching sagittal slides of CTa, EPIC-µCT and histology (see appendix 1 below this figure caption fot the methods used for preparation and staining of the bone-cartilage specimen with safranin-O). The attenuation of cartilage is visualized in color: A high attenuation represents a low sGAG content of cartilage and a low attenuation represents a high sGAG content. A high intensity of safranin-O staining on histology represents a high sGAG content and a low intensity or discoloration represents a low or absent sGAG content. The top row shows visual agreement in high cartilage sGAG content and the bottom row shows visual agreement for low cartilage sGAG content.*

Appendix 1: After acquiring all cartilage biopsies for the EPIC-µCT specimen, the bone-cartilage specimens were fixed using a paraformaldehyde solution for one week. Next, the specimens were decalcified using formic acid for four weeks and embedded in paraffin. After embedding, sagittal sections of 5 µm were acquired in the central (non)-weight-bearing area of the specimen which was determined visually. Those slices were stained with safranin-O to image the sGAG distribution. All specimens were stained in one batch. After staining the images we visually selected two slices, which matched with the imaging outcomes on approximately the same sagittal slice through the central (non)-weight-bearing area of the particular specimen.

By calculating the p-values of the contour probability of the different correlations we observed that the correlation between CTa and EPIC-μCT was significantly different from the correlation between CTa and sGAG or collagen content (contour probability > 0.99). The correlation between EPIC-μCT and sGAG content was significantly different from the correlation between EPIC-μCT and collagen content (contour probability = 0.002). The other correlation coefficients did not differ significantly from each other.

The matched images of CTa, EPIC-μCT and histology (visual representation of sGAG content using Safranin-O staining) representing cartilage with relatively high and low sGAG content shown in *figure 3* confirmed the good correlation between CTa and EPIC-μCT and cartilage sGAG content.

DISCUSSION

Quantitative imaging biomarkers that non-invasively estimate cartilage biochemical composition are essential for development and monitoring of DMOADs in OA. This study was performed to assess the correlation between *in vivo* CTa in human OA knees and *ex vivo* reference standards for sGAG and collagen content.

Our results show a good correlation between X-ray attenuation of CTa and EPIC-μCT and a somewhat less pronounced correlation between CTa and cartilage sGAG content determined by the DMMB assay. These results are in agreement with previous research showing a good correlation between outcomes of CTa acquired in *ex vivo* human cadaveric knee joints and EPIC-μCT [200]. The results are also consistent with several previous *in vitro* studies examining the correlation between contrast-enhanced (micro) CT and the sGAG content of articular cartilage [78, 79, 203]. Therefore, we believe that CTa X-ray attenuation may be used as a quantitative estimate for sGAG content of articular cartilage in future clinical OA research.

The difference in strength of correlation between CTa and sGAG content measured using EPIC-μCT versus DMMB assay might be caused by the fact that the attenuation of EPIC-μCT and cartilage sGAG content are well correlated, but not by a linear relationship. This indicates that, although not fully specific, EPIC-μCT is good reference test for cartilage sGAG content. Due to the aforementioned, we think that we observed a difference in strength of the correlation between CTa and EPIC-μCT compared to CTa and sGAG content as measured using the DMMB assay. Another explanation for the difference in strength of correlation may be that the ROIs in CTa and EPIC-μCT were matched exactly by image registration while the DMMB assay was limited to assessment of sGAG content in representative cartilage explants that did not correspond exactly with the cartilage volume of the imaging ROIs. We chose this approach since we considered it to be reliable to analyze representative focal cartilage explants taken

from standardized locations out of the cartilage ROIs analyzed using CTa and EPIC-μCT. Since there were no large spatial differences in sGAG distribution within cartilage ROIs in EPIC-μCT (data not shown), we are convinced that this did not influence our results compared to analyzing total cartilage ROIs using the DMMB assay.

We found a moderate correlation between outcomes of CTa and collagen content of cartilage measured using the hydroxyproline assay. This result could potentially be explained by a strong relation between collagen and sGAG content of cartilage and a concomitant loss of sGAG and collagen in the OA process. Cartilage sGAG and collagen content were, however, only weakly correlated in our study (r=0.40, data not shown). This indicates that, in addition to sGAG content, the integrity of the collagen network also influences contrast influx into cartilage as suggested in previous *ex vivo* research [200]. It is important to note that in CTa, there is no equilibrium between cartilage sGAG content and the contrast agent because CTa images are acquired already 10 minutes after contrast administration. This is unlike EPIC-μCT in which cartilage is incubated in contrast agent for 24 hours [78, 79, 203]. Therefore, measurements from non-equilibrium CTa are also influenced by other factors than sGAG content alone [207-209]. In particular, the collagen network of the extracellular matrix of the cartilage, which determines the permeability of the cartilage, influences the diffusion rate of contrast agent into the cartilage besides its sGAG content [210, 211]. Contrast diffusion goes slowly in healthy cartilage, in which an intact collagen network and densely packed collagen parallel to the cartilage surface result a relative low permeability of the cartilage [212, 213]. When the collagen network is impaired, e.g. in case of loss of collagen content, cartilage permeability increases, resulting in higher diffusion rate of contrast into the cartilage. The influence of collagen content of cartilage on CTa outcomes, however, is less pronounced compared to the influence of cartilage sGAG content since the correlations were significantly different. This suggests that, although not totally sGAG specific, CTa may be considered a useful imaging biomarker to estimate cartilage sGAG content in future human OA research.

CTa might be a worthwhile quantitative biochemical cartilage imaging technique in future clinical research additional to contrast-enhanced MRI based techniques used for the same purpose. CTa has a relatively fast acquisition time and can be acquired already ten minutes after contrast administration, while the delay between intravenous contrast administration in knee dGEMRIC is at least 1.5 hours [95]. This makes CTa more patient friendly and clinically feasible than MRI. Moreover, in the generally middle-aged or elderly OA population, the relative long acquisition time of MRI compared to CT (minutes versus seconds) and the number of patients with possible contra-indication for MRI (for example non MRI compatible implants) may favor CTa as an alternative to MRI in clinical OA research [244]. CTa might also be applicable as imaging biomarker for

cartilage biochemical composition in large cohort studies since it is relatively cheap and widely available [245].

Potential limitations of CTa include concerns of ionizing radiation. The effective radiation dose used for CTa as presented in this paper (0.4 mSv) is four times higher than a regular CT of the knee [220]. However, it has been shown that CTa acquired using only 10% of this dose also has a good correlation with cartilage sGAG content *ex vivo* in cadaveric knees [246]. Besides, active knee flexion and extension may be impossible for the full range of motion for OA patients, resulting in variations in contrast concentration across the knee joint. Recent research by Silvast *et al.*, however, shows that differences in contrast concentration do not influence the speed of contrast influx into cartilage and would therefore not influence the reliability of CTa outcomes [198]. Finally, although not observed in our study and also not reported in other studies applying CTa *in vivo* in humans [236, 237, 247], the intra-articular injection introduces the risk of infection and increases the risk of knee pain after injection. It may be worthwhile to perform fluoroscopic-guided intra-articular injections in future research with CTa since this may overcome the problem of extra-articular contrast agent deposition, which happened in one of our study participants, however against increased costs and logistic complexity of the procedure.

Based on our results and despite the potential drawbacks we propose that CTa may be applicable in future clinical OA research. Of course, more research is needed, particularly to assess reproducibility in OA patients before CTa could be applied in cross-sectional and longitudinal studies. Such a reproducibility study might also benefit from including more participants and different delays between contrast administration and CT acquisition to assess if this influences the correlation between CTa and cartilage composition in full thickness ROIs. In addition, a depth-wise analysis to assess the effect of different concentrations of cartilage composites throughout the extracellular matrix and across the cartilage layer would be interesting. For such a study it would be interesting to include patellar cartilage, which is thicker and has been shown to have a different composition than femoral and tibial cartilage [248]. In addition, nowadays OA is considered a whole joint disease in which not only cartilage, but also subchondral bone, menisci and synovium play important roles in disease development and progression [22]. The simultaneous analysis of cartilage and subchondral bone was also described previously in *in vitro* studies using contrast-enhanced μCT [232, 249]. It would also be worthwhile to assess the ability of CTa to evaluate cartilage and meniscus composition within one examination. Simultaneous analysis of cartilage and meniscus composition has recently been described for contrast-enhanced MRI [143, 250] and contrast-enhanced CT *in vitro* [251, 252]. Finally, future research might assess the possibility of injecting the contrast agent intravenously instead of intra-articularly to make the technique more patient friendly. This dGEMRIC like approach will, however, be challenging because the

intra-articular contrast is also used for the purpose of cartilage segmentation. Moreover, an intravenous approach requires a longer delay between contrast administration and acquisition of the CT scan.

In conclusion, our study shows that when applied *in vivo* in human OA knees, X-ray attenuation of CTa correlates well with sGAG content. Outcomes of CTa also slightly correlate with cartilage collagen content. However, since outcomes of CTa are mainly sGAG dependent, CTa may be suitable as quantitative imaging biomarker to estimate cartilage sGAG content in future clinical OA research.

Chapter 10

General discussion, conclusions and future perspectives

QUANTITATIVE IMAGING BIOMARKERS OF CARTILAGE COMPOSITION IN OSTEOARTHRITIS RESEARCH

For a long time, radiography and subsequently conventional magnetic resonance imaging (MRI) were used as imaging biomarkers for evaluating cartilage morphological disease state in osteoarthritis (OA) research [253]. Because research is switching its focus towards disease-modifying OA drugs (DMOADs) in order to target OA at an early stage of disease, quantitative imaging biomarkers for cartilage composition became of interest during the last decade [128, 129, 254, 255]. Therefore, several MRI based techniques to (indirectly) measure the sulphated glycosaminoglycan (sGAG) content of the extracellular matrix of articular cartilage were or are being translated to clinical OA research. Examples of such techniques are delayed gadolinium-enhanced MRI of cartilage (dGEMRIC) [93, 95], T1rho-mapping [131, 132], sodium imaging [74, 75] and sGAG specific chemical exchange saturation transfer (gagCEST) [76, 256].

Despite all efforts with regard to translation, validation and application of these techniques in clinical research, until now, only dGEMRIC has been shown to be a robust and valid imaging biomarker for cartilage sGAG content in human OA subjects [88, 91, chapters 3 and 4]. Contrary to what was suggested *in vitro* or *ex vivo* [134], T1rho-mapping seems not suitable as an imaging biomarker for sGAG content in human OA cartilage [69, 90, chapter 4]. Sodium imaging and gagCEST are both validated and reproducible *in vivo* as sGAG biomarkers [72, 76, 77, 257] and are therefore promising techniques. However, both are best applied at ultra-high field MRI systems, e.g. 7 Tesla [256], which are not widely available for human application yet.

An alternative to MRI based biomarkers could be computed tomography (CT) based quantitative sGAG imaging. Similar to dGEMRIC, contrast-enhanced CT utilizes the inverse relation between a contrast agent and the sGAG distribution throughout the articular cartilage [78, 79]. Although CT arthrography (CTa) was already an established technique for the assessment of knee pathology [82, 83], it has only recently been implemented and used to evaluate OA cartilage composition [236, 237, chapters 7,8 and 9]. However, CTa has yet to be assessed clinically with regard to its reproducibility and to the willingness of patients to undergo an intra-articular injection with contrast agent. Future developments in CT scanner technology and image post processing, for example novel dual energy CT scanners and iterative reconstruction algorithms, might lead to imaging protocols which need less or even no contrast agent and less radiation dose [230, 231, 258, 259], which would be favorable for the application of CTa in clinical research. However, to date, CTa is a more invasive technique compared to dGEMRIC and the use of potentially harmful ionizing radiation is a drawback of the technique with regard to implementation on a large scale in OA research.

Despite the aforementioned lack of availability of thoroughly tested quantitative imaging biomarkers for cartilage in human OA subjects, recent consensus driven guidelines for OA research encourage the implementation of imaging biomarkers in general in OA intervention trials and cohort studies [260]. This is surprising since besides dGEMRIC, until now, no other imaging biomarker for cartilage composition has been shown to be valid and robust in humans OA. Furthermore, only some small size therapeutic OA studies using dGEMRIC as an outcome have been reported [156, 261-263, chapter 5], while large scale OA intervention trials have not yet been performed due to the lack of potent DMOADs.

One may question what the exact place of imaging biomarkers for cartilage composition is in the current OA research field? When the first quantitative imaging biomarker, e.g. dGEMRIC, was introduced in 1996 [64], the expectations were high. Quantitative imaging biomarkers could be used to assess the efficacy of DMOADs or to predict OA progression in the future [264]. Rather than a diagnostic or prognostic tool, by the year 2015, imaging OA biomarkers are only used in small size trials as outcome for cartilage sGAG content. Furthermore, imaging biomarkers might be used select subjects for studies targeting cartilage with differences in disease stage within the joint at a compositional level in terms of its sGAG content.

To assess if imaging biomarkers are capable of being used as primary endpoint in OA trials, a lot of future research needs to be performed. This research should focus on further validation, implementation and comparison of potential and already established quantitative imaging biomarkers, for example the potential of gagCEST versus dGEMRIC. In addition, compositional imaging biomarker for cartilage collagen content, e.g. T2- of T2*-mapping [233, 265], may be of additional value to sGAG biomarkers. When this research is performed, attention should be paid that these sequences are widely available, such that they can be feasibly applied on a large scale in order to compare the results of different researchers.

To assess the potential of imaging biomarkers to serve as a predictor of cartilage degeneration within disease course and outcome, imaging biomarkers should be included in large scale cohort studies like the OsteoArthritis Initiative (OAI) in the USA (http://www.oai.ucsf.edu/) or the Cohort Hip and Cohort Knee in The Netherlands (http://www.check-onderzoek.nl/) in which OA progression or clinical outcome measures of OA, like pain can be correlated to outcomes of imaging biomarkers. A potential alternative to compositional imaging biomarkers are quantitative thickness measurements of articular cartilage thickness to determine and follow articular cartilage in OA [45, 46]. Despite the fact that the segmentation is time consuming and that a relative long follow-up period of several years is required [266], it has been shown that quantitative morphometric measurements of cartilage may predict progression of knee OA [267, 268]. Therefore, it could be of interest to compare its outcomes to those of imaging biomarkers for cartilage composition in cross-sectional and longitudinal cohort studies. In

addition, it may be of interest to also look at other tissues in the knee for prediction of OA progression. For example, it has recently been shown that specific bone shapes are predictors of end stage knee [269-271]. Moreover, the European League Against Rheumatism (EULAR) has recently recommended to also focus on non-cartilaginous tissues in OA research [272].

IMAGING BIOMARKERS TO IMAGE THE WHOLE OSTEOARTHRITIC JOINT

Nowadays, OA is considered to be a whole joint disease in which, besides cartilage, also (subchondral) bone, menisci, synovium, and Hoffa's fat pad in the knee, play an import role in disease development and progression [22, 273]. Therefore, MRI based whole organ scoring systems which assess morphological changes of all these tissues have been proposed. Examples are the Knee Osteoarthritis Scoring System (KOSS) [40], the Whole-Organ MRI Score (WORMS) [41], the Boston Leeds Osteoarthritis Knee Score (BLOKS) [42] and MRI Osteoarthritis Knee Score (MOAKS) [43, 44]. These scoring systems are increasingly used in OA research [25]. A drawback of those scoring systems is that they rely on morphological tissue changes, which may not always be present in early stage disease.

Quantitative imaging biomarkers may be used to image composition of multiple key tissues other than articular cartilage in any stage of knee OA. Using this information, the complex and simultaneous mechanisms in different tissues in OA development and progression might be further analyzed. This information might eventually lead to the identification of new disease pathways which may lead to the development of novel treatment options for OA. Until now, however, only a few studies have been performed to assess the capability of imaging biomarkers to assess other tissues in the knee joint other than cartilage.

Using MRI, cartilage and meniscal tissue can be assessed within one examination [186, 250, 274, 275, chapter 6], ultra short echo time imaging might be used to assess the calcified cartilage and subchondral bone [276, 277] and several contrast-enhanced and non-contrast-enhanced options to quantitatively assess synovitis have been proposed [278-280]. CTa might also be a very usefully technique for the purpose of imaging cartilage, meniscus and also subchondral bone changes in OA [249, 252, 281, 282].

Future research with the purpose of assessing multiple tissues within the OA joint might benefit from using a multimodality approach, e.g. combining CT and MRI biomarkers, like already performed in animal research [283]. CT or MRI could also be combined with other emerging techniques for quantitative assessment of bone metabolism, macrophage activity within the synovium, but also meniscal and anterior cruciate ligament tears. These techniques use single photon emission CT (SPECT) and positron emission

tomography (PET) and have recently been validated *in vivo* in animal research [245, 254, 284, 285] and are already also applied for bone metabolism and meniscal and anterior cruciate ligament tears in human research [286-290]. Combing these datasets with high resolution CT or MRI scans enables accurate localization of bone or macrophage activity or meniscal and ligamentous injuries throughout the joint.

In addition to assessing OA pathophysiology and progression, imaging of multiple OA affected tissues might be helpful to different subtypes of OA which have recently been identified in the OAI [291]. Since different subtypes of OA have been shown to have their own etiology, speed of progression and clinical characteristics, a combination of specific imaging biomarkers and clinical tests may be developed to identify these subgroups that might benefit from specific treatment or even preventive strategies in future studies [292, 293].

IMAGE POST PROCESSING OF QUANTITATIVE MRI BASED IMAGING BIOMARKERS

Taking into account that future research will include quantitative analyses of multiple tissues, the need for accurate and reliable image post processing algorithms will be of utmost importance. This is especially the case in MRI based biomarkers since quantitative analysis of OA tissues needs multiple acquisitions during which patient motion can cause inaccurate quantitative outcomes. This has been reported for dGEMRIC [84, 85, chapter 2], but may also be the case for other quantitative MRI biomarkers. Image registration is also helpful in longitudinal studies since it makes the analysis of the data less time consuming because region of interest (ROI) drawing is only needed once.

An imaging post processing tool should also include the quantification of other, non-motion related, inaccuracies. Such inaccuracies could be caused by partial volume effects, low signal to noise ratios throughout datasets, or B0 or B1 inhomogeneity. In present imaging biomarker research, the accuracy of quantitative MRI measures is usually presented using the coefficient of determination for all analyzed images. This information may be used to evaluate the overall accuracies and reliability of quantitative MRI datasets for a specific patient or group of study patients. However, it may be better to use a measure for inaccuracy which is calculated per voxel in the analyzed images instead of all images of one or more patients together. This voxel based information on accuracy can be used to calculate a weighted outcome of quantitative MRI data in which voxels with a high inaccuracy contribute less to the outcome of the analysis compared to accurate voxels. This way, inaccurate voxels throughout a specific patient or even multiple patients have less influence on the calculated outcomes of quantitative imaging biomarkers [chapter 2].

Currently, not much research is performed related to the development, validation and implementation of image post processing tools for quantitative imaging biomarkers. This is striking because of the potential large impact these biomarkers can have in OA research. Therefore, more research with regard to image registration and assessment of accuracy in data analyses is necessary. Implementation of semi-automated or automated ROI segmentation algorithms may also be beneficial for biomarker image processing. Such segmentation was recently proposed for hip and knee cartilage [294-297] and may result in relative fast image post processing tools. This is especially of interest if imaging biomarkers are being included as an outcome measure in large OA trials or cohort studies in the future.

CONCLUSIONS

The research on which this thesis is based forms a contribution towards the application of quantitative imaging biomarkers of cartilage composition in OA. The most important results can be summarized as follows:

- Until now, dGEMRIC is the only validated and robust imaging biomarker for quantifying cartilage sGAG content in human OA subjects in clinical research.
- dGEMRIC and dGEMRIM may be capable of assessing cartilage and meniscus sGAG content within one contrast-enhanced MRI examination.
- T1rho-mapping appears not suitable as an alternative to dGEMRIC for quantifying cartilage sGAG content in articular cartilage and seems therefore not applicable as an imaging biomarker for OA research.
- CT arthrography may be suitable as an imaging biomarker for quantitative measurement of cartilage sGAG content in clinical OA research and therefore could be considered an alternative to MRI.
- Sophisticated imaging post processing tools are of utmost importance to generate reliable outcomes of quantitative MRI biomarkers of cartilage composition.

FUTURE PERSPECTIVES

Quantitative imaging biomarkers in OA research have not yet held to the high initial expectations. Despite the fact that quantitative imaging biomarkers for cartilage composition are therefore not yet applicable at a large scale in clinical OA research for reasons discussed before, a lot of interesting and important research is to be carried out within the coming years. This research should focus on implementing promising new imaging biomarkers, e.g. gagCEST, in clinical research and compare its outcomes

to dGEMRIC. In addition, the relation between imaging biomarkers and clinically important outcome measure for OA, like pain should be assessed, as well as the ability to predict OA development or progression by using these imaging biomarkers in large cohort studies. Based on this research, the OA community must reach consensus about the role of quantitative imaging biomarkers as an outcome measure or predictor of disease in OA research.

chapter 1

Summary

For a long time, radiography and subsequently conventional magnetic resonance imaging (MRI) were used as imaging biomarkers for evaluating cartilage morphological disease state in osteoarthritis (OA). Because research is switching its focus towards disease modification or even prevention to target OA at an early stage, imaging techniques that measure cartilage composition rather than its morphology became of interest. Several MRI and computed tomography (CT) based quantitative imaging biomarkers for cartilage composition were developed. These techniques were advocated to allow a quantitative measure of the sulphated glycosaminoglycan (sGAG) content, an important composite of the cartilage extracellular matrix. The main aims of this thesis is based have been divided between MRI and CT based quantitative imaging biomarkers since their different stage of application in research. MRI has already been applied in human OA research, whereas CT was still to be translated and implemented in clinical research.

PART 1: MRI BASED QUANTITATIVE IMAGING BIOMARKERS OF CARTILAGE SULPHATED GLYCOSAMINOGLYCAN CONTENT

The first part of this thesis focused on MRI based techniques and aimed at optimization of image post processing, assessing reproducibility, comparison of different MRI sequences and application in clinical OA research.

1.1 Optimization of image processing and reproducibility of dGEMRIC

Since accurate image post processing is of utmost importance to generate reliable and robust quantitative MRI outcomes, an imaging post processing tool was developed and described in chapter 2. This tool corrects for intra-sequence patient motion during acquisition of quantitative MR images, by applying image registration reducing errors and incorrect outcomes. This resulted in 6-14% improvement in accuracy of delayed gadolinium-enhanced MRI of cartilage (dGEMRIC) T1 relaxation time. Using image registration, the tool also allows assessment of the same cartilage region throughout multiple MRI acquisitions, which makes analyses less time consuming. Finally, the algorithm also involves a fitting technique which corrects for unreliable quantitative MRI biomarker data by calculating a weighted mean outcome for all voxels in a specific cartilage region based on the inaccuracy of each voxel. Because of these abilities and the fact that this tool could be used in any quantitative MRI biomarker, e.g. T1rho-mapping or T2-mapping, the image post processing tool was used in all chapters in this thesis where MRI based measures were used for cartilage sGAG content.

Along with robust image processing tools, the outcomes of the MRI exam itself should also be reproducible in order to be able to apply the particular technique in cross-sectional or longitudinal study designs. Therefore, chapter 3 described a reproducibility

study of dGEMRIC acquired at 3 Tesla in early stage knee OA patient. It was shown that dGEMRIC is highly reproducible in terms of results in large cartilage regions, as well as for differentiating between spatial distributions of diverse cartilage quality within a single slice. dGEMRIC can therefore be used as an imaging biomarker in cross-sectional and longitudinal study designs. In addition, a threshold for defining significant changes in dGEMRIC results for longitudinal follow-up was determined.

1.2 Validation and comparison of dGEMRIC and T1rho-mapping as imaging biomarker in human osteoarthritis research

T1rho-mapping has been proposed as a non-contrast-enhanced alternative to dGEMRIC for sGAG quantification in clinical studies. However, no thorough validation has been performed comparing both techniques within the same OA patients using a reference standard for cartilage sGAG. Therefore, in chapter 4 an *in vivo* comparison and validation study assessing the capability of dGEMRIC and T1rho-mapping was performed. In knee OA patients, dGEMRIC results strongly correlate with cartilage sGAG content, whereas T1rho-mapping did not. Therefore, it appears that T1rho-mapping cannot be regarded as an alternative for dGEMRIC to measure cartilage sGAG content in clinical OA research. It was also shown that results of dGEMRIC are also partially influenced by the collagen content of cartilage. Despite the fact that dGEMRIC cannot be regarded as entirely sGAG specific, the difference in strength in correlation between dGEMRIC and sGAG (r=0.73) and collagen content (r=0.40) suggests that dGEMRIC may be used as an imaging biomarker for sGAG content. The outcomes of T1rho-mapping did also not correlate with cartilage collagen content. Therefore, the use of T1rho-mapping as imaging biomarker in OA is questionable.

1.3 Application of dGEMRIC in clinical osteoarthritis research

Since dGEMRIC has been shown to be a robust and valid sGAG imaging biomarker in longitudinal studies, in Chapter 5 we used dGEMRIC to assess the effects of a potential disease-modifying OA drug, i.e. intra-articular injections with hyaluronic acid, in patients with early stage knee. This therapy has been advocated to improve cartilage composition by increasing the cartilage sGAG content. There was, however, no effect of the injections on cartilage sGAG content measured with dGEMRIC and using the threshold for change as defined in chapter 3. Although promising results were and are still being generated in *in vitro* and *in vivo* animal research with regard to improving cartilage composition using disease-modifying therapies, large human OA treatment trials have yet to be set up. The use of quantitative image biomarkers for cartilage composition is, in addition to clinical examination and questionnaires, a desirable outcome measure in such studies.

OA is nowadays regarded as a whole joint disease rather than a disease of only cartilage, therefore protocols imaging several relevant tissues within the knee joint became of interest in clinical research. Since articular cartilage and the meniscus are both partially composed of sGAG, the ability of dGEMRIC to serve as imaging biomarker for both tissues in one MR examination was assessed in chapter 6. It was shown that T1 relaxation times of degenerated menisci on conventional MRI were borderline significantly lower compared to healthy menisci. These differences in outcomes of morphologically healthy and degenerated menisci were highly reproducible independent of the anatomical location of the assessed menisci, showing the potential of contrast-enhanced MRI as a quantitative imaging biomarker for assessment of cartilage and meniscal composition. However, future research is needed to assess the role of contrast-enhanced MRI for multiple OA tissues within one examination.

PART 2: CT BASED QUANTITATIVE IMAGING BIOMARKERS OF CARTILAGE SULPHATED GLYCOSAMINOGLYCAN CONTENT

The second part of this thesis focused on CT based techniques and aimed at translating CT arthrography from a microscopic to a macroscopic setup and making suitable to be used in clinical OA research.

2.1 Translation of µCT arthrography to clinically applicable CT arthrography

Similar to dGEMRIC, contrast-enhanced CT can be used as a quantitative imaging biomarker for cartilage composition. Previously, microCT arthrography (µCTa) was successfully used as sGAG biomarker in *in vivo* animal OA research. Chapter 7 describes an *ex vivo* study in human cadaveric knee joints in which results of CT arthrography (CTa) are shown to be strongly correlated with cartilage sGAG content measured using a reference standard for sGAG. This study shows the potential of CTa as an imaging biomarker in human OA research.

Compared to MRI, CT has the disadvantage of using ionizing radiation. In chapter 8 it was shown that when only 10% of the radiation dose used in chapter 7 was used, it is still possible to measure cartilage sGAG content in cadaveric human knee joints. Using such a low radiation dose could be of interest especially if CTa would be used in longitudinal study designs or if the technique would be used in relatively young patients. Moreover, chapter 8 showed that CTa can determine spatial differences in sGAG content in adjacent cartilage regions. However, this capability is reduced at lower radiation dose and the amount of radiation used to acquire CTa should therefore be adjusted to the research question.

2.2 Validation of CT arthrography as imaging biomarker in human osteoarthritis research

After translating μCTa to a clinically applicable CTa protocol, chapter 9 describes an *in vivo* validation study for CTa to measure cartilage sGAG content in humans with knee OA. It was shown that outcomes of CTa have a strong correlation with cartilage sGAG content in human OA tibial and femoral cartilage. In agreement with chapter 4, it was again shown that contrast distribution throughout the cartilage is also partially influenced by its collagen content. The correlation of CTa with the collagen content of cartilage (r=0.56), however, less strong compared to the correlation between CTa and its sGAG content (r=76). Because of its high relative high resolution, low coasts and speed of acquisition, CTa may be used as an alternative to dGEMRIC in future human OA research. This is also true for patients with relative or absolute contra-indications for MRI.

CONCLUSIONS

The research on which this thesis is based forms a contribution towards the application of quantitative imaging biomarkers of cartilage composition in OA. The most important results can be summarized as follows:

- Until now, dGEMRIC is the only validated and robust imaging biomarker for quantifying cartilage sGAG content in human OA subjects in clinical research.
- dGEMRIC and dGEMRIM may be capable of assessing cartilage and meniscus sGAG content within one contrast-enhanced MRI examination.
- T1rho-mapping appears not suitable as an alternative to dGEMRIC for quantifying cartilage sGAG content in articular cartilage and seems therefore not applicable as an imaging biomarker for OA research.
- CT arthrography may be suitable as an imaging biomarker for quantitative measurement of cartilage sGAG content in clinical OA research and therefore could be considered an alternative to MRI.
- Sophisticated imaging post processing tools are of utmost importance to generate reliable outcomes of quantitative MRI biomarkers of cartilage composition.

chapter 12

Nederlandse samenvatting

Röntgenfoto's en later ook magnetic resonance imaging (MRI) werden lange tijd gebruikt als beeldvormende technieken om de ernst van slijtage van een gewricht, ook wel artrose genoemd, te bepalen. Dit werd gedaan aan de hand van de kraakbeendikte of vormafwijkingen van het kraakbeen welke gedurende de loop van de ziekte ontstaan en in ernst toenemen. Wetenschappelijk onderzoek naar artrose richt zich tegenwoordig op behandelingen welke toepasbaar zijn in een vroeg stadium van de ziekte, wanneer er nog geen verlies van dikte of vorm van kraakbeen zichtbaar is. In dit stadium is het namelijk wellicht mogelijk het ziekteproces te vertragen of zelfs ongedaan te maken. Om het effect van dergelijke behandelingen te kunnen meten is er de laatste jaren een aantal geavanceerde beeldvormende technieken ontwikkeld die niet de vorm of dikte van kraakbeen, maar de samenstelling van kraakbeen in maat en getal bepalen. Voorbeelden hiervan zijn MRI en computed tomography (CT) technieken welke, al dan niet met gebruik van een contrastmiddel, bepaalde bestanddelen van het kraakbeen zouden kunnen bepalen. Een belangrijk bestanddeel van kraakbeen dat bepaald kan worden is een schakeling van lange suikerketens welke ervoor zorgt dat kraakbeen water opzuigt als een spons om vervolgens op te zwellen, zoals een binnenband van een fiets met lucht wordt gevuld. Een ander belangrijk bestanddeel welke voor stevigheid van het kraakbeen is een netwerk van collageenvezels dat als een soort rubber van een opgeblazen binnenband een stevig, maar ook in zekere mate flexibel, loopvlak geeft. In dit proefschrift werden een aantal op MRI en CT gebaseerde, geavanceerde beeldvormende technieken voor kraakbeensamenstelling grondig bestudeerd. De onderzoeksdoelstellingen waren verschillend voor geavanceerde MRI en CT technieken, omdat deze niet dezelfde manier worden toegepast in wetenschappelijk onderzoek naar artrose. MRI wordt namelijk al gebruikt voor artroseonderzoek bij mensen, terwijl CT tot op heden vooral wordt gebruikt in dierexperimenteel onderzoek.

DEEL 1: GEAVANCEERDE MRI TECHNIEKEN OM KRAAKBEENSAMENSTELLING IN MAAT EN GETAL TE BEPALEN

Het eerste deel van dit proefschrift richtte zich op het verbeteren en nauwkeuriger maken van het berekenen van de uitkomsten van geavanceerde MRI technieken en het onderzoeken van de meetfout van deze technieken. Daarnaast werd van verschillende MRI technieken hun verband met kraakbeensamenstelling bekeken en vergeleken en werden deze technieken toegepast in artroseonderzoek bij mensen.

1.1 Verbeteren en nauwkeuriger maken van het berekenen van uitkomsten van geavanceerde MRI technieken en het onderzoeken van de meetfout van deze technieken

Om betrouwbare en nauwkeurige uitkomsten van geavanceerde MRI technieken te verkrijgen is het belangrijk om over goede beeldverwerkingssoftware te beschikken. In hoofdstuk 2 is dergelijke software ontwikkeld en getest voor een bepaalde geavanceerde MRI techniek, namelijk delayed gadolinium-enhanced MRI of cartilage (dGEMRIC). De software corrigeert voor bewegingen van de patiënt tussen de verschillende beelden die worden gemaakt bij een dGEMRIC scan. Door de beelden, die door beweging zijn verschoven, op een specifieke manier te bewerken en weer op de goede plek te zetten worden de uitkomsten van dGEMRIC 6-14% meer nauwkeurig. Dit bewegen en bewerken wordt beeldregistratie genoemd en kan ook worden toegepast om exact hetzelfde stuk kraakbeen op verschillende scans in de loop van de tijd met elkaar te vergelijken. Dit is veel nauwkeuriger en tijdsefficiënter dan iedere keer hetzelfde stukje op te zoeken en handmatig aan te geven. Daarnaast zorgt de software ervoor dat uitkomsten van dGEMRIC in een stuk kraakbeen die, ondanks beeldregistratie, nog erg onnauwkeurig zijn minder zwaar wegen bij het berekenen van de gemiddelde uitkomst van een geanalyseerd deel van het kraakbeen. De software is getest op dGEMRIC scans, maar kan ook worden gebruikt om uitkomsten van andere geavanceerde MRI technieken nauwkeurig te berekenen. De beeldverwerkingssoftware is daarom toegepast in elk hoofdstuk van dit proefschrift waar geavanceerde MRI technieken worden gebruikt.

Naast goede beeldverwerkingssoftware om nauwkeurig de uitkomsten van dGEMRIC te bepalen is het van belang dat de uitkomsten van de techniek geen grote meetfout hebben en dat uitkomsten vergelijkbaar zijn als de techniek meerdere malen binnen korte tijd wordt herhaald. Het onderzoeken van deze meetfout wordt ook wel het onderzoeken van de reproduceerbaarheid van de meting genoemd. Wanneer zowel de uitkomsten nauwkeurig zijn als de meting zelf goed reproduceerbaar is, kan een techniek als robuust worden beschouwd en worden ingezet in artroseonderzoek. In hoofdstuk 3 is gekeken of dGEMRIC reproduceerbare uitkomsten geeft in patiënten met een vroeg stadium van artrose. Het bleek dat de uitkomsten van dGEMRIC goed reproduceerbaar waren als het gaat om grote gebieden van kraakbeen en ook als werd gekeken naar verschillen binnen kraakbeen in een gebied op een bepaald beeld van de gehele scan. Dit laatste is van belang wanneer er gekeken wordt naar lokale afwijkingen van kraakbeen zoals het verlies van lange suikerketens. Daarnaast werd er een drempelwaarde berekend die gebruikt kan worden om te zien of de uitkomst van de dGEMRIC scan in de loop van de tijd is verbeterd of verslechterd.

1.2 Verband tussen uitkomsten van geavanceerde MRI technieken met kraakbeensamenstelling en onderlinge vergelijking van verschillende MRI technieken

Een nadeel van dGEMRIC is dat er voor het maken van deze MRI scan contrastmiddel moet worden ingespoten in een ader van de patiënt. Dit contrastmiddel verdeelt zich in het kraakbeen naargelang de hoeveelheid eiwitketens die het bevat. De hoeveelheid contrastmiddel in een bepaald gebied kan worden gemeten met behulp van de MRI scan. Aan het gebruik van het contrastmiddel kleven een aantal risico's en daarom werd gezocht naar een alternatieve geavanceerde MRI techniek om de samenstelling van gewichtskraakbeen in maat en getal te bepalen zonder dat daarvoor contrastmiddel noodzakelijk zou zijn. Een techniek waarmee dit mogelijk zou kunnen is T1rho-mapping. Tot op heden waren echter nog geen onderzoeken gedaan waarin uitkomsten van dGEMRIC en T1rho-mapping vergeleken werden met zogenaamde gouden standaard metingen in het laboratorium. Daarnaast werden ook de uitkomsten van beide technieken nog niet eerder met elkaar vergeleken. Een dergelijk validatie- en vergelijkingsonderzoek is daarom uitgevoerd en beschreven in hoofdstuk 4. De uitkomsten van dGEMRIC lieten een goed verband zien met de hoeveelheid suikerketens in het kraakbeen. Voor T1rho-mapping bleek dit echter niet het geval te zijn. De uitkomsten van dGEMRIC bleken ook deels te worden beïnvloed door de hoeveelheid collageen in het kraakbeen, al was dit verband minder sterk dan het verband met de suikerketens. dGEMRIC lijkt daarom geschikt om in toekomstig onderzoek in mensen met artrose te worden gebruikt als maat voor de hoeveelheid suikerketens. Uitkomsten van T1rho-mapping hadden, net als met de suikerketens, geen verband met de hoeveelheid collageen in kraakbeen. T1rho-mapping lijkt daarom ongeschikt om in toekomstig onderzoek gebruikt te worden om kraakbeensamenstelling te meten bij mensen met artrose.

1.3 Toepassing van geavanceerde MRI technieken in onderzoek bij mensen met knieartrose

In hoofdstuk 3 en 4 is aangetoond dat dGEMRIC een reproduceerbare meting is welke een goed verband heeft met de hoeveelheid suikerketens in het kraakbeen. In hoofdstuk 5 is dGEMRIC daarom gebruikt om het effect van een potentieel artrose-vertragend middel, namelijk hyaluronzuur, dat in de knie wordt geïnjecteerd op de hoeveelheid suikerketens in gewrichtskraakbeen te bepalen. Dit effect werd in eerder laboratoriumonderzoek al waargenomen. In het kraakbeen van de patiënten werd er echter geen toename van de hoeveelheid suikerketens gemeten met dGEMRIC, terwijl de injecties met hyaluronzuur wel een positief effect hadden op pijnklachten, stijfheid en de functie van de knie. Deze positieve effecten kunnen dus zeer waarschijnlijk niet worden toegeschreven aan een toename van suikerketens in het kraakbeen. Mogelijk

komen uit laboratorium- en dierexperimenteel onderzoek in de toekomst nieuwe mogelijk artrose-vertragende of -beïnvloedende therapieën voort. Als het effect van deze therapieën wordt bestudeerd is het aan te raden om ook gebruik te maken van geavanceerde beeldvormende technieken om kraakbeensamenstelling te meten, naast scorelijsten en functie-onderzoek. Op deze manier kan dan worden gekeken of bepaalde effecten daadwerkelijk verklaard kunnen worden door een verandering in de samenstelling van gewrichtskraakbeen.

Tegenwoordig wordt artrose niet alleen gezien als een ziekte waarbij het kraakbeen in het gewricht slijt en uiteindelijk te gronde gaat. Namelijk, ook andere weefsels van het gewricht slijten of raken aangedaan. Voorbeelden van dergelijke weefsels zijn het bot dat net onder het gewrichtsoppervlak ligt, de binnenbekleding van het gewrichtskapsel welke verantwoordelijk is voor de aanmaak van gewrichtsvloeistof (het synovium) en ook de meniscus van de knie. De meniscus is een structuur die qua samenstelling lijkt op kraakbeen met suikerketens en collageen en die ervoor zorgt dat de knie goed kan bewegen, stabiel is en dat de kracht van het bovenbeen naar het onderbeen wordt verplaatst op een gelijkwaardige manier. In hoofdstuk 6 is gekeken of met een dGEMRIC scan, naast de hoeveelheid suikerketens in het kraakbeen, ook de hoeveelheid suikerketens in de meniscus kan worden gemeten. De resultaten van dit onderzoek toonden aan dat dit waarschijnlijk het geval is als gekeken wordt naar het verschil in uitkomst van de scan in menisci die intact waren vergeleken met menisci die slijtage toonden in het kader van artrose. Ondanks dit veelbelovende resultaat zal toekomstig onderzoek met een zelfde studieopzet als in hoofdstuk 4 (uitkomsten vergelijken met gouden standaard metingen in het laboratorium) nog moeten uitwijzen of dit daadwerkelijk het geval is.

DEEL 2: GEAVANCEERDE CT TECHNIEKEN OM KRAAKBEENSAMENSTELLING IN MAAT EN GETAL TE BEPALEN

Het tweede deel van dit proefschrift richtte zich op het toepasbaar maken van een geavanceerde CT scan met contrastmiddel in wetenschappelijk onderzoek met mensen. Deze techniek werd tot op heden alleen nog gebruikt in dierexperimenteel onderzoek.

2.1 Het toepasbaar maken van een geavanceerde CT scan met contrastmiddel in knieën van mensen

Net als bij dGEMRIC wordt bij een geavanceerde CT scan met contrastmiddel gebruik gemaakt van de verdeling van het contrastmiddel naargelang de hoeveelheid suikerketens van het gewrichtskraakbeen. Het contrastmiddel wordt echter niet in de aderen, maar direct in het kniegewricht geïnjecteerd. Deze techniek werd tot nu toe voorna-

melijk gebruikt bij dierexperimenteel onderzoek en wordt een CT artrografie genoemd. In hoofdstuk 7 werd, in een onderzoek met knieën van patiënten die hun lichaam ter beschikking aan de wetenschap hadden gesteld, gekeken of het CT artrogram ook bij menselijke knieën kan worden gebruikt om suikerketens te meten. Er bleek een sterk verband te bestaan tussen de uitkomsten van de CT scan en de hoeveelheid suikerketens die werden gemeten met een gouden standaard meting in het laboratorium. Het CT artrogram zou dus waarschijnlijk kunnen worden toegepast om gewichtskraakbeen samenstelling te kunnen meten in menselijke knieën.

Een nadeel van CT ten opzichte van MRI is dat voor het maken van een CT scan röntgenstraling wordt gebruikt welke, bij veelvuldige toepassing, mogelijk een schadelijk effect op de weefsels zou kunnen hebben. Om te kijken of het ook mogelijk is om suikerketens te meten met een lage dosis röntgenstraling is in hoofdstuk 8 een onderzoek beschreven waarbij CT scans met verschillende hoeveelheden straling werden vergeleken met de uitkomst van een gouden standaard meting. Het bleek dat als 10% van de hoeveelheid straling in hoofdstuk 7 werd gebruikt, er door middel van een CT artrogram alsnog suikerketens in gewrichtskraakbeen kunnen worden gemeten. Dit maakt deze geavanceerde techniek ook geschikt en veilig om te gebruiken om patiënten in de loop van de tijd te vervolgen met meerdere CT scans. Ook werd gekeken naar de mogelijkheid om met een CT artrogram verschillen in de hoeveelheid suikerketens te meten binnen een bepaald gebied binnen het kraakbeen op een beeld van de gehele scan. Dit bleek, net als bij dGEMRIC, mogelijk. Echter de mogelijkheid om onderscheid te maken tussen verschillen in suikerketens op een bepaald beeld werd minder goed mogelijk bij het gebruik van een lage röntgenstralingsdosis. De hoeveelheid röntgenstraling die gebruikt wordt voor een CT artrogram moet dus worden aangepast aan het doel van de CT scan wanneer deze in het kader van wetenschappelijk onderzoek wordt gemaakt.

2.2 Validatie van het CT artrogram om kraakbeen samenstelling te meten in mensen met knieartrose

Nadat in hoofdstuk 7 en 8 de toepassing van het CT artrogram in knieën van overleden mensen werd onderzocht, is in hoofdstuk 9 gekeken naar het verband tussen uitkomsten van een CT artrogram en de hoeveelheid suikerketens in levende menselijke knieën. De uitkomsten van de CT scan hadden ook in levende knieën een sterk verband met de hoeveelheid suikerketens in het kraakbeen, maar waren, net als bij dGEMRIC, ook deels gerelateerd aan de hoeveelheid collageen van het gewrichtskraakbeen. CT heeft een relatief hoge resolutie, een lagere prijs en is sneller vergeleken met MRI. Het CT artrogram zou daarom een uitstekend alternatief kunnen zijn voor dGEMRIC om, in toekomstig wetenschappelijk onderzoek, de hoeveelheid suikerketens in gewrichtskraakbeen van levende mensen kunnen meten.

CONCLUSIES

Het onderzoek waarop dit proefschrift is gebaseerd vormt een bijdrage aan de mogelijke toepassing van geavanceerde beeldvormende technieken om kraakbeensamenstelling in maat en getal te bepalen bij onderzoek naar artrose. De belangrijkste resultaten kunnen als volgt worden samengevat:

- Tot op heden is dGEMRIC de enige goed gevalideerde en robuuste geavanceerde beeldvormende techniek waarmee kraakbeensamenstelling in de vorm van suikerketens kan worden gemeten bij patiënten met knieartrose.
- dGEMRIC kan, naast kraakbeensamenstelling, mogelijk ook in dezelfde scan de hoeveelheid suikerketens in de meniscus meten.
- T1rho-mapping lijkt niet geschikt als geavanceerde beeldvormende techniek om kraakbeensamenstelling te meten bij mensen met knieartrose.
- CT artrografie is mogelijk geschikt als geavanceerde beeldvormende techniek om de hoeveelheid suikerketens in gewrichtskraakbeen te meten bij mensen met knieartrose en is daarom een mogelijk alternatief voor MRI.
- Geavanceerde beeldverwerkingssoftware verbetert de nauwkeurigheid van uitkomsten van geavanceerde beeldvormende MRI technieken.

chapter 13

References

1. Gommer AM, Poos MJ. Tweede nationale studie naar ziekten en verrichtingen in de huisartspraktijk: klachten en aandoeningen in de bevolking en in de huisartspraktijk. In: Nationaal Kompas Volksgezondheid. Bilthoven: Rijksinstituut voor Volksgezondheid en Milieu 2010.
2. van de Linden MW, Westert GP, de Bakker DH, Schellevis FG. Tweede Nationale Studie naar ziekten en verrichtingen in de huisartspraktijk: klachten en aandoeningen in de bevolking en in de huisartspraktijk. In: Nationaal Kompas Volksgezondheid. Bilthoven: Rijksinstituut voor Volksgezondheid en Milieu 2004.
3. van Meurs JB, Bierma-Zeinstra SM, Uitterlinden AG. Artrose samengevat. In: Nationaal Kompas Volksgezondheid. Bilthoven: Rijksinstituut voor Volksgezondheid en Milieu 2014.
4. The burden of musculoskeletal conditions at the start of the new millennium. In: WHO technical report series 919. Geneva: World Health Organisation 2003.
5. Buckwalter JA, Martin JA. Osteoarthritis. Adv Drug Deliv Rev 2006;58:150-67.
6. Poos MJ, Gommer AM. Neemt het aantal mensen met artrose toe of af? In: Nationaal Kompas Volksgezondheid. Bilthoven: Rijksinstituut voor Volksgezondheid en Milieu 2009.
7. Hermans J, Koopmanschap MA, Bierma-Zeinstra SMA, van Linge JH, Verhaar JAN, Reijman M, et al. Productivity Costs and Medical Costs Among Working Patients With Knee Osteoarthritis. Arthritis Care & Research 2012;64:853-61.
8. Litwic A, Edwards MH, Dennison EM, Cooper C. Epidemiology and burden of osteoarthritis. Br Med Bull 2013;105:185-99.
9. Wenham CY, Conaghan PG. New horizons in osteoarthritis. Age Ageing 2013;42:272-8.
10. Brooks PM. The burden of musculoskeletal disease - a global perspective. Clinical Rheumatology 2006;25:778-81.
11. Slobbe LC, Smit JM, Groen J, Poos MJ, Kommer GJ. Trends in Kosten van Ziekten in Nederland 1999-2010. In. Bilthoven: Rijksinstituut voor volksgezondheid en milieu 2011.
12. Poos MJ, Smit JM, Groen J, Kommer GJ, Slobbe LC. Kosten van Ziekten in Nederland 2005 Zorg voor euro's – 8. In. Bilthoven: Rijksinstituut voor volksgezondheid en milieu 2008.
13. Hunter DJ. Pharmacologic therapy for osteoarthritis-the era of disease modification. Nature Reviews Rheumatology 2011;7:13-22.
14. Bos PK, van Melle ML, van Osch GJVM. Articular cartilage repair and the evolving role of regenerative medicine. Open Access Surgery 2010:109 – 22.
15. Liu Y, Wu J, Zhu Y, Han J. Therapeutic application of mesenchymal stem cells in bone and joint diseases. Clin Exp Med 2012.
16. Wiegant K, van Roermund PM, Intema F, Cotofana S, Eckstein F, Mastbergen SC, et al. Sustained clinical and structural benefit after joint distraction in the treatment of severe knee osteoarthritis. Osteoarthritis Cartilage 2013;21:1660-7.
17. Intema F, Van Roermund PM, Marijnissen AC, Cotofana S, Eckstein F, Castelein RM, et al. Tissue structure modification in knee osteoarthritis by use of joint distraction: an open 1-year pilot study. Ann Rheum Dis 2011;70:1441-6.
18. Brouwer RW, Raaij VTM, Bierma-Zeinstra SMA, Verhagen AP, Jakma TSC, Verhaar JAN. Osteotomy for treating knee osteoarthritis (Withdrawn Paper. 2007, art. no. CD004019). Cochrane Database of Systematic Reviews 2007:CD004019.
19. Runhaar J, van Middelkoop M, Reijman M, Vroegindeweij D, Oei EH, Bierma-Zeinstra SM. Malalignment: a possible target for prevention of incident knee osteoarthritis in overweight and obese women. Rheumatology (Oxford) 2014;53:1618-24.

20. Jones RK, Chapman GJ, Findlow AH, Forsythe L, Parkes MJ, Sultan J, et al. A new approach to prevention of knee osteoarthritis: reducing medial load in the contralateral knee. J Rheumatol 2013;40:309-15.
21. Runhaar J, van Middelkoop M, Reijman M, Willemsen S, Oei EH, Vroegindeweij D, et al. Prevention of Knee Osteoarthritis in Overweight Females: The First Preventive Randomized Controlled Trial in Osteoarthritis. Am J Med 2015.
22. Loeser RF, Goldring SR, Scanzello CR, Goldring MB. Osteoarthritis: A disease of the joint as an organ. Arthritis and Rheumatism 2012;64:1697-707.
23. Cubukcu D, Sarsan A, Alkan H. Relationships between Pain, Function and Radiographic Findings in Osteoarthritis of the Knee: A Cross-Sectional Study. Arthritis 2012;2012:984060.
24. Finan PH, Buenaver LF, Bounds SC, Hussain S, Park RJ, Haque UJ, et al. Discordance Between Pain and Radiographic Severity in Knee Osteoarthritis Findings From Quantitative Sensory Testing of Central Sensitization. Arthritis and Rheumatism 2013;65:363-72.
25. Roemer FW, Eckstein F, Hayashi D, Guermazi A. The role of imaging in osteoarthritis. Best Pract Res Clin Rheumatol 2014;28:31-60.
26. Huang M, Schweitzer ME. The role of radiology in the evolution of the understanding of articular disease. Radiology 2014;273:S1-S22.
27. Hunter DJ, Guermazi A. Imaging Techniques in Osteoarthritis. Pm&R 2012;4:S68-S74.
28. Kellgren JH, Lawrence JS. Radiological assessment of osteo-arthrosis. Ann Rheum Dis 1957;16:494-502.
29. Kijowski R, Blankenbaker D, Stanton P, Fine J, De Smet A. Correlation between radiographic findings of osteoarthritis and arthroscopic findings of articular cartilage degeneration within the patellofemoral joint. Skeletal Radiology 2006;35:895-902.
30. Kijowski R, Blankenbaker DG, Stanton PT, Fine JP, De Smet AA. Radiographic findings of osteoarthritis versus arthroscopic findings of articular cartilage degeneration in the tibiofemoral joint. Radiology 2006;239:818-24.
31. Gale DR, Chaisson CE, Totterman SMS, Schwartz RK, Gale ME, Felson D. Meniscal subluxation: association with osteoarthritis and joint space narrowing. Osteoarthritis and Cartilage 1999;7:526-32.
32. Hunter DJ, Zhang YQ, Tu X, LaValley M, Niu JB, Amin S, et al. Change in joint space width - Hyaline articular cartilage loss or alteration in meniscus? Arthritis and Rheumatism 2006;54:2488-95.
33. Guermazi A, Roemer FW, Burstein D, Hayashi D. Why radiography should no longer be considered a surrogate outcome measure for longitudinal assessment of cartilage in knee osteoarthritis. Arthritis Research & Therapy 2011;13:247.
34. Schiphof D, Boers M, Bierma-Zeinstra SMA. Differences in descriptions of Kellgren and Lawrence grades of knee osteoarthritis. Ann Rheum Dis 2008;67:1034-36.
35. Felson DT, Nevitt MC, Yang M, Clancy M, Niu JB, Torner JC, et al. A new approach yields high rates of radiographic progression in knee osteoarthritis. Journal of Rheumatology 2008;35:2047-54.
36. Amin S, LaValley MP, Guermazi A, Grigoryan M, Hunter DJ, Clancy M, et al. The relationship between cartilage loss on magnetic resonance imaging and radiographic progression in men and women with knee osteoarthritis. Arthritis and Rheumatism 2005;52:3152-59.
37. Bedson J, Croft PR. The discordance between clinical and radiographic knee osteoarthritis: a systematic search and summary of the literature. BMC Musculoskelet Disord 2008;9:116.
38. Hannan MT, Felson DT, Pincus T. Analysis of the discordance between radiographic changes and knee pain in osteoarthritis of the knee. Journal of Rheumatology 2000;27:1513-17.
39. Guermazi A, Roemer FW, Haugen IK, Crema MD, Hayashi D. MRI-based semiquantitative scoring of joint pathology in osteoarthritis. Nature Reviews Rheumatology 2013;9:236-51.

40. Kornaat PR, Ceulemans RY, Kroon HM, Riyazi N, Kloppenburg M, Carter WO, et al. MRI assessment of knee osteoarthritis: Knee Osteoarthritis Scoring System (KOSS)—inter-observer and intra-observer reproducibility of a compartment-based scoring system. Skeletal Radiol 2005;34:95-102.
41. Peterfy CG, Guermazi A, Zaim S, Tirman PF, Miaux Y, White D, et al. Whole-Organ Magnetic Resonance Imaging Score (WORMS) of the knee in osteoarthritis. Osteoarthritis Cartilage 2004;12:177-90.
42. Hunter DJ, Lo GH, Gale D, Grainger AJ, Guermazi A, Conaghan PG. The reliability of a new scoring system for knee osteoarthritis MRI and the validity of bone marrow lesion assessment: BLOKS (Boston Leeds Osteoarthritis Knee Score). Ann Rheum Dis 2008;67:206-11.
43. Hunter DJ, Guermazi A, Lo GH, Grainger AJ, Conaghan PG, Boudreau RM, et al. Evolution of semi-quantitative whole joint assessment of knee OA: MOAKS (MRI Osteoarthritis Knee Score). Osteoarthritis Cartilage 2011;19:990-1002.
44. Runhaar J, Schiphof D, van Meer B, Reijman M, Bierma-Zeinstra SM, Oei EH. How to define subregional osteoarthritis progression using semi-quantitative MRI Osteoarthritis Knee Score (MOAKS). Osteoarthritis Cartilage 2014;22:1533-6.
45. Buck RJ, Wyman BT, Le Graverand MPH, Hunter D, Vignon E, Wirth W, et al. Using ordered values of subregional cartilage thickness change increases sensitivity in detecting risk factors for osteoarthritis progression. Osteoarthritis and Cartilage 2011;19:302-08.
46. Buck RJ, Wyman BT, Le Graverand MPH, Wirth W, Eckstein F, Investigators A. An Efficient Subset of Morphological Measures for Articular Cartilage in the Healthy and Diseased Human Knee. Magnetic Resonance in Medicine 2010;63:680-90.
47. Koster IM, Oei EHG, Hensen JHJ, Boks SS, Koes BW, Vroegindeweij D, et al. Predictive factors for new onset or progression of knee osteoarthritis one year after trauma: MRI follow-up in general practice. European Radiology 2011;21:1509-16.
48. Oei EH. Magnetic resonance imaging for traumatic knee injury In: Department of Radiology, Erasmus MC. Rotterdam: Erasmus University 2009.
49. Kijowski R, Blankenbaker DG, Davis KW, Shinki K, Kaplan LD, De Smet AA. Comparison of 1.5-and 3.0-T MR Imaging for Evaluating the Articular Cartilage of the Knee Joint. Radiology 2009;250:839-48.
50. Zhang M, Min ZG, Rana N, Liu HJ. Accuracy of Magnetic Resonance Imaging in Grading Knee Chondral Defects. Arthroscopy-the Journal of Arthroscopic and Related Surgery 2013;29:349-56.
51. Burstein D, Gray M, Mosher T, Dardzinski B. Measures of Molecular Composition and Structure in Osteoarthritis. Radiologic Clinics of North America 2009;47:675-+.
52. Choi JA, Gold GE. MR Imaging of Articular Cartilage Physiology. Magnetic Resonance Imaging Clinics of North America 2011;19:249-+.
53. Binks DA, Hodgson RJ, Ries ME, Foster RJ, Smye SW, McGonagle D, et al. Quantitative parametric MRI of articular cartilage: a review of progress and open challenges. British Journal of Radiology 2013;86:20120163.
54. Muir H. The Chondrocyte, Architect of Cartilage - Biomechanics, Structure, Function and Molecular-Biology of Cartilage Matrix Macromolecules. Bioessays 1995;17:1039-48.
55. Venn M, Maroudas A. Chemical composition and swelling of normal and osteoarthrotic femoral head cartilage. I. Chemical composition. Ann Rheum Dis 1977;36:121-9.
56. Buckwalter JA, Mankin HJ. Articular cartilage: Degeneration and osteoarthritis, repair, regeneration, and transplantation. Instructional Course Lectures, Vol 47 - 1998 1998;47:487-504.
57. Maroudas A, Bayliss MT, Venn MF. Further-Studies on the Composition of Human Femoral-Head Cartilage. Ann Rheum Dis 1980;39:514-23.
58. Maroudas A, Ziv I, Weisman N, Venn M. Studies of Hydration and Swelling Pressure in Normal and Osteoarthritic Cartilage. Biorheology 1985;22:159-69.

59. Maroudas A, Venn M. Chemical composition and swelling of normal and osteoarthrotic femoral head cartilage. II. Swelling. Ann Rheum Dis 1977;36:399-406.
60. Franzen A, Inerot S, Hejderup SO, Heinegard D. Variations in the Composition of Bovine Hip Articular-Cartilage with Distance from the Articular Surface. Biochemical Journal 1981;195:535-43.
61. Gomez S, Toffanin R, Bernstorff S, Romanello M, Amenitsch H, Rappolt M, et al. Collagen fibrils are differently organized in weight-bearing and not-weight-bearing regions of pig articular cartilage. Journal of Experimental Zoology 2000;287:346-52.
62. Mosher TJ. Functional anatomy and structure of the "osteochondral unit". In: Arthritis in color: advanced imaging of arthritis, Bruno MA, Mosher TJ, Gold GE Eds. Philadelphia: Elsevier Saunders 2009:23-32.
63. Dijkgraaf LC, Debont LGM, Boer G, Liem RSB. The Structure, Biochemistry, and Metabolism of Osteoarthritic Cartilage - a Review of the Literature. Journal of Oral and Maxillofacial Surgery 1995;53:1182-92.
64. Bashir A, Gray ML, Burstein D. Gd-DTPA2- as a measure of cartilage degradation. Magn Reson Med 1996;36:665-73.
65. Bashir A, Gray ML, Hartke J, Burstein D. Nondestructive imaging of human cartilage glycosaminoglycan concentration by MRI. Magnetic Resonance in Medicine 1999;41:857-65.
66. Duvvuri U, Reddy R, Patel SD, Kaufman JH, Kneeland JB, Leigh JS. T1rho-relaxation in articular cartilage: effects of enzymatic degradation. Magn Reson Med 1997;38:863-7.
67. Regatte RR, Akella SVS, Borthakur A, Reddy R. Proton spin-lock ratio imaging for quantitation of glycosaminoglycans in articular cartilage. Journal of Magnetic Resonance Imaging 2003;17:114-21.
68. Duvvuri U, Kudchodkar S, Reddy R, Leigh JS. T(1rho) relaxation can assess longitudinal proteoglycan loss from articular cartilage in vitro. Osteoarthritis Cartilage 2002;10:838-44.
69. Nishioka H, Hirose J, Nakamura E, Oniki Y, Takada K, Yamashita Y, et al. T1rho and T2 mapping reveal the in vivo extracellular matrix of articular cartilage. Journal of Magnetic Resonance Imaging 2012;35:147-55.
70. Wang L, Regatte RR. T MRI of human musculoskeletal system. J Magn Reson Imaging 2014.
71. Wolff SD, Balaban RS. Magnetization transfer contrast (MTC) and tissue water proton relaxation in vivo. Magn Reson Med 1989;10:135-44.
72. Ling W, Regatte RR, Navon G, Jerschow A. Assessment of glycosaminoglycan concentration in vivo by chemical exchange-dependent saturation transfer (gagCEST). Proceedings of the National Academy of Sciences of the United States of America 2008;105:2266-70.
73. Granot J. Sodium imaging of human body organs and extremities in vivo. Radiology 1988;167:547-50.
74. Insko EK, Kaufman TH, Leigh JS, Reddy R. Sodium NMR evaluation of articular cartilage degradation. Magnetic Resonance in Medicine 1999;41:30-34.
75. Shapiro EM, Borthakur A, Gougoutas A, Reddy R. 23Na MRI accurately measures fixed charge density in articular cartilage. Magn Reson Med 2002;47:284-91.
76. Schmitt B, Zbyn S, Stelzeneder D, Jellus V, Paul D, Lauer L, et al. Cartilage Quality Assessment by Using Glycosaminoglycan Chemical Exchange Saturation Transfer and Na-23 MR Imaging at 7 T. Radiology 2011;260:257-64.
77. Madelin G, Babb J, Xia D, Chang G, Krasnokutsky S, Abramson SB, et al. Articular Cartilage: Evaluation with Fluid-suppressed 7.0-T Sodium MR Imaging in Subjects with and Subjects without Osteoarthritis. Radiology 2013;268:481-91.
78. Palmer AW, Guldberg RE, Levenston ME. Analysis of cartilage matrix fixed charge density and three-dimensional morphology via contrast-enhanced microcomputed tomography. Proceedings of the National Academy of Sciences of the United States of America 2006;103:19255-60.

79. Xie L, Lin AS, Guldberg RE, Levenston ME. Nondestructive assessment of sGAG content and distribution in normal and degraded rat articular cartilage via EPIC-microCT. Osteoarthritis Cartilage 2010;18:65-72.
80. Piscaer TM, Waarsing JH, Kops N, Pavljasevic P, Verhaar JA, van Osch GJ, et al. In vivo imaging of cartilage degeneration using microCT-arthrography. Osteoarthritis Cartilage 2008;16:1011-7.
81. Siebelt M, Waarsing JH, Kops N, Piscaer TM, Verhaar JAN, Oei EHG, et al. Quantifying Osteoarthritic Cartilage Changes Accurately Using In Vivo MicroCT Arthrography in Three Etiologically Distinct Rat Models. Journal of Orthopaedic Research 2011;29:1788-94.
82. De Filippo M, Bertellini A, Pogliacomi F, Sverzellati N, Corradi D, Garlaschi G, et al. Multidetector computed tomography arthrography of the knee: diagnostic accuracy and indications. Eur J Radiol 2009;70:342-51.
83. Subhas N, Freire M, Primak AN, Polster JM, Recht MP, Davros WJ, et al. CT arthrography: in vitro evaluation of single and dual energy for optimization of technique. Skeletal Radiology 2010;39:1025-31.
84. Miese F, Kropil P, Ostendorf B, Scherer A, Buchbender C, Quentin M, et al. Motion correction improves image quality of dGEMRIC in finger joints. European Journal of Radiology 2011;80:E427-E31.
85. Studler U, White LM, Andreisek G, Luu S, Cheng HLM, Sussman MS. Impact of Motion on T1 Mapping Acquired With Inversion Recovery Fast Spin Echo and Rapid Spoiled Gradient Recalled-Echo Pulse Sequences for Delayed Gadolinium-Enhanced MRI of Cartilage (dGEMRIC) in Volunteers. Journal of Magnetic Resonance Imaging 2010;32:394-98.
86. Szumowski J, Durkan MG, Foss EW, Brown DS, Schwarz E, Crawford DC. Signal polarity restoration in a 3D inversion recovery sequence used with delayed gadolinium-enhanced magnetic resonance imaging of cartilage (dGEMRIC). Journal of Magnetic Resonance Imaging 2012;36:1248-55.
87. Multanen J, Rauvala E, Lammentausta E, Ojala R, Kiviranta I, Hakkinen A, et al. Reproducibility of imaging human knee cartilage by delayed gadolinium-enhanced MRI of cartilage (dGEMRIC) at 1.5 Tesla. Osteoarthritis and Cartilage 2009;17:559-64.
88. Siversson C, Tiderius CJ, Neuman P, Dahlberg L, Svensson J. Repeatability of T1-Quantification in dGEMRIC for Three Different Acquisition Techniques: Two-Dimensional Inversion Recovery, Three-Dimensional Look Locker, and Three-Dimensional Variable Flip Angle. Journal of Magnetic Resonance Imaging 2010;31:1203-09.
89. Mosher TJ, Zhang Z, Reddy R, Boudhar S, Milestone BN, Morrison WB, et al. Knee articular cartilage damage in osteoarthritis: analysis of MR image biomarker reproducibility in ACRIN-PA 4001 multicenter trial. Radiology 2011;258:832-42.
90. Wong CS, Yan CH, Gong NJ, Li T, Chan Q, Chu YC. Imaging biomarker with T1rho and T2 mappings in osteoarthritis - In vivo human articular cartilage study. Eur J Radiol 2013;82:647-50.
91. Watanabe A, Wada Y, Obata T, Ueda T, Tamura M, Ikehira H, et al. Delayed gadolinium-enhanced MR to determine glycosaminoglycan concentration in reparative cartilage after autologous chondrocyte implantation: Preliminary results. Radiology 2006;239:201-08.
92. Lawrence RC, Felson DT, Helmick CG, Arnold LM, Choi H, Deyo RA, et al. Estimates of the prevalence of arthritis and other rheumatic conditions in the United States. Part II. Arthritis Rheum 2008;58:26-35.
93. Bashir A, Gray ML, Boutin RD, Burstein D. Glycosaminoglycan in articular cartilage: in vivo assessment with delayed Gd(DTPA)(2-)-enhanced MR imaging. Radiology 1997;205:551-8.
94. McKenzie CA, Williams A, Prasad PV, Burstein D. Three-dimensional delayed gadolinium-enhanced MRI of cartilage (dGEMRIC) at 1.5T and 3.0T. Journal of Magnetic Resonance Imaging 2006;24:928-33.
95. Tiderius CJ, Olsson LE, Leander P, Ekberg O, Dahlberg L. Delayed gadolinium-enhanced MRI of cartilage (dGEMRIC) in early knee osteoarthritis. Magnetic Resonance in Medicine 2003;49:488-92.

96. Sijbers J, den Dekker AJ, Raman E, Van Dyck D. Parameter estimation from magnitude MR images. International Journal of Imaging Systems and Technology 1999;10:109-14.
97. Cavassila S, Deval S, Huegen C, van Ormondt D, Graveron-Demilly D. Cramer-Rao bounds: an evaluation tool for quantitation. Nmr in Biomedicine 2001;14:278-83.
98. Rao CR. Minimum variance and the estimation of several parameters. Cambridge Univ Press 1946;43:280-83.
99. Spandonis Y, Heese FP, Hall LD. High resolution MRI relaxation measurements of water in the articular cartilage of the meniscectomized rat knee at 4.7 T. Magnetic Resonance Imaging 2004;22:943-51.
100. Li K, Zu Z, Xu J, Janve VA, Gore JC, Does MD, et al. Optimized inversion recovery sequences for quantitative T1 and magnetization transfer imaging. Magn Reson Med 2010;64:491-500.
101. Poot DHJ, den Dekker AJ, Achten E, Verhoye M, Sijbers J. Optimal Experimental Design for Diffusion Kurtosis Imaging. Ieee Transactions on Medical Imaging 2010;29:819-29.
102. Klein S, Staring M, Murphy K, Viergever MA, Pluim JPW. elastix: A Toolbox for Intensity-Based Medical Image Registration. Ieee Transactions on Medical Imaging 2010;29:196-205.
103. Klein S, van der Heide UA, Lips IM, van Vulpen M, Staring M, Pluim JPW. Automatic segmentation of the prostate in 3D MR images by atlas matching using localized mutual information. Medical Physics 2008;35:1407-17.
104. Shrout PE, Fleiss JL. Intraclass Correlations - Uses in Assessing Rater Reliability. Psychological Bulletin 1979;86:420-28.
105. McGraw KO, Wong SP. Forming inferences about some intraclass correlation coefficients. Psychological Methods 1996;1:30-46.
106. Petráš I, Bednárová D. Total least squares approach to modeling: a Matlab toolbox. Acta Montanistica Slovaca 2010;15:158-70.
107. Golub GH, Vanloan CF. An Analysis of the Total Least-Squares Problem. Siam Journal on Numerical Analysis 1980;17:883-93.
108. Buckwalter JA, Saltzman C, Brown T. The impact of osteoarthritis - Implications for research. Clinical Orthopaedics and Related Research 2004:S6-S15.
109. Woolf AD, Pfleger B. Burden of major musculoskeletal conditions. Bulletin of the World Health Organization 2003;81:646-56.
110. Tiderius CJ, Olsson LE, Nyquist F, Dahlberg L. Cartilage glycosaminoglycan loss in the acute phase after an anterior cruciate ligament injury - Delayed gadolinium-enhanced magnetic resonance imaging of cartilage and synovial fluid analysis. Arthritis and Rheumatism 2005;52:120-27.
111. Vasiliadis HS, Danielson B, Ljunberg M, McKeon B, Lindahl A, Peterson L. Autologous Chondrocyte Implantation in Cartilage Lesions of the Knee Long-term Evaluation With Magnetic Resonance Imaging and Delayed Gadolinium-Enhanced Magnetic Resonance Imaging Technique. American Journal of Sports Medicine 2010;38:943-49.
112. Gillis A, Bashir A, McKeon B, Scheller A, Gray ML, Burstein D. Magnetic resonance imaging of relative glycosaminoglycan distribution in patients with autologous chondrocyte transplants. Invest Radiol 2001;36:743-48.
113. Trattnig S, Burstein D, Szomolanyi P, Pinker K, Welsch GH, Mamisch TC. T1 (Gd) Gives Comparable Information as Delta T1 Relaxation Rate in dGEMRIC Evaluation of Cartilage Repair Tissue. Invest Radiol 2009;44:598-602.
114. Trattnig S, Marlovits S, Gebetsroither S, Szomolanyi P, Welsch GH, Salomonowitz E, et al. Three-dimensional delayed gadolinium-enhanced MRI of cartilage (dGEMRIC) for in vivo evaluation of reparative cartilage after matrix-associated autologous chondrocyte transplantation at 3.0T: Preliminary results. Journal of Magnetic Resonance Imaging 2007;26:974-82.

115. Burstein D, Velyvis J, Scott KT, Stock KW, Kim YJ, Jaramillo D, et al. Protocol issues for delayed Gd(DTPA)(2-)-enhanced MRI: (dGEMRIC) for clinical evaluation of articular cartilage. Magnetic Resonance in Medicine 2001;45:36-41.
116. Felson DT, Lawrence RC, Dieppe PA, Hirsch R, Helmick CG, Jordan JM, et al. Osteoarthritis: new insights. Part 1: the disease and its risk factors. Ann Intern Med 2000;133:635-46.
117. Jensen MP, Miller L, Fisher LD. Assessment of pain during medical procedures: A comparison of three scales. Clinical Journal of Pain 1998;14:343-49.
118. Ferraz MB, Quaresma MR, Aquino LRL, Atra E, Tugwell P, Goldsmith CH. Reliability of Pain Scales in the Assessment of Literate and Illiterate Patients with Rheumatoid-Arthritis. Journal of Rheumatology 1990;17:1022-24.
119. Mayerhoefer ME, Welsch GH, Mamisch TC, Kainberger F, Weber M, Nemec S, et al. The in vivo effects of unloading and compression on T1-Gd (dGEMRIC) relaxation times in healthy articular knee cartilage at 3.0 Tesla. European Radiology 2010;20:443-49.
120. Eckstein F, Ateshian G, Burgkart R, Burstein D, Cicuttini F, Dardzinski B, et al. Proposal for a nomenclature for Magnetic Resonance Imaging based measures of articular cartilage in osteoarthritis. Osteoarthritis and Cartilage 2006;14:974-83.
121. Tiderius CJ, Tjornstrand J, Akeson P, Sodersten K, Dahlberg L, Leander P. Delayed gadolinium-enhanced MRI of cartilage (dGEMRIC): Intra- and interobserver variability in standardized drawing of regions of interest. Acta Radiologica 2004;45:628-34.
122. Tiderius CJ, Olsson LE, de Verdier H, Leander P, Ekberg O, Dahlberg L. Gd-DTPA2)-enhanced MRI of femoral knee cartilage: a dose-response study in healthy volunteers. Magn Reson Med 2001;46:1067-71.
123. Bron EE, van Tiel J, Smit H, Poot DHJ, Niessen WJ, Krestin GP, et al. Image registration improves human knee cartilage T1 mapping with delayed gadolinium-enhanced MRI of cartilage (dGEMRIC). European Radiology 2013;23:246-52.
124. Atkinson G, Nevill AM. Statistical methods for assessing measurement error (reliability) in variables relevant to sports medicine. Sports Med 1998;26:217-38.
125. Bland JM, Altman DG. Statistical Methods for Assessing Agreement between Two Methods of Clinical Measurement. Lancet 1986;1:307-10.
126. Bedi A, Feeley BT, Williams RJ. Management of Articular Cartilage Defects of the Knee. Journal of Bone and Joint Surgery-American Volume 2010;92A:994-1009.
127. Hawezi ZK, Lammentausta E, Svensson J, Dahlberg LE, Tiderius CJ. In Vivo Transport of Gd-DTPA(2-) in Human Knee Cartilage Assessed by Depth-Wise dGEMRIC Analysis. Journal of Magnetic Resonance Imaging 2011;34:1352-58.
128. Neu CP. Functional imaging in OA: role of imaging in the evaluation of tissue biomechanics. Osteoarthritis Cartilage 2014;22:1349-59.
129. Oei EH, van Tiel J, Robinson WH, Gold GE. Quantitative radiologic imaging techniques for articular cartilage composition: toward early diagnosis and development of disease-modifying therapeutics for osteoarthritis. Arthritis Care Res (Hoboken) 2014;66:1129-41.
130. Wang L, Regatte RR. T1rho MRI of human musculoskeletal system. J Magn Reson Imaging 2015;41:586-600.
131. Regatte RR, Akella SV, Wheaton AJ, Lech G, Borthakur A, Kneeland JB, et al. 3D-T1rho-relaxation mapping of articular cartilage: in vivo assessment of early degenerative changes in symptomatic osteoarthritic subjects. Acad Radiol 2004;11:741-9.
132. Li X, Han ET, Ma CB, Link TM, Newitt DC, Majumdar S. In vivo 3T spiral imaging based multi-slice T(1rho) mapping of knee cartilage in osteoarthritis. Magn Reson Med 2005;54:929-36.

133. Keenan KE, Besier TF, Pauly JM, Han E, Rosenberg J, Smith RL, et al. Prediction of glycosaminoglycan content in human cartilage by age, T1rho and T2 MRI. Osteoarthritis Cartilage 2011;19:171-9.
134. Li X, Cheng J, Lin K, Saadat E, Bolbos RI, Jobke B, et al. Quantitative MRI using T1rho and T2 in human osteoarthritic cartilage specimens: correlation with biochemical measurements and histology. Magn Reson Imaging 2011;29:324-34.
135. Chen W, Takahashi A, Han ET. 3D Quantitative Imaging of T1rho and T2. In: 19th Ed. International Society for Magnetic Resonance in Medicine: Annual Meeting & Exhibition. Montréal 2011.
136. van Tiel J, Bron EE, Tiderius CJ, Bos PK, Reijman M, Klein S, et al. Reproducibility of 3D delayed gadolinium enhanced MRI of cartilage (dGEMRIC) of the knee at 3.0 T in patients with early stage osteoarthritis. Eur Radiol 2013;23:496-504.
137. Tiderius C, Hori M, Williams A, Sharma L, Prasad PV, Finnell M, et al. dGEMRIC as a function of BMI. Osteoarthritis Cartilage 2006;14:1091-7.
138. Farndale RW, Buttle DJ, Barrett AJ. Improved quantitation and discrimination of sulphated glycosaminoglycans by use of dimethylmethylene blue. Biochim Biophys Acta 1986;883:173-7.
139. Bank RA, Krikken M, Beekman B, Stoop R, Maroudas A, Lafeber FP, et al. A simplified measurement of degraded collagen in tissues: application in healthy, fibrillated and osteoarthritic cartilage. Matrix Biol 1997;16:233-43.
140. Lunn DJ, Thomas A, Best N, Spiegelhalter D. WinBUGS – A Bayesian modelling framework: Concepts, structure, and extensibility. Statistics and Computing 2000;10:325-37.
141. Watanabe A, Boesch C, Anderson SE, Brehm W, Mainil Varlet P. Ability of dGEMRIC and T2 mapping to evaluate cartilage repair after microfracture: a goat study. Osteoarthritis Cartilage 2009;17:1341-9.
142. Salo EN, Nissi MJ, Kulmala KA, Tiitu V, Toyras J, Nieminen MT. Diffusion of Gd-DTPA(2)(-) into articular cartilage. Osteoarthritis Cartilage 2012;20:117-26.
143. van Tiel J, Kotek G, Reijman M, Bos PK, Bron EE, Klein S, et al. Delayed gadolinium-enhanced MRI of the meniscus (dGEMRIM) in patients with knee osteoarthritis: relation with meniscal degeneration on conventional MRI, reproducibility, and correlation with dGEMRIC. Eur Radiol 2014;24:2261-70.
144. Balazs EA. The physical properties of synovial fluid and the specific role of hyaluronic acid. J B Lippincott, Philadelphia 1982:61-74.
145. Divine JG, Zazulak BT, Hewett TE. Viscosupplementation for knee osteoarthritis: a systematic review. Clin Orthop Relat Res 2007;455:113-22.
146. Bellamy N, Campbell J, Robinson V, Gee T, Bourne R, Wells G. Viscosupplementation for the treatment of osteoarthritis of the knee. Cochrane Database Syst Rev 2006:CD005321.
147. Goldberg VM, Buckwalter JA. Hyaluronans in the treatment of osteoarthritis of the knee: evidence for disease-modifying activity. Osteoarthritis and Cartilage 2005;13:216-24.
148. Moreland LW. Intra-articular hyaluronan (hyaluronic acid) and hylans for the treatment of osteoarthritis: mechanisms of action. Arthritis Research & Therapy 2003;5:54-67.
149. Kawasaki K, Ochi M, Uchio Y, Adachi N, Matsusaki M. Hyaluronic acid enhances proliferation and chondroitin sulfate synthesis in cultured chondrocytes embedded in collagen gels. J Cell Physiol 1999;179:142-48.
150. Frean SP, Abraham LA, Lees P. In vitro stimulation of equine articular cartilage proteoglycan synthesis by hyaluronan and carprofen. Res Vet Sci 1999;67:183-90.
151. Stove J, Gerlach C, Huch K, Gunther KP, Puhl W, Scharf HP. Effects of hyaluronan on proteoglycan content of osteoarthritic chondrocytes in vitro. Journal of Orthopaedic Research 2002;20:551-55.
152. Kikuchi T, Yamada H, Fujikawa K. Effects of high molecular weight hyaluronan on the distribution and movement of proteoglycan around chondrocytes cultured in alginate beads. Osteoarthritis and Cartilage 2001;9:351-56.

153. Grushko G, Schneiderman R, Maroudas A. Some biochemical and biophysical parameters for the study of the pathogenesis of osteoarthritis: a comparison between the processes of ageing and degeneration in human hip cartilage. Connect Tissue Res 1989;19:149-76.
154. Crema MD, Roemer FW, Marra MD, Burstein D, Gold GE, Eckstein F, et al. Articular Cartilage in the Knee: Current MR Imaging Techniques and Applications in Clinical Practice and Research. Radiographics 2011;31:37-U76.
155. Roemer FW, Crema MD, Trattnig S, Guermazi A. Advances in Imaging of Osteoarthritis and Cartilage. Radiology 2011;260:332-54.
156. McAlindon TE, Nuite M, Krishnan N, Ruthazer R, Price LL, Burstein D, et al. Change in knee osteoarthritis cartilage detected by delayed gadolinium enhanced magnetic resonance imaging following treatment with collagen hydrolysate: a pilot randomized controlled trial. Osteoarthritis and Cartilage 2011;19:399-405.
157. Prasad PV, Li W, Schnitzer T, Krishnan N, Burstein D. Preliminary Evaluation of Potential Disease Modification by Hylan G-F 20 (Synvisc®) Using dGEMRIC. J Mol Imag Dynamic 2012;2.
158. Roos EM, Toksvig-Larsen S. Knee injury and Osteoarthritis Outcome Score (KOOS) - validation and comparison to the WOMAC in total knee replacement. Health Qual Life Outcomes 2003;1:17.
159. de Groot IB, Favejee MM, Reijman M, Verhaar JA, Terwee CB. The Dutch version of the Knee Injury and Osteoarthritis Outcome Score: a validation study. Health Qual Life Outcomes 2008;6:16.
160. Hermans J, Bierma-Zeinstra SMA, Bos PK, Verhaar JAN, Reijman M. The Most Accurate Approach for Intra-Articular Needle Placement in the Knee Joint: A Systematic Review. Semin Arthritis Rheum 2011;41:106-15.
161. Holm S. A Simple Sequentially Rejective Multiple Test Procedure. Scandinavian Journal of Statistics 1979;6:65-70.
162. Chan AOO, Jim MH, Lam KF, Morris JS, Siu DCW, Tong T, et al. Prevalence of colorectal neoplasm among patients with newly diagnosed coronary artery disease. Jama-Journal of the American Medical Association 2007;298:1412-19.
163. Kimelman T, Vu A, Storey P, McKenzie C, Burstein D, Prasad P. Three-dimensional T1 mapping for dGEMRIC at 3.0 T using the look locker method. Invest Radiol 2006;41:198-203.
164. Williams A, Mikulis B, Krishnan N, Gray M, McKenzie C, Burstein D. Suitability of T-1Gd as the "dGEMRIC Index" at 1.5T and 3.0T. Magnetic Resonance in Medicine 2007;58:830-34.
165. Zhang W, Nuki G, Moskowitz RW, Abramson S, Altman RD, Arden NK, et al. OARSI recommendations for the management of hip and knee osteoarthritis Part III: changes in evidence following systematic cumulative update of research published through January 2009. Osteoarthritis and Cartilage 2010;18:476-99.
166. Ghosh P, Holbert C, Read R, Armstrong S. Hyaluronic-Acid (Hyaluronan) in Experimental Osteoarthritis. Journal of Rheumatology 1995;22:155-57.
167. Larsen NE, Lombard KM, Parent EG, Balazs EA. Effect of Hylan on Cartilage and Chondrocyte Cultures. Journal of Orthopaedic Research 1992;10:23-32.
168. Yoshioka M, Shimizu C, Harwood FL, Coutts RD, Amiel D. The effects of hyaluronan during the development of osteoarthritis. Osteoarthritis and Cartilage 1997;5:251-60.
169. Huang GS, Lee HS, Chou MC, Shih YYI, Tsai PH, Lin MH, et al. Quantitative MR T2 measurement of articular cartilage to assess the treatment effect of intra-articular hyaluronic acid injection on experimental osteoarthritis induced by ACLX. Osteoarthritis and Cartilage 2010;18:54-60.
170. Wang YY, Hall S, Hanna F, Wluka AE, Grant G, Marks P, et al. Effects of Hylan G-F 20 supplementation on cartilage preservation detected by magnetic resonance imaging in osteoarthritis of the knee: a two-year single-blind clinical trial. Bmc Musculoskeletal Disorders 2011;12:195.

171. von den Hoff JW, van Kampen GP, van de Stadt RJ, van der Korst JK. Kinetics of proteoglycan turnover in bovine articular cartilage explants. Matrix 1993;13:195-201.
172. van Kampen GP, van de Stadt RJ, van der Korst JK. 'Resident' proteoglycans in mature articular cartilage. Trans. Orthop. Res. Soc. 1991;16.
173. Maroudas A, Leaback DH, Stockwell RA. Glycosaminoglycan Turn-over in Articular-Cartilage. Philosophical Transactions of the Royal Society of London Series B-Biological Sciences 1975;271:293-313.
174. Guidolin DD, Ronchetti IP, Lini E, Guerra D, Frizziero L. Morphological analysis of articular cartilage biopsies from a randomized. clinical study comparing the effects of 500-730 kDa sodium hyaluronate (Hyalgan (R)) and methylprednisolone acetate on primary osteoarthritis of the knee. Osteoarthritis and Cartilage 2001;9:371-81.
175. Pasquali Ronchetti I, Guerra D, Taparelli F, Boraldi F, Bergamini G, Mori G, et al. Morphological analysis of knee synovial membrane biopsies from a randomized controlled clinical study comparing the effects of sodium hyaluronate (Hyalgan) and methylprednisolone acetate (Depomedrol) in osteoarthritis. Rheumatology (Oxford) 2001;40:158-69.
176. Frizziero L, Govoni E, Bacchini P. Intra-articular hyaluronic acid in the treatment of osteoarthritis of the knee: Clinical and morphological study. Clin Exp Rheumatol 1998;16:441-49.
177. Scanzello CR, Goldring SR. The role of synovitis in osteoarthritis pathogenesis. Bone 2012;51:249-57.
178. Sofat N, Ejindu V, Kiely P. What makes osteoarthritis painful? The evidence for local and central pain processing. Rheumatology (Oxford) 2011;50:2157-65.
179. Conaghan PG, Kloppenburg M, Schett G, Bijlsma JW. Osteoarthritis research priorities: a report from a EULAR ad hoc expert committee. Ann Rheum Dis 2014.
180. Yelin E, Murphy L, Cisternas MG, Foreman AJ, Pasta DJ, Helmick CG. Medical care expenditures and earnings losses among persons with arthritis and other rheumatic conditions in 2003, and comparisons with 1997. Arthritis Rheum 2007;56:1397-407.
181. Hunter DJ, Zhang YQ, Niu JB, Tu X, Amin S, Clancy M, et al. The association of meniscal pathologic changes with cartilage loss in symptomatic knee osteoarthritis. Arthritis Rheum 2006;54:795-801.
182. Englund M, Guermazi A, Roemer FW, Aliabadi P, Yang M, Lewis CE, et al. Meniscal Tear in Knees Without Surgery and the Development of Radiographic Osteoarthritis Among Middle-Aged and Elderly Persons The Multicenter Osteoarthritis Study. Arthritis and Rheumatism 2009;60:831-39.
183. Englund M, Guermazi A, Lohmander SL. The role of the meniscus in knee osteoarthritis: a cause or consequence? Radiol Clin North Am 2009;47:703-12.
184. Mcnicol D, Roughley PJ. Extraction and Characterization of Proteoglycan from Human Meniscus. Biochemical Journal 1980;185:705-13.
185. Hellio Le Graverand MP, Vignon E, Otterness IG, Hart DA. Early changes in lapine menisci during osteoarthritis development: Part I: cellular and matrix alterations. Osteoarthritis Cartilage 2001;9:56-64.
186. Krishnan N, Shetty SK, Williams A, Mikulis B, McKenzie C, Burstein D. Delayed gadolinium-enhanced magnetic resonance imaging of the meniscus: an index of meniscal tissue degeneration? Arthritis Rheum 2007;56:1507-11.
187. Mayerhoefer ME, Mamisch TC, Riegler G, Welsch GH, Dobrocky T, Weber M, et al. Gadolinium diethylenetriaminepentaacetate enhancement kinetics in the menisci of asymptomatic subjects: a first step towards a dedicated dGEMRIC (delayed gadolinium-enhanced MRI of cartilage)-like protocol for biochemical imaging of the menisci. Nmr in Biomedicine 2011;24:1210-15.
188. Herwig J, Egner E, Buddecke E. Chemical-Changes of Human Knee-Joint Menisci in Various Stages of Degeneration. Ann Rheum Dis 1984;43:635-40.

189. van Tiel J, Reijman M, Bos PK, Hermans J, van Buul GM, Bron EE, et al. Delayed gadolinium-enhanced MRI of cartilage (dGEMRIC) shows no change in cartilage structural composition after viscosupplementation in patients with early-stage knee osteoarthritis. PLoS One 2013;8:e79785.
190. Crues JV, Mink J, Levy TL, Lotysch M, Stoller DW. Meniscal Tears of the Knee - Accuracy of Mr Imaging. Radiology 1987;164:445-48.
191. Reicher MA, Hartzman S, Duckwiler GR, Bassett LW, Anderson LJ, Gold RH. Meniscal Injuries - Detection Using Mr Imaging. Radiology 1986;159:753-57.
192. Meredith DS, Losina E, Mahorned NN, Wright J, Katz JN. Factors predicting functional and radiographic outcomes after arthroscopic partial meniscectomy: A review of the literature. Arthroscopy-the Journal of Arthroscopic and Related Surgery 2005;21:211-23.
193. Salata MJ, Gibbs AE, Sekiya JK. A Systematic Review of Clinical Outcomes in Patients Undergoing Meniscectomy. American Journal of Sports Medicine 2010;38:1907-16.
194. Nieminen MT, Rieppo J, Toyras J, Hakumaki JM, Silvennoinen J, Hyttinen MM, et al. T2 relaxation reveals spatial collagen architecture in articular cartilage: a comparative quantitative MRI and polarized light microscopic study. Magn Reson Med 2001;46:487-93.
195. Zarins ZA, Bolbos RI, Pialat JB, Link TM, Li X, Souza RB, et al. Cartilage and meniscus assessment using T1rho and T2 measurements in healthy subjects and patients with osteoarthritis. Osteoarthritis and Cartilage 2010;18:1408-16.
196. Li W, Edelman RR, Prasad PV. Delayed Contrast Enhanced MRI of Meniscus With Ionic and Non-ionic Agents. Journal of Magnetic Resonance Imaging 2011;33:731-35.
197. Li W, Scheidegger R, Wu Y, Edelman RR, Farley M, Krishnan N, et al. Delayed Contrast-Enhanced MRI of Cartilage: Comparison of Nonionic and Ionic Contrast Agents. Magnetic Resonance in Medicine 2010;64:1267-73.
198. Silvast TS, Jurvelin JS, Tiitu V, Quinn TM, Töyräs J. Bath Concentration of Anionic Contrast Agents Does Not Affect Their Diffusion and Distribution in Articular Cartilage In Vitro. Cartilage 2013;4:42-51.
199. Wiener E, Settles M, Weirich G, Schmidt C, Diederichs G. The Influence of Collagen Network Integrity on the Accumulation of Gadolinium-Based MR Contrast Agents in Articular Cartilage. Rofo-Fortschritte Auf Dem Gebiet Der Rontgenstrahlen Und Der Bildgebenden Verfahren 2011;183:226-32.
200. Siebelt M, van Tiel J, Waarsing JH, Piscaer TM, Straten M, Booij R, et al. Clinically applied CT arthrography to measure the sulphated glycosaminoglycan content of cartilage. Osteoarthritis and Cartilage 2011;19:1183-89.
201. Son M, Goodman SB, Chen W, Hargreaves BA, Gold GE, Levenston ME. Regional Variation in T1rho and T2 Times in Osteoarthritic Human Menisci: Correlation with Mechanical Properties and Matrix Composition. Osteoarthritis Cartilage 2013.
202. Williams A, Qian Y, Golla S, Chu CR. UTE-T2* mapping detects sub-clinical meniscus injury after anterior cruciate ligament tear. Osteoarthritis and Cartilage 2012;20:486-94.
203. Kallioniemi AS, Jurvelin JS, Nieminen MT, Lammi MJ, Toyras J. Contrast agent enhanced pQCT of articular cartilage. Physics in Medicine and Biology 2007;52:1209-19.
204. Xie L, Lin AS, Levenston ME, Guldberg RE. Quantitative assessment of articular cartilage morphology via EPIC-microCT. Osteoarthritis Cartilage 2009;17:313-20.
205. Eckstein F, Burstein D, Link TM. Quantitative MRI of cartilage and bone: degenerative changes in osteoarthritis. Nmr in Biomedicine 2006;19:822-54.
206. Eckstein F, Cicuttini F, Raynauld JP, Waterton JC, Peterfy C. Magnetic resonance imaging (MRI) of articular cartilage in knee osteoarthritis (OA): morphological assessment. Osteoarthritis and Cartilage 2006;14:A46-A75.

207. Silvast TS, Jurvelin JS, Aula AS, Lammi MJ, Toyras J. Contrast Agent-Enhanced Computed Tomography of Articular Cartilage: Association with Tissue Composition and Properties. Acta Radiologica 2009;50:78-85.
208. Silvast TS, Jurvelin JS, Lammi MJ, Toyras J. pQCT study on diffusion and equilibrium distribution of iodinated anionic contrast agent in human articular cartilage - associations to matrix composition and integrity. Osteoarthritis and Cartilage 2009;17:26-32.
209. Silvast TS, Kokkonen HT, Jurvelin JS, Quinn TM, Nieminen MT, Toyras J. Diffusion and near-equilibrium distribution of MRI and CT contrast agents in articular cartilage. Physics in Medicine and Biology 2009;54:6823-36.
210. Maroudas A. Distribution and diffusion of solutes in articular cartilage. Biophys J 1970;10:365-79.
211. Perlewitz TJ, Haughton VM, Riley LH, NguyenMinh C, George V. Effect of molecular weight on the diffusion of contrast media into cartilage. Spine 1997;22:2707-10.
212. Bullough PG, Yawitz PS, Tafra L, Boskey AL. Topographical Variations in the Morphology and Biochemistry of Adult Canine Tibial Plateau Articular-Cartilage. Journal of Orthopaedic Research 1985;3:1-16.
213. Weiss C, Mirow S. An ultrastructural study of osteoarthritis changes in the articular cartilage of human knees. J Bone Joint Surg Am 1972;54:954-72.
214. Bryant D, Havey TC, Roberts R, Guyatt G. How many patients? How many limbs? Analysis of patients or limbs in the orthopaedic literature: a systematic review. J Bone Joint Surg Am 2006;88:41-5.
215. Park MS, Kim SJ, Chung CY, Choi IH, Lee SH, Lee KM. Statistical Consideration for Bilateral Cases in Orthopaedic Research. Journal of Bone and Joint Surgery-American Volume 2010;92A:1732-37.
216. Bansal PN, Joshi NS, Entezari V, Grinstaff MW, Snyder BD. Contrast enhanced computed tomography can predict the glycosaminoglycan content and biomechanical properties of articular cartilage. Osteoarthritis Cartilage 2010;18:184-91.
217. Julkunen P, Korhonen RK, Nissi MJ, Jurvelin JS. Mechanical characterization of articular cartilage by combining magnetic resonance imaging and finite-element analysis - a potential functional imaging technique. Physics in Medicine and Biology 2008;53:2425-38.
218. Kiviranta P, Rieppo J, Korhonen RK, Julkunen P, Toyras J, Jurvelin JS. Collagen network primarily controls Poisson's ratio of bovine articular cartilage in compression. Journal of Orthopaedic Research 2006;24:690-99.
219. Urban JPG, Hall AC, Gehl KA. Regulation of Matrix Synthesis Rates by the Ionic and Osmotic Environment of Articular Chondrocytes. J Cell Physiol 1993;154:262-70.
220. Biswas D, Bible JE, Bohan M, Simpson AK, Whang PG, Grauer JN. Radiation Exposure from Musculoskeletal Computerized Tomographic Scans. Journal of Bone and Joint Surgery-American Volume 2009;91A:1882-89.
221. Trattnig S, Domayer S, Welsch GW, Mosher T, Eckstein F. MR imaging of cartilage and its repair in the knee - a review. European Radiology 2009;19:1582-94.
222. Gatehouse PD, Thomas RW, Robson MD, Hamilton G, Herlihy AH, Bydder GM. Magnetic resonance imaging of the knee with ultrashort TE pulse sequences. Magnetic Resonance Imaging 2004;22:1061-67.
223. Bieri O, Scheffler K, Welsch GH, Trattnig S, Mamisch TC, Ganter C. Quantitative mapping of T2 using partial spoiling. Magn Reson Med 2011;66:410-8.
224. Williams A, Qian Y, Bear D, Chu CR. Assessing degeneration of human articular cartilage with ultrashort echo time (UTE) T2* mapping. Osteoarthritis Cartilage 2010;18:539-46.
225. Neu CP, Walton JH. Displacement encoding for the measurement of cartilage deformation. Magnetic Resonance in Medicine 2008;59:149-55.

226. Guermazi A, Burstein D, Conaghan P, Eckstein F, Le Graverand-Gastineau MPH, Keen H, et al. Imaging in osteoarthritis. Rheumatic Disease Clinics of North America 2008;34:645-+.
227. Gray ML, Burstein D, Kim YJ, Maroudas A. 2007 Elizabeth Winston Lanier Award Winner. Magnetic resonance imaging of cartilage glycosaminoglycan: basic principles, imaging technique, and clinical applications. J Orthop Res 2008;26:281-91.
228. Maes F, Collignon A, Vandermeulen D, Marchal G, Suetens P. Multimodality image registration by maximization of mutual information. Ieee Transactions on Medical Imaging 1997;16:187-98.
229. Vande Berg BC, Lecouvet FE, Poilvache P, Maldague B, Malghem J. Spiral CT arthrography of the knee: technique and value in the assessment of internal derangement of the knee. Eur Radiol 2002;12:1800-10.
230. Gervaise A, Osemont B, Lecocq S, Noel A, Micard E, Felblinger J, et al. CT image quality improvement using adaptive iterative dose reduction with wide-volume acquisition on 320-detector CT. European Radiology 2012;22:295-301.
231. Tamm EP, Rong XJ, Cody DD, Ernst RD, Fitzgerald NE, Kundra V. Quality initiatives: CT radiation dose reduction: how to implement change without sacrificing diagnostic quality. Radiographics 2011;31:1823-32.
232. Aula AS, Jurvelin JS, Toyras J. Simultaneous computed tomography of articular cartilage and subchondral bone. Osteoarthritis Cartilage 2009;17:1583-8.
233. Mosher TJ, Dardzinski BJ. Cartilage MRI T2 relaxation time mapping: overview and applications. Semin Musculoskelet Radiol 2004;8:355-68.
234. Bansal PN, Joshi NS, Entezari V, Malone BC, Stewart RC, Snyder BD, et al. Cationic contrast agents improve quantification of glycosaminoglycan (GAG) content by contrast enhanced CT imaging of cartilage. J Orthop Res 2011;29:704-9.
235. Bansal PN, Stewart RC, Entezari V, Snyder BD, Grinstaff MW. Contrast agent electrostatic attraction rather than repulsion to glycosaminoglycans affords a greater contrast uptake ratio and improved quantitative CT imaging in cartilage. Osteoarthritis Cartilage 2011;19:970-6.
236. Hirvasniemi J, Kulmala KA, Lammentausta E, Ojala R, Lehenkari P, Kamel A, et al. In vivo comparison of delayed gadolinium-enhanced MRI of cartilage and delayed quantitative CT arthrography in imaging of articular cartilage. Osteoarthritis Cartilage 2013;21:434-42.
237. Kokkonen HT, Suomalainen JS, Joukainen A, Kroger H, Sirola J, Jurvelin JS, et al. In vivo diagnostics of human knee cartilage lesions using delayed CBCT arthrography. J Orthop Res 2014;32:403-12.
238. Fisher RA. Frequency distribution of the values of the correlation coefficient in samples of an indefinitely large population. Biometrika 1915;10:507–21.
239. Mason RO, Lind DA, Marchal WG. Statistics: An Introduction. New York, Harcourt Brace Jovanovich, Inc 1983.
240. Zhang D, Cagnon CH, Villablanca JP, McCollough CH, Cody DD, Stevens DM, et al. Peak skin and eye lens radiation dose from brain perfusion CT based on Monte Carlo simulation. AJR Am J Roentgenol 2012;198:412-7.
241. Waarsing JH, Day JS, Weinans H. An improved segmentation method for in vivo microCT imaging. Journal of Bone and Mineral Research 2004;19:1640-50.
242. Gelman A, Meng XL, Stern H. Posterior predictive assessment of model fitness via realized discrepancies. Statistica Sinica 1996;6:733-807.
243. Lesaffre E, Lawson AB. Bayesian Biostatistics. New York, John Wiley & Sons 2012.
244. Guermazi A, Hayashi D, Roemer FW, Felson DT. Osteoarthritis: a review of strengths and weaknesses of different imaging options. Rheum Dis Clin North Am 2013;39:567-91.

245. Siebelt M, Agricola R, Weinans H, Kim YJ. The role of imaging in early hip OA. Osteoarthritis Cartilage 2014;22:1470-80.
246. van Tiel J, Siebelt M, Waarsing JH, Piscaer TM, van Straten M, Booij R, et al. CT arthrography of the human knee to measure cartilage quality with low radiation dose. Osteoarthritis Cartilage 2012;20:678-85.
247. Kokkonen HT, Aula AS, Kröger H, Suomalainen JS, Lammentausta E, Mervaala E, et al. Delayed Computed Tomography Arthrography of Human Knee Cartilage In Vivo. Cartilage 2012;3:334-41.
248. Kiviranta P, Rieppo J, Korhonen RK, Julkunen P, Toyras J, Jurvelin JS. Collagen network primarily controls Poisson's ratio of bovine articular cartilage in compression. J Orthop Res 2006;24:690-9.
249. Turunen M, Toyras J, Kokkonen H, Jurvelin J. Quantitative Evaluation of Knee Subchondral Bone Mineral Density Using Cone Beam Computed Tomography. IEEE Trans Med Imaging 2015.
250. Sigurdsson U, Siversson C, Lammentausta E, Svensson J, Tiderius CJ, Dahlberg LE. In vivo transport of Gd-DTPA2- into human meniscus and cartilage assessed with delayed gadolinium-enhanced MRI of cartilage (dGEMRIC). BMC Musculoskelet Disord 2014;15:226.
251. Lakin BA, Grasso DJ, Stewart RC, Freedman JD, Snyder BD, Grinstaff MW. Contrast enhanced CT attenuation correlates with the GAG content of bovine meniscus. J Orthop Res 2013;31:1765-71.
252. Honkanen JT, Danso EK, Suomalainen JS, Tiitu V, Korhonen RK, Jurvelin JS, et al. Contrast enhanced imaging of human meniscus using cone beam CT. Osteoarthritis Cartilage 2015.
253. McAlindon TE, Driban JB, Henrotin Y, Hunter DJ, Jiang GL, Skou ST, et al. OARSI Clinical Trials Recommendations: Design, conduct, and reporting of clinical trials for knee osteoarthritis. Osteoarthritis Cartilage 2015;23:747-60.
254. Roemer FW, Guermazi A. Osteoarthritis year in review 2014: imaging. Osteoarthritis Cartilage 2014;22:2003-12.
255. Eckstein F, Guermazi A, Gold G, Duryea J, Hellio Le Graverand MP, Wirth W, et al. Imaging of cartilage and bone: promises and pitfalls in clinical trials of osteoarthritis. Osteoarthritis Cartilage 2014;22:1516-32.
256. Singh A, Haris M, Cai KJ, Kassey VB, Kogan F, Reddy D, et al. Chemical exchange saturation transfer magnetic resonance imaging of human knee cartilage at 3 T and 7 T. Magnetic Resonance in Medicine 2012;68:588-94.
257. Madelin G, Babb JS, Xia D, Chang G, Jerschow A, Regatte RR. Reproducibility and repeatability of quantitative sodium magnetic resonance imaging in vivo in articular cartilage at 3 T and 7 T. Magn Reson Med 2012;68:841-9.
258. He J, Wang Q, Ma X, Sun Z. Dual-energy CT angiography of abdomen with routine concentration contrast agent in comparison with conventional single-energy CT with high concentration contrast agent. Eur J Radiol 2015;84:221-7.
259. Mileto A, Ramirez-Giraldo JC, Marin D, Alfaro-Cordoba M, Eusemann CD, Scribano E, et al. Nonlinear image blending for dual-energy MDCT of the abdomen: can image quality be preserved if the contrast medium dose is reduced? AJR Am J Roentgenol 2014;203:838-45.
260. Hunter DJ, Altman RD, Cicuttini F, Crema MD, Duryea J, Eckstein F, et al. OARSI Clinical Trials Recommendations: Knee imaging in clinical trials in osteoarthritis. Osteoarthritis Cartilage 2015;23:698-715.
261. Rutgers M, Bartels LW, Tsuchida AI, Castelein RM, Dhert WJ, Vincken KL, et al. dGEMRIC as a tool for measuring changes in cartilage quality following high tibial osteotomy: a feasibility study. Osteoarthritis Cartilage 2012;20:1134-41.
262. Anandacoomarasamy A, Leibman S, Smith G, Caterson I, Giuffre B, Fransen M, et al. Weight loss in obese people has structure-modifying effects on medial but not on lateral knee articular cartilage. Ann Rheum Dis 2012;71:26-32.

263. Vasiliadis HS, Danielson B, Ljungberg M, McKeon B, Lindahl A, Peterson L. Autologous chondrocyte implantation in cartilage lesions of the knee: long-term evaluation with magnetic resonance imaging and delayed gadolinium-enhanced magnetic resonance imaging technique. Am J Sports Med 2010;38:943-9.
264. Meulenbelt I, Kraus VB, Sandell LJ, Loughlin J. Summary of the OA biomarkers workshop 2010 - genetics and genomics: new targets in OA. Osteoarthritis Cartilage 2011;19:1091-4.
265. Williams A, Qian Y, Chu CR. UTE-T2 * mapping of human articular cartilage in vivo: a repeatability assessment. Osteoarthritis Cartilage 2011;19:84-8.
266. Eckstein F, Mc Culloch CE, Lynch JA, Nevitt M, Kwoh CK, Maschek S, et al. How do short-term rates of femorotibial cartilage change compare to long-term changes? Four year follow-up data from the osteoarthritis initiative. Osteoarthritis Cartilage 2012;20:1250-7.
267. Eckstein F, Kwoh CK, Boudreau RM, Wang Z, Hannon MJ, Cotofana S, et al. Quantitative MRI measures of cartilage predict knee replacement: a case-control study from the Osteoarthritis Initiative. Ann Rheum Dis 2013;72:707-14.
268. Hitzl W, Wirth W, Maschek S, Cotofana S, Nevitt M, John MR, et al. Greater Lateral Femorotibial Cartilage Loss in Osteoarthritis Initiative Participants with Incident Knee Replacement: A Prospective Cohort Study. Arthritis Care Res (Hoboken) 2015.
269. Agricola R, Waarsing JH, Arden NK, Carr AJ, Bierma-Zeinstra SM, Thomas GE, et al. Cam impingement of the hip: a risk factor for hip osteoarthritis. Nature Reviews Rheumatology 2013;9:630-4.
270. Agricola R, Heijboer MP, Bierma-Zeinstra SM, Verhaar JA, Weinans H, Waarsing JH. Cam impingement causes osteoarthritis of the hip: a nationwide prospective cohort study (CHECK). Ann Rheum Dis 2013;72:918-23.
271. Castano-Betancourt MC, Van Meurs JB, Bierma-Zeinstra S, Rivadeneira F, Hofman A, Weinans H, et al. The contribution of hip geometry to the prediction of hip osteoarthritis. Osteoarthritis Cartilage 2013;21:1530-6.
272. Felson DT. Osteoarthritis: priorities for osteoarthritis research: much to be done. Nature Reviews Rheumatology 2014;10:447-8.
273. Atukorala I, Kwoh CK, Guermazi A, Roemer FW, Boudreau RM, Hannon MJ, et al. Synovitis in knee osteoarthritis: a precursor of disease? Ann Rheum Dis 2014.
274. Wang L, Chang G, Xu J, Vieira RL, Krasnokutsky S, Abramson S, et al. T1rho MRI of menisci and cartilage in patients with osteoarthritis at 3T. Eur J Radiol 2012;81:2329-36.
275. Bolbos RI, Link TM, Ma CB, Majumdar S, Li X. T1rho relaxation time of the meniscus and its relationship with T1rho of adjacent cartilage in knees with acute ACL injuries at 3 T. Osteoarthritis Cartilage 2009;17:12-8.
276. Bae WC, Chen PC, Chung CB, Masuda K, D'Lima D, Du J. Quantitative ultrashort echo time (UTE) MRI of human cortical bone: correlation with porosity and biomechanical properties. Journal of Bone and Mineral Research 2012;27:848-57.
277. Du J, Carl M, Bae WC, Statum S, Chang EY, Bydder GM, et al. Dual inversion recovery ultrashort echo time (DIR-UTE) imaging and quantification of the zone of calcified cartilage (ZCC). Osteoarthritis Cartilage 2013;21:77-85.
278. Guermazi A, Hayashi D, Roemer FW, Zhu Y, Niu J, Crema MD, et al. Synovitis in knee osteoarthritis assessed by contrast-enhanced magnetic resonance imaging (MRI) is associated with radiographic tibiofemoral osteoarthritis and MRI-detected widespread cartilage damage: the MOST study. Journal of Rheumatology 2014;41:501-8.
279. de Lange-Brokaar BJ, Ioan-Facsinay A, Yusuf E, Visser AW, Kroon HM, Andersen SN, et al. Degree of synovitis on MRI by comprehensive whole knee semi-quantitative scoring method correlates with

histologic and macroscopic features of synovial tissue inflammation in knee osteoarthritis. Osteoarthritis Cartilage 2014;22:1606-13.
280. McWalter EJ, Sveinsson B, Oei EH, Robinson WH, Genovese MC, Gold GE, et al. Non-contrast Diffusion-weighted MRI for Detection of Synovitis using DESS. In: 22nd Ed. International Society for Magnetic Resonance in Medicine: Annual Meeting & Exhibition. Milan 2014.
281. Bousson V, Lowitz T, Laouisset L, Engelke K, Laredo JD. CT imaging for the investigation of subchondral bone in knee osteoarthritis. Osteoporos Int 2012;23 Suppl 8:S861-5.
282. Eckstein F, Putz R, Muller-Gerbl M, Steinlechner M, Benedetto KP. Cartilage degeneration in the human patellae and its relationship to the mineralisation of the underlying bone: a key to the understanding of chondromalacia patellae and femoropatellar arthrosis? Surg Radiol Anat 1993;15:279-86.
283. Bernsen MR, Vaissier PE, Van Holen R, Booij J, Beekman FJ, de Jong M. The role of preclinical SPECT in oncological and neurological research in combination with either CT or MRI. Eur J Nucl Med Mol Imaging 2014;41 Suppl 1:S36-49.
284. Piscaer TM, Sandker M, van der Jagt OP, Verhaar JA, de Jong M, Weinans H. Real-time assessment of bone metabolism in small animal models for osteoarthritis using multi pinhole-SPECT/CT. Osteoarthritis Cartilage 2013;21:882-8.
285. Piscaer TM, Muller C, Mindt TL, Lubberts E, Verhaar JA, Krenning EP, et al. Imaging of activated macrophages in experimental osteoarthritis using folate-targeted animal single-photon-emission computed tomography/computed tomography. Arthritis Rheum 2011;63:1898-907.
286. Cook GJ, Ryan PJ, Clarke SE, Fogelman I. SPECT bone scintigraphy of anterior cruciate ligament injury. J Nucl Med 1996;37:1353-6.
287. Hart R, Konvicka M, Filan P, deCordeiro J. SPECT scan is a reliable tool for selection of patients undergoing unicompartmental knee arthroplasty. Arch Orthop Trauma Surg 2008;128:679-82.
288. Knupp M, Pagenstert GI, Barg A, Bolliger L, Easley ME, Hintermann B. SPECT-CT compared with conventional imaging modalities for the assessment of the varus and valgus malaligned hindfoot. J Orthop Res 2009;27:1461-6.
289. Ryan PJ, Reddy K, Fleetcroft J. A prospective comparison of clinical examination, MRI, bone SPECT, and arthroscopy to detect meniscal tears. Clin Nucl Med 1998;23:803-6.
290. So Y, Chung JK, Seong SC, Sohn YJ, Kang HS, Lee DS, et al. Usefulness of 99Tcm-MDP knee SPET for pre-arthroscopic evaluation of patients with internal derangements of the knee. Nucl Med Commun 2000;21:103-9.
291. Waarsing JH, Bierma-Zeinstra SM, Weinans H. Distinct subtypes of knee osteoarthritis: data from the Osteoarthritis Initiative. Rheumatology (Oxford) 2015.
292. Felson DT. Identifying different osteoarthritis phenotypes through epidemiology. Osteoarthritis Cartilage 2010;18:601-4.
293. Bierma-Zeinstra SM, Verhagen AP. Osteoarthritis subpopulations and implications for clinical trial design. Arthritis Research & Therapy 2011;13:213.
294. Iranpour-Boroujeni T, Watanabe A, Bashtar R, Yoshioka H, Duryea J. Quantification of cartilage loss in local regions of knee joints using semi-automated segmentation software: analysis of longitudinal data from the Osteoarthritis Initiative (OAI). Osteoarthritis Cartilage 2011;19:309-14.
295. Xia Y, Chandra SS, Engstrom C, Strudwick MW, Crozier S, Fripp J. Automatic hip cartilage segmentation from 3D MR images using arc-weighted graph searching. Physics in Medicine and Biology 2014;59:7245-66.
296. Siversson C, Akhondi-Asl A, Bixby S, Kim YJ, Warfield SK. Three-dimensional hip cartilage quality assessment of morphology and dGEMRIC by planar maps and automated segmentation. Osteoarthritis Cartilage 2014;22:1511-5.

297. Lee JG, Gumus S, Moon CH, Kwoh CK, Bae KT. Fully automated segmentation of cartilage from the MR images of knee using a multi-atlas and local structural analysis method. Medical Physics 2014;41:092303.

chapter 14

Appendices

List of abbreviations

PhD portfolio

List of publications

Dankwoord

Curriculum vitae

LIST OF ABBREVIATIONS

3D: three-dimensional
90%-CRLBσ: 90% percentile of the CRLBσ in a region of interest
95%CI: 95% confidence interval
ACLT: anterior cruciate ligament tear
ADL: activities of daily living
aMEN: anterior horn of the meniscus
BLOKS: Boston Leeds osteoarthritis knee score
BMI: body mass index
CEST: chemical exchange saturation transfer
CI: 95% confidence interval
CRLB: Cramér–Rao lower bound
CRLBσ: square root of the Cramér–Rao lower bound
CT: computed tomography
CTa: using CT arthrography
CTDIvol: CT-Dose Index
CV: coefficient of variation
dGEMRIC: delayed gadolinium-enhanced MRI of cartilage
dGEMRIM: delayed gadolinium-enhanced MRI of the meniscus
DMMB assay: dimethylmethylene blue assay
DMOADs: disease-modifying osteoarthritis drugs
ECM: extracellular matrix
EDTA: ethylenediaminetetraacetic acid
EPIC- μCT: equilibrium partitioning of an ionic contrast agent using micro-CT
EULAR: European league against rheumatism
FCD: fixed-charge density
FOV: field of view
FSE: fast spin echo
FSPGR: fast spoiled gradient-recalled echo
gagCEST: glycosaminoglycan specific chemical exchange saturation transfer
HA: hyaluronic acid
ICC: intraclass correlation coefficient
ICC(2,1): two-way random intraclass correlation coefficient
IRB: Institutional Review Board
IR: inversion recovery
IR SPGR: inversion recovery spoiled gradient-echo
KL: Kellgren & Lawrence grading system
KOOS: knee injury and osteoarthritis outcome score

KOSS: knee osteoarthritis scoring system
LMI: localized mutual information
McMC: Markov chain Monte Carlo
MIRIT: multimodality image registration using information theory
MOAKS: MRI Osteoarthritis Knee Score
mpP: mid-portion of patellar cartilage
MRI: magnetic resonance imaging
ncCT: non-contrast CT
NRS: numeric rating scale
OA: osteoarthritis
OAI: OsteoArthritis Imitative
PBS: phosphate buffered saline
PCC: posterior predictive check
PET: positron emission tomography
pFC: posterior non weight-bearing cartilage of the femoral condyle
PG: proteoglycans
pLC: posterior non-weight bearing area of the lateral femoral condyle
pMC: posterior non-weight bearing area of the medial femoral condyle
pMEN: posterior horn of the meniscus
QoL: knee-related quality of life
r: Pearson's correlation coefficient
ROIs: regions of interest
sGAG: sulphated glycosaminoglycan
SNR: signal-to-noise ratio
SPARCK: software for post processing and registration of cartilage of the knee
SPECT: single photon emission computed tomography
SPGR: spoiled gradient-echo
T: Tesla
$T1_{GD:}$ post contrast T1 relaxation time
TI: inversion time
TKR: total knee replacement
TR: repetition time
TSL: spin lock time
µCT: micro computed tomography
µCTa: micro computed tomography arthrography
VGA: visual grading analysis
wbFC: weight-bearing cartilage of the femoral condyle
wbFCa: anterior weight-bearing cartilage of the femoral condyle
wbFCp: posterior weight-bearing cartilage of the femoral condyle

wbLC: lateral femoral condyle
wbLP: weight-bearing lateral tibial plateau
wbMC: medial femoral condyle
wbMP: weight-bearing medial tibial plateau
wbTP: weight-bearing cartilage of the tibial plateau
WORMS: whole-Organ MRI Score

PHD PORTFOLIO

Name PhD student: J. van Tiel
Erasmus MC Department: Orthopedic Surgery and Radiology
Research School: Molmed / NIHES
PhD period: 15-03-2010 – 31-12-2013
Promotors: Prof.dr.ir. H.H. Weinans and Prof.dr. G.P. Krestin
Daily supervisor: Dr. E.H.G. Oei

General courses / Workshops	**Year**	**Workload (ECTS)**
MRI Safety and Scanning Course (Department of Radiology, Erasmus MC)	2010	2
Introduction to Data Analysis (NIHES)	2010	2
Biomedical Scientific English writing course (Molmed)	2011	4
Translational Imaging Workshop by AMIE "From mouse to man" (Molmed)	2011	1
Basiscursus Regelgeving en Organisatie van Klinische trials / Good Clinical Practice (Molmed)	2011	1
Diagnostic Research (NIHES)	2012	1
Writing a successful grant proposal (Molmed)	2012	1
(Inter)national podium presentations	**Year**	**Workload (ECTS)**
Clinical application of CT-arthrography as a measure for cartilage quality, validated by in-vitro contrast-enhanced µCT. *European congress of Radiology, Vienna, Austria*	2011	1
CT arthrography to measure cartilage quality: influence of sulphated glycosaminoglycan content and structural composition of extracellular matrix on contrast agent diffusion into cartilage. *5th OARSI imaging workshop, Salzburg, Austria*	2011	1
CT-arthrography to measure cartilage quality: influence of sulphated glycosaminoglycan content and structural composition of extracellular matrix on contrast agent diffusion into cartilage. *Radiologendagen, Maastricht, The Netherlands*	2011	1
Reproducibility of 3D delayed Gadolinium Enhanced MRI of Cartilage of the knee at 3.0 Tesla in patients with early stage osteoarthritis. *Radiologendagen, Maastricht, The Netherlands*	2011	1
Reproducibility of 3D delayed Gadolinium Enhanced MRI of Cartilage (dGEMRIC) of the knee at 3.0 Tesla in patients with early stage osteoarthritis. *European society of skeletal radiology, Innsbruck, Austria*	2012	1
3D Delayed Gadolinium-Enhanced MRI of Cartilage at 3.0 Tesla used to evaluate the effect of hyaluronic acid on cartilage quality in knee osteoarthritis patients. *Radiologendagen, 's Hertogenbosch, The Netherlands* Awarded with Best Scientific Paper Award	2012	1

Effectiviteit van hyaluronzuur injecties bij knieartrose geëvalueerd met dGEMRIC. *Najaarscongres Nederlandse Orthopaedische Vereniging, Veldhoven, The Netherlands*	2012	1
Reproducibility of 3D delayed Gadolinium Enhanced MRI of Cartilage of the knee at 3.0 Tesla in patients with early stage osteoarthritis. *Annual Meeting of the Radiological Society of North America, Chicago, United States of America*	2012	1
3D Delayed Gadolinium-Enhanced MRI of Cartilage at 3.0 Tesla used to evaluate the effect of hyaluronic acid on cartilage quality in knee osteoarthritis patients. *European congress of Radiology, Vienna, Austria*	2013	1
Correlation between quantitative delayed contrast-enhancement in meniscus and cartilage in knee osteoarthritis. *Annual meeting of the International Society for Magnetic Resonance in Medicine, Salt Lake City, United States of America*	2013	1
CT arthrography of the human knee to quantitatively measure cartilage biochemical composition: preliminary results of an *in-vivo* validation study *European congress of Radiology, Vienna, Austria*	2014	1
Delayed gadolinium-enhanced MRI of cartilage (dGEMRIC) is superior to T1rho-mapping in measuring cartilage sulphated glycosaminoglycan content: preliminary results of an *in vivo* validation study *European congress of Radiology, Vienna, Austria*	2014	1
Delayed gadolinium-enhanced MRI of the Meniscus (dGEMRIM) in patients with knee osteoarthritis: relation with meniscal degeneration on conventional MRI, reproducibility, and correlation with dGEMRIC *European congress of Radiology, Vienna, Austria*	2014	1
Delayed gadolinium-enhanced MRI of cartilage (dGEMRIC) is superior to T1rho-mapping in measuring cartilage sulphated glycosaminoglycan content: preliminary results of an *in-vivo* validation study using an *ex-vivo* reference standard for cartilage sulphated glycosaminoglycan content *Annual meeting of the International Society for Magnetic Resonance in Medicine, Milano, Italia*	2014	1
Quantitative CT arthrography of the human knee to measure cartilage biochemical composition: results of an *in-vivo* validation study against *ex-vivo* reference standards *Radiologendagen, 's Hertogenbosch, The Netherlands* Nominated for Best Scientific Paper Award	2014	1
Delayed gadolinium-enhanced MRI of cartilage (dGEMRIC) is superior to T1rho-mapping in measuring cartilage glycosaminoglycan content: results of an *in-vivo* validation study against *ex-vivo* reference standards for cartilage composition *Radiologendagen, 's Hertogenbosch, The Netherlands* Nominated for RSNA travel grant	2014	1
Quantitative CT arthrography of the human knee to measure cartilage biochemical composition: results of an *in-vivo* validation study against *ex-vivo* reference standards *Annual Meeting of the Radiological Society of North America, Chicago, United States of America*	2014	1

(Inter)national poster presentations	Year	Workload (ECTS)
CT arthrography of the knee to measure cartilage quality with low radiation exposure. *OARSI World Congress on Osteoarthritis. San Diego, United States of America*	2011	1
CT arthrography of the knee to measure cartilage quality with low radiation exposure. *Annual Meeting of the Orthopedic Research Society, San Francisco, United States of America*	2012	1
CT arthrography of the knee to measure cartilage quality with low radiation exposure. *European congress of Radiology, Vienna, Austria*	2012	1
Reproducibility of 3D delayed Gadolinium Enhanced MRI of Cartilage (dGEMRIC) of the knee at 3.0 Tesla in patients with early stage osteoarthritis. *OARSI World Congress on Osteoarthritis. Barcelona, Spain*	2012	1
Effectiveness of hyaluronic acid in knee osteoarthritis patients evaluated using delayed gadolinium-enhanced MRI of cartilage. *6th OARSI imaging workshop, Hilton Head Island, United States of America*	2012	1
The relation between quantitative delayed contrast-enhancement in meniscus and cartilage in knee osteoarthritis. *OARSI World Congress on Osteoarthritis, 2013, Philadelphia, United States of America*	2013	1
CT arthrography of the human knee to quantitatively measure cartilage biochemical composition: preliminary results of an *in-vivo* validation study using *ex-vivo* reference standards for cartilage composition. *OARSI World Congress on Osteoarthritis. Paris, France*	2014	1
Delayed gadolinium-enhanced MRI of cartilage (dGEMRIC) is superior to T1rho-mapping in measuring cartilage sulphated glycosaminoglycan content: preliminary results of an *in-vivo* validation study using an *ex-vivo* reference standard for cartilage sulphated glycosaminoglycan content *OARSI World Congress on Osteoarthritis. Paris, France*	2014	1

Teaching Activities	Year	Workload (ECTS)
Co-supervising Masters project of Esther E. Bron: "*Optimization of registration in assessment of human knee cartilage T1 mapping with dGEMRIC*"	2011	4
Co-supervising Internship of Vincent Dahi: "*Implementation of T1rho- and T2-mapping into SPARCK*"	2012	1
Co-supervising Masters Internship of Koen Dijkstra: "*dGEMRIM, T2- and T1rho-mapping MRI of the meniscus and the capability to quantitatively measure meniscal tissue composition*"	2013	4
Grant proposals	**Year**	
"*Quantitative MRI techniques to measure knee cartilage quality: Clinical validation and evaluation*" Anna foundation | NOREF Main applicant: *€ 10.000,00*	2013	4

Peer reviewing for International journals on regular basis		
European Radiology, Arthritis Care and Research, Arthritis and Rheumatology, PLoS One, Cartilage	2012-2015	5

LIST OF PUBLICATIONS

1. J. van Tiel, M. Siebelt, J.H. Waarsing, T.M. Piscaer, M. van Straten, R. Booij, M.L. Dijkshoorn, G.J. Kleinrensink, J.A. Verhaar, G.P. Krestin, H. Weinans, E.H. Oei.
   Clinically applied CT arthrography to measure the sulphated glycosaminoglycan content of cartilage.
   Osteoarthritis Cartilage. 2011 Oct;19(10):1183-9.

2. J. van Tiel, M. Siebelt, J.H. Waarsing, T.M. Piscaer, M. van Straten, R. Booij, M.L. Dijkshoorn, G.J. Kleinrensink, J.A. Verhaar, G.P. Krestin, H. Weinans, E.H. Oei.
   CT arthrography of the human knee to measure cartilage quality with low radiation dose.
   Osteoarthritis Cartilage. 2012 Jul;20(7):678-85.

3. E.E. Bron, J. van Tiel, H. Smit, D.H.J. Poot, W.J. Niessen, G.P. Krestin, H. Weinans, E.H. Oei, G. Kotek, S. Klein.
   Image registration improves human knee cartilage T1 mapping with delayed -enhanced MRI of cartilage (dGEMRIC).
   Eur Radiol. 2013 Jan;23(1):246-52.

4. J. van Tiel, E.E. Bron, C.J. Tiderius, P.K. Bos, M. Reijman, S. Klein, J.A. Verhaar, G.P. Krestin, H. Weinans, G. Kotek, E.H. Oei.
   Reproducibility of 3D delayed gadolinium-enhanced MRI of cartilage (dGEMRIC) of the knee at 3.0 T in patients with early stage osteoarthritis.
   Eur Radiol. 2013 Feb;23(2):496-504.

5. S. Matzat, J. van Tiel, G.E. Gold, E.H. Oei.
   Quantitative MRI Techniques of Cartilage Composition.
   Quant Imaging Med Surg. 2013 Jun;3(3):162-74.

6. J. van Tiel, E.H. Oei.
   Quantitative measurement of articular cartilage quality using MRI.
   Ned Tijdschr Geneeskd. 2013;157:A6340.

7. A.C. Kok, G.J.M. Tuijthof, S. den Dunnen, J. van Tiel, M. Siebelt, V. Everts, C.N. van Dijk, G.M. Kerkhoffs.
   Hole geometry of bone marrow stimulation does not influence cartilage repair in talar osteochondral defects in the goat.
   Clin Orthop Relat Res. 2013 Nov;471(11):3653-3662.

8. J. van Tiel, M. Reijman, P.K. Bos, J. Hermans, G.M. van Buul, E.E. Bron, S. Klein, J.A. Verhaar, G.P. Krestin, S.M. Bierma-Zeinstra, H. Weinans, G. Kotek, E.H. Oei.

Delayed gadolinium-enhanced MRI of cartilage (dGEMRIC) shows no change in cartilage structural composition after viscosupplementation in patients with early stage knee osteoarthritis.
PLoS One. 2013 Nov;8(11):e79785

9. E.H. Oei, J. van Tiel, W.H. Robinson, G.E. Gold.
Quantitative Radiological Imaging Techniques for Articular Cartilage Composition: Towards Early Diagnosis and Development of Disease-Modifying Therapeutics for Osteoarthritis.
Arthritis Care Res (Hoboken). 2014 Aug;66(8):1129-41.

10. J. van Tiel, G. Kotek, M. Reijman, P.K. Bos, E.E. Bron, S. Klein, J.A. Verhaar, G.P. Krestin, H. Weinans, E.H. Oei.
Delayed Gadolinium-Enhanced MRI of the Meniscus (dGEMRIM) in patients with knee osteoarthritis: relation with meniscal degeneration on conventional MRI, reproducibility and correlation with dGEMRIC.
Eur Radiol. 2014 Sep;24(9):2261-70.

11. J. van Tiel, G. Kotek, M. Reijman, P.K. Bos, E.E. Bron, S. Klein, K. Nasserinejad, G.J. van Osch, J.A. Verhaar, G.P. Krestin, H. Weinans, E.H. Oei.
Is T1rho-mapping an alternative to delayed gadolinium-enhanced MRI of
Cartilage (dGEMRIC) in assessing sulphated glycosaminoglycan content in human osteoarthritic knees? An in vivo validation study
Radiology. 2015. Accepted for publication

12. J van Tiel, M. Siebelt, M. Reijman, P.K. Bos, J.H. Waarsing, A.M. Zuurmond, K. Nasserinejad, G.J. van Osch, J.A. Verhaar, G.P. Krestin, H. Weinans, E.H. Oei.
Quantitative in vivo CT arthrography of the human osteoarthritic knee to estimate cartilage sulphated glycosaminoglycan content: correlation with ex-vivo reference standards
Osteoarthritis Cartilage. 2015. Revision submitted

13. R.A. van der Heijden, E.H. Oei, E.E. Bron, J. van Tiel, P.L. van Veldhoven, S. Klein, J.A. Verhaar, G.P. Krestin, S.M. Bierma-Zeinstra, M. van Middelkoop.
Quantitative MRI shows no difference in patellofemoral cartilage composition between patients with patellofemoral pain and healthy control subjects.
Am J Sport Med. 2015. Submited

14. P.R. Moshtagh, B. Pouran, J. van Tiel, J.Rauker, M.R. Zuiddam, F.W. Dirne, V. Arbabi, N.M. Korthagen, H. Weinans, A.A. Zadpoor.
Micro- and nano-mechanics of osteoarthritic cartilage: the effects of tonicity and disease severity.
Osteoarthritis Cartilage. 2015. Submitted.

DANKWOORD

Iemand die mij zeer dierbaar is schreef eens: "promoveren is als topsport". Toen ik dit vijf jaar geleden las had ik nog geen goed idee waar zij het over had. Nu ik inmiddels zelf alle frustratie, teleurstellingen, maar natuurlijk vooral de mooie en leuke momenten van het doen van promotieonderzoek mee heb gemaakt kan ik alleen maar stellen dat ik het met haar eens ben. Onderzoek doen is inderdaad als topsport en er is een sterk team voor nodig om dit tot een goed einde te brengen.

Allereerst wil ik de patiënten bedanken die het voor mij mogelijk hebben gemaakt om mijn onderzoek te kunnen uitvoeren. Doordat deze mensen hun tijd of hun lichaam aan de wetenschap hebben besteed heb ik dit proefschrift kunnen realiseren. Hartelijk dank hiervoor!

En dan wil ik nu de mensen uit mijn onderzoeksteam bedanken.

Prof.dr.ir. Weinans, beste Harrie, bedankt dat je me de mogelijkheid hebt gegeven om onderzoek te komen doen in Rotterdam. Achteraf ben ik ontzettend blij met jouw keuze mij niet in eerste instantie, maar in tweede instantie aan te nemen op een ander project dan waar ik aanvankelijk op solliciteerde. Jouw bevlogenheid en enthousiaste kijk op de wereld van de wetenschap hebben mij erg geïnspireerd en gemotiveerd gedurende de afgelopen jaren. Ik hoop, ondanks dat jij nu in het UMC Utrecht werkt, dat wij in de toekomst nog veel samen zullen werken.

Prof.dr. Krestin, beste professor, ook u wil ik bedanken dat u mij de mogelijkheid heeft gegeven een belangrijk deel van mijn onderzoek op de afdeling radiologie uit te voeren. Bedankt voor uw altijd snelle, kritische en opbouwende commentaren op mijn manuscripten en ander werk. Ondanks dat ik geen radioloog word hoop ik toch in de toekomst zowel op klinisch, als op onderzoeksgebied met u samen te mogen werken.

Dr. Oei, beste Edwin, ik was jouw eerste promovendus, maar daar was niets van te merken. Je was en bent nog steeds een fantastische begeleider en een prettig mens om mee samen te werken. Ondanks een drukke baan als radioloog en je vele extra taken daarnaast was je altijd benaderbaar voor een korte of lange vraag en heb je een zeer waardevolle input geleverd aan mijn proefschrift, op zowel wetenschappelijk als tekstueel gebied. Ik hoop dat er de komende jaren nog veel onderzoek zal volgen op wat wij tot nu toe hebben gedaan en ik hoop dat wij hier een gezamenlijke bijdrage aan kunnen blijven leveren.

Leden van de leescommissie en promotiecomissie: prof.dr. Bierma - Zeinstra, prof.dr. Maas, prof.dr. Niessen, prof.dr. Stam en prof.dr. Verhaar, hartelijk dank voor het lezen en het beoordelen van dit manuscript en het als opponent zitting nemen in de promotiecommissie. Prof.dr. Trattnig, thank you for reading my thesis and for your willingness to serve as an opponent on the thesis committee.

Naast bovengenoemde mensen wil ik nog een aantal mensen in het bijzonder bedanken voor hun hulp, input en niet onderzoek gebonden tijdverdrijf tijdens mijn onderzoeksperiode.

Prof.dr. Verhaar, beste professor, ondanks dat u niet in de vorm van promotor bij mijn onderzoek betrokken was wil ik u hartelijk danken voor uw input en het met een zeer klinisch gerichte blik meedenken over mijn onderzoek en manuscripten. Ik heb het altijd gewaardeerd met u over mijn onderzoek te praten en zo tot nieuwe (klinische) inzichten te komen waar ik weer mee verder kon. Ik hoop de komende jaren nog veel van u te leren tijdens mijn opleiding tot orthopedisch chirurg.

Dr. Reijman en dr. Bos, beste Max en Koen, dank voor jullie hulp en input tijdens het opzetten van mijn klinische studies en het opschrijven van de resultaten hiervan. Koen, als opleider hoop ik de komende jaren nog veel van jou te leren, al hoop ik dat we het naast vakinhoudelijke zaken toch ook nog over wetenschap kunnen hebben, bijvoorbeeld op een mooi congres.

Beste Dirk Poot, Esther Bron, Gavin Houston, Gyula Kotek, Mika Vogel en Stefan Klein, dank voor jullie hulp bij het opzetten van alle MRI protocollen en het analyseren hiervan. Zonder jullie hulp was dit nooit gelukt!

Hetzelfde geldt voor Marcel Dijkshoorn, Marcel van Straten, Ronald Booij en Wim Vermeule. Dank voor jullie hulp en flexibiliteit als het gaat om het opzetten, testen en maken van de CT artrogrammen.

Our international collaborators, dear prof.dr. Garry Gold, prof.dr. Jukka Jurvelin, dr. Eveliina Lammentausta, prof.dr. Miika Nieminen, dr. Carl Johan Tiderius and prof.dr. Juha Töyräs, thank you for collaborating with us during the implementation phase, protocol setup and clinical application of our translational and clinical MRI and CT studies in humans. I hope we can expand our collaboration in the future, which may eventually lead towards the application of quantitative imaging biomarkers of cartilage composition as a primary outcome measure for future clinical trials in osteoarthritis research in humans.

Beste staf, arts-assistenten, onderzoekers en andere medewerkers van de afdeling orthopedie en het orthopedisch research laboratorium van het Erasmus MC, dank voor jullie medewerking en meedenken als het gaat om mijn onderzoek. Natuurlijk ook bedankt voor de gezelligheid de afgelopen jaren. Vooral voor mijn ex-collegae op het lab, ik hoop dat ik jullie niet teveel heb geïrriteerd met mijn immer flauwe grappen, mijn gefluit, mijn getik, of enigerlei andere dingen die anderen altijd lijken te storen…

Beste onderzoekers, laboranten en andere medewerkers van de afdeling radiologie van het Erasmus MC, ook aan jullie mijn dank voor jullie hulp en gezelligheid tijdens alle borrels, etentjes en andere activiteiten gedurende de afgelopen jaren.

Beste chirurgen en arts-assistenten chirurgie uit het Reinier de Graaf Gasthuis in Delft, bedankt voor de enorm leerzame en leuke vooropleiding die ik bij jullie heb gehad! Ook dank voor het geven van voldoende tijd en support om mijn promotie af te ronden tijdens mijn tijd bij jullie.

Beste Rintje en Michiel, mijn paranimfen, samen werden wij de afgelopen jaren ook wel "de drie musketiers" genoemd. Ik vind het fantastisch dat ik met jullie aan mijn zijde mijn proefschrift mag verdedigen!

Beste Rintje, ik weet nog goed dat toen ik begon op EE16:18 ik mij af vroeg van wie die stapels papier toch waren die het gehele bureau tegenover mij in beslag namen. Toen er vervolgens een goedlachse, met een tulband gesierde, Friesche jongeman achter kwam zitten was het al gauw over met de rust daar. 538 Party en Fresh FM Friday, met ons gefluit maakten we iedereen gek! Gelukkig liet jij je vooral door Michiel en een beetje door mij overtuigen je studentenonderzoek door te zetten tot een promotieonderzoek; de rest is natuurlijk geschiedenis…! Naast collega en vriend, want vrienden schijn je pas te zijn als je samen dronken bent geweest heb ik weleens iemand horen zeggen, werden we ook stadsgenoten. Dus samen in de trein naar Roffa en ook 's avonds op de racefiets een rondje doen. Dat laatste en bier drinken hebben we de laatste tijd te weinig gedaan, dus daar moeten we wat aan gaan doen! Op naar een mooie opleidingstijd met veel borrels op de NOV, cursus en wie weet wat nog meer!

Beste Michiel, tijdens onze eerste kennismaking werd ik door jou doorgezaagd over wat ik nu precies met de MRI en die magnetron ging doen. Toen beide projecten vervolgens om totaal verschillende redenen vertraging opliepen, hebben wij samen een middag zitten brainstormen met als resultaat in ieder geval 3 papers! Daarnaast zijn er natuurlijk ook voldoende memorabele tripjes uit deze middagsessie koffie drinken voort gekomen. Ik denk dan bijvoorbeeld aan ons tripje naar Oulu, de congressen, maar natuurlijk

ook de borrels in Boudewijn. Ook wij zijn na al dit drankgelach gelukkig vrienden en ik hoop dat nog lang te zijn! Wat dat betreft dezelfde wens als voor Rintje, op naar een mooie tijd met zoveel mogelijke leuke uitstapjes de komende jaren!

Boys van JC Kopstuk, veel dank voor alle leuke, mooie, brakke en minder brakke dingen die we samen hebben gedaan gedurende de afgelopen 10 jaar. Ik hoop dat we, ondanks dat iedereen zijn eigen weg zoekt, al dan niet met of zonder vriendin/vrouw/kind(eren), de komende jaren nog veel mooie dingen samen zullen doen. Op naar ons Lustrum-Lustrum!

Lieve familie en schoonfamilie, bedankt voor jullie interesse. Lieve Sofie, Koen, Léon, Alexandra, Diger, Marieke en natuurlijk Thijn, ook jullie bedankt voor jullie interesse. Ik ben trots en blij dat jullie mijn (schoon)zussen, (schoon)broers en neefje zijn. Lieve Grad en Hetty, bedankt voor jullie gastvrijheid, waardering, gezelligheid en natuurlijk het oppassen op de kinderen waardoor ik soms nog wat extra tijd had om naast mijn opleiding dit werk af te ronden.

Lieve papa en mama, fijn dat jullie mij altijd hebben gesteund! Bedankt voor het vertrouwen en jullie liefde, ondanks dat ik wellicht niet altijd jullie makkelijkste kind was. Ook aan jullie veel dank voor het oppassen op onze kleintjes waardoor Wen en ik soms ook nog wat leuke tijd samen konden doorbrengen.

Lieve Wen en kids, wat is het altijd heerlijk om na een dag hard werken thuis te komen en jullie weer te zien en te kunnen knuffelen. Ik zal beloven dat ik de komende tijd niet al mijn vrije uren aan het afronden van mijn onderzoek en het voorbereiden van poli's en operaties zal besteden, maar vooral aan jullie! Bedankt voor alle leuke, grappige en ontroerende momenten de afgelopen maand, ruim 2 jaar en meer dan afgelopen 10 jaar. Jullie zijn mijn toppers waar ik het meest van hou, voor altijd!

CURRICULUM VITAE

Jasper van Tiel was born in Utrecht, the Netherlands on the 7th of December 1984. He attended secondary school at 'College Blaucapel' in Utrecht from which he graduated in 2003. In that same year he started his medical study at Utrecht University. From the beginning of his study onwards, Jasper was fascinated by the musculoskeletal system and its pathophysiology. During his study he also became interested in medical research. Therefore, after graduating as a medical doctor, in March 2010, he started his research project on quantitative cartilage imaging as a joint project of the Department of Orthopedic Surgery and the Department of Radiology of the Erasmus MC Rotterdam. He worked as a full time PhD student for almost four years under supervision of prof. dr.ir. H.H. Weinans, prof.dr. G.P. Krestin and dr. E.H.G. Oei. The research carried out during this period was rewarded with the Best Scientific Abstract Award in 2012 by the Radiological Society of the Netherlands and resulted in the current thesis. After finishing this research project, Jasper started his training to become an orthopedic surgeon in January 2014. He worked at the Department of General Surgery at the Reinier de Graaf Gasthuis in Delft (supervisor dr. M. van der Elst) and continued his training at the Department of Orthopedic Surgery at the Erasmus MC in July 2015 (supervisor dr. P.K. Bos). Jasper lives together with his girlfriend Wendy and their son and daughter.